Contents

Publication policy

The ECMWF Newsletter is published quarterly. Its purpose is to make users of ECMWF products, collaborators with ECMWF and the wider meteorological community aware of new developments at ECMWF and the use that can be made of ECMWF products. Most articles are prepared by staff at ECMWF, but articles are also welcome from people working elsewhere, especially those from Member States and Co-operating States. The ECMWF Newsletter is not peer-reviewed.

Editor: Bob Riddaway

Typesetting and Graphics: Rob Hine

Any queries about the content or distribution of the ECMWF Newsletter should be sent to Bob.Riddaway@ecmwf.int

Contacting ECMWF

Shinfield Park, Reading, Berkshire RG2 9AX, UK

Fax: . . . . . +44 118 986 9450

Telephone: National 0118 949 9000

International . . . . . +44 118 949 9000

ECMWF Web site . . . . . http://www.ecmwf.int

Front cover

ECMWF's successful 4D-Var data assimilation system has now been in operations for ten years.

EDITORIAL

Contributing to climate change studies

ECMWF's core mission is to develop its global weather forecasting system, run it operationally and distribute the results to its Member States. It is not to carry out climate simulations. However, through its core activity, ECMWF is contributing significantly to climate change studies.

The first major contribution is with reanalyses. Initially a by-product of the assimilation system developed for global weather forecasting, it was aimed at:

- Studying the evolution of the observing system and evaluating the impact on the quality of the forecast.
- Testing forecasting techniques over a long period and developing calibrations.

However the quality and ease of use of recent reanalyses has attracted a growing interest from the climate community: the IPCC Fourth Assessment Report published in 2007 contains many references to the ECMWF reanalysis, ERA-40. Recent work on homogenization of the observations and detailed comparisons between satellite instruments is still increasing the credibility of climate trends deduced from reanalyses. Such work will be further developed in the coming years, thanks to the continuous improvement of the assimilation techniques, in particular those associated with atmospheric chemistry, oceans and continental surfaces.

A second important contribution is emerging with the concept of seamless systems unifying weather and climate predictions. There are important synergies between numerical weather prediction (NWP) and climate prediction. The first synergy is that many of the key feedbacks which lead to uncertainty in climate predictions are associated with processes such as clouds, convection or boundary-layer turbulence, whose intrinsic timescales lie within the domain of NWP. Another one is that, due to obvious time constraints (you do not want to issue a forecast after its target range), NWP has developed code optimisation and supercomputing tools that can also benefit climate prediction: this, in particular, is key to increasing the resolution of climate predictions. This contribution is fully recognised and ECMWF was requested by the World Climate Research Programme (WCRP) and the World Weather Research Programme (WWRP) to host their "World Modelling Summit for Climate Prediction" which aims at identifying and developing such synergies. This is not a one-way road and NWP is also benefiting from developments in climate prediction, in particular in addressing model errors. From this point of view, the EC-EARTH initiative by several Member States, which aims at developing a climate version of the IFS, is most welcome and will be of benefit to the ECMWF forecasting system.

Finally ECMWF's core activities will contribute to the adaptation of our societies to climate change. The ECMWF strategy puts the early warning of severe weather at the heart of its principal goals. As severe weather events are likely to increase in frequency or magnitude with climate change, early warnings will become even more crucial for mitigating the consequences of these events. Recent examples when such warnings were available 3 to 5 days in advance (e.g. storm Kyrill in January 2007 and the storm surge in the North Sea in November 2007) have shown that early warnings are crucial for enabling civil protection authorities to make appropriate and timely decisions.

Dominique Marbouty

Changes to the operational forecasting system

DAVID RICHARDSON

Implementation of VarEPS-Monthly forecasting system

ECMWF has now integrated its Monthly Forecasting System with the medium-range Ensemble Prediction System (EPS). The new combined system, called VarEPS-Monthly, enables users to be provided with EPS output uniformly up to 32 days ahead, once a week. It also introduces a coupled ocean-atmosphere model for the forecast range day 10 to 15 for the forecast started from the 00 UTC analysis, on a daily basis.

VarEPS-Monthly was implemented on 11 March 2008; the first monthly run from the new system was on 13 March. The main changes are:

- Use of persisted SST anomalies in all atmospheric forecasts.
- Daily ocean-coupling for day 10 to 15 of EPS forecasts from 00 UTC analyses.
- Modified EFI products using the new unified re-forecasts.
- New GRIB description for all monthly forecast products, analogous to the current medium-range EPS data.

Further information about VarEPS-Monthly

There is an article about VarEPS-Monthly starting on page 35 of this edition of the *ECMWF Newsletter*. This includes a comparison between the performance of VarEPS-Monthly and the previous Monthly Forecasting System in terms of:

- Bias and probabilistic scores.
- Two case studies of extreme weather events.

Also detailed information about the new VarEPS-Monthly system, including a technical description, can be found on the following web page:

www.ecmwf.int/products/changes/vareps-monthly

New items on the ECMWF web site

ANDY BRADY

GRIB API 1.4.0 released

Version 1.4.0 of ECMWF's GRIB encoding/decoding software was released on 8 February 2008 and can be freely downloaded from:

www.ecmwf.int/products/data/software/download/grib_api

A new FORTRAN 90 interface has been added. Documentation and examples are available at:

www.ecmwf.int/publications/manuals/grib_api/

World Modelling Summit for Climate Prediction

The *World Modelling Summit for Climate Prediction* will be held from 6 to 9 May 2008, with the first half day featuring talks related to the five themes followed by another one and a half days of discussions in breakout groups. The summit will end with a plenary discussion and a declaration of the outcome of the meeting.

www.ecmwf.int/newsevents/meetings/workshops/

Forecast Products – Users Meeting

ECMWF organizes annually a meeting of users of its medium-range and extended-range products. The purpose of the meetings is to give forecasters the opportunity to:

- Discuss their experience with and to exchange views on the use of the medium-range and extended-range products, including the ensemble.
- Review the development of the operational system.
- Discuss future developments including forecast products.

The meeting will be held from 11 to 13 June 2008.

www.ecmwf.int/newsevents/meetings/forecast_products_user/

Magics++ 2.4.0 released

Version 2.4.0 of ECMWF's graphics library Magics++ was released on 27 February 2008. Documentation is available at:

www.ecmwf.int/publications/manuals/magics/magplus/

Subscribe to the RSS feed for more announcements at:

www.ecmwf.int/publications/manuals/magics/news/graphicsnews.rss

ESA Projects – SMOS

ECMWF participates in a number of collaborative research projects funded by the European Space Agency (ESA). ESA's Soil Moisture and Ocean Salinity (SMOS) mission has been designed to observe soil moisture over land and salinity over the oceans. ECMWF plays a major role in developing and implementing the use of SMOS brightness temperature data in NWP models (see the news item about ECMWF's contribution to SMOS on page 5 of this edition of the *ECMWF Newsletter*).

www.ecmwf.int/research/ESA_projects/SMOS/

First meeting of the TAC Subgroup on the RMDCN

TONY BAKKER, RÉMY GIRAUD

At its 37th session (October 2007), the ECMWF Technical Advisory Committee (TAC) established a Subgroup to plan for the provision of the Regional Meteorological Data Communication Network (RMDCN) service beyond 2010 and nominated R. Skålin (Norway) as its Convenor. The Subgroup includes representatives from Member States and Co-operating States, with EUMETSAT, WMO/RA VI and the WMO Secretariat being involved as observers as appropriate.

The first meeting of the TAC Subgroup on the RMDCN took place on 6–7 February 2008.

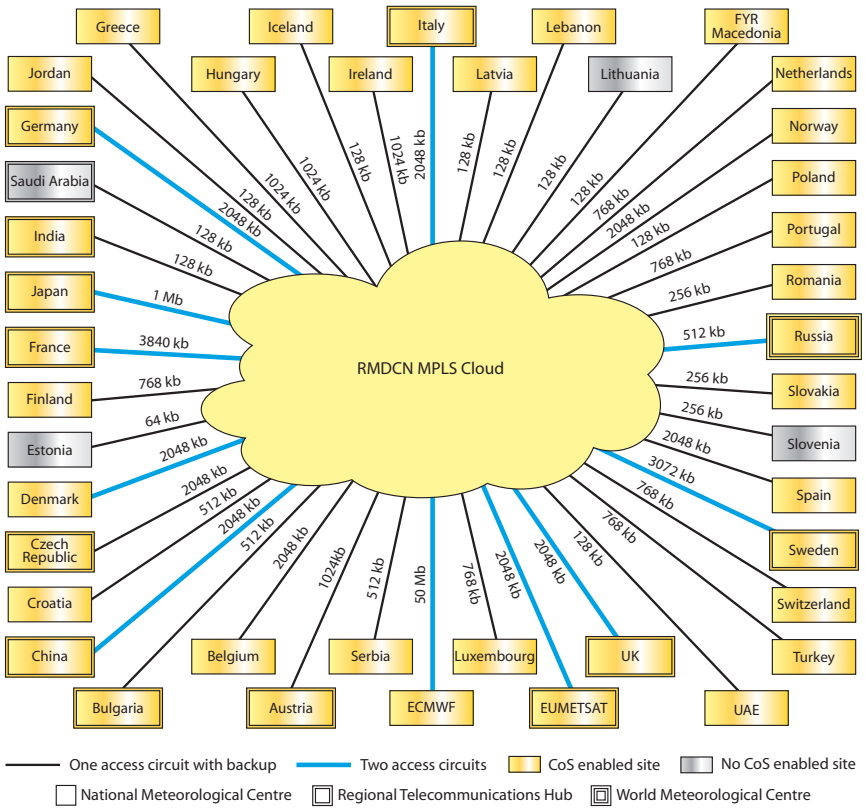

RMDCN (Regional Meteorological Data Communications Network) as at June 2007.

Representatives from ECMWF Member States, Co-operating States and EUMETSAT met with ECMWF staff to discuss network requirements and possible network architectures for the RMDCN. The Subgroup discussed the scope and methodology of the planned networking market survey to be carried out by a specialist networking consultancy company in spring 2008. The service of the current provider of the MPLS network for the RMDCN, Orange Business Services, will be compared with:

◆ Services of other providers of similar MPLS networks.
◆ MPLS networks provided by Virtual Network Operators.
◆ Solutions using the Internet to access a core MPLS Network.

The market survey will also encompass a financial analysis of the network with a perspective of five years, based on increased bandwidth requirements as well as on possible performance increases for a constant budget.

Over the next few months, two expert teams will focus on specific networking issues:

◆ The consequences of using the Internet as a medium for providing access to the RMDCN or as a backup to the RMDCN.
◆ The opportunities for using EUMETCast to complement the RMDCN.

The next meeting of the Subgroup will take place on 23–24 June 2008. A further meeting is planned for 8–9 September 2008. The final report of the Subgroup will be presented to the Technical Advisory Committee at its next meeting in October 2008.

Information about the migration to the current MPLS IPVPN based RMDCN can be found in the article on "Improving the Regional Meteorological Data Communications Network (RMDCN)" in *ECMWF Newsletter No.113*.

Third WCRP International Conference on Reanalysis

SAKARI UPPALA, DICK DEE, SHINYA KOBAYASHI, MAGDALENA BALMASEDA, ADRIAN SIMMONS

The *Third WCRP International Conference on Reanalysis* took place in Tokyo from 28 January to 1 February 2008. It provided an opportunity to assess current reanalysis activities and consider strategies and international cooperation for future reanalyses. The first reanalysis conference, Washington 1997, was held just after the completion of the NCEP (National Centers for Environmental Prediction) reanalysis and the ERA-15 reanalysis at ECMWF. The second conference, Reading 1999, was held before the start of ERA-40. Now, after the completion of the Japanese 25-year Reanalysis (JRA-25), there are more products to compare and additional assessments need to be made of the uncertainties in each reanalysis. Also the products are distributed and made available much more widely. The benefit of more open data policies was clear from the discussions and it was recognised that such policies have opened the way for collaboration on the preparation of data (calibrating satellite data, releasing their own archives, preparing boundary forcing fields etc.).

Reanalyses are now an established component in studies of planet Earth and the interest of the climate change community for reanalysis products is growing. Reanalysis centres have been able to correct the main defects in the products by improving assimilating models, observation bias handling, use of reprocessed data, exchanging of blacklist information, data recovery etc. Also new sophisticated applications of reanalyses, such as for driving chemical transport models, have emerged. These have proved the usefulness of reanalyses in estimating sensitive quantities such as the age of air. In addition the ocean community has been able to use atmospheric

reanalyses to force ocean reanalyses.

Coupled reanalysis is gradually becoming a reality. The new NCEP reanalysis from 1979 onwards has started and includes a model with a weak coupling between the ocean, sea ice, land surface and atmospheric components. It is an integral part of NCEP's seasonal forecasting system and a new reanalysis is planned after each major model upgrade. The reanalysis is expected to be available in near-real-time in about two years from now.

The new JRA-50 project (1957 onwards) has been accepted as one of the core activities of the Japan Meteorological Agency (JMA). While the first Japanese reanalysis, JRA-25, relied upon computer resources from the Central Research Institute of Electric Power Industry (CRIEPI), JRA-50 will run on JMA's own computer system. It will be an atmospheric reanalysis using 4D-Var with the ERA-40 observations as input.

The new reanalyses from NCEP and JMA are being prepared using substantial in-house resources:

- NCEP reanalysis consists of a core team of 9–11 people with substantial resources from the Global Branch, Analysis Branch of Climate Prediction Center, NESDIS (National Environmental Satellite, Data, and Information Service) and JCSDA (Joint Center for Satellite Data Assimilation).
- JRA group consists of four full-time members as of March 2008.

Comparisons between NCEP, ERA-40 and JRA-25 were presented at the conference. The overall quality of ERA-40 still seems generally high (apart from the known defects), but its future usefulness is restricted due to the limited period covered. ERA-Interim, which started with data from January 1989, will be a clear improvement and users will now have access to the first ten years of data. The NCEP reanalysis, from 1948 onwards, is still the longest and most frequently used. It is however based on a 15-year old data assimilation system and does not include the assimilation of radiances, which is crucial especially for the analysis quality from 2000 onwards.

At the end of the conference a common statement in support of reanalyses was issued, including directions for future developments. The statement will be available in the conference proceedings, which will be available soon.

Addition information about reanalyses

Current and future reanalyses

A reanalysis is a comprehensive global, multi-decadal dataset generated by the latest numerical data assimilation techniques using various past observations. Reanalyses have consistent technical quality over decades and provide vital context to many types of meteorological and climatological research and applications. The following reanalyses are available:

- NCEP reanalysis: 1948 onwards
- NASA/DAO: 1980 to 1995
- ERA-15: 1979 to 1993
- ERA-40: mid-1957 to mid-2002
- JRA-25: 1979 onwards

New reanalyses are being prepared: by NCEP (1979 onwards), JMA (JRA-50: 1957 onwards), NASA (1979 onwards) and ECWMF (ERA-Interim: 1989 onwards).

Conference proceedings

The Third WCRP International Conference on Reanalysis focused on the following.

- Introduction of reanalyses.
- Applications using reanalysis data.
- Comparison and validation of characteristics of each reanalysis.
- Data assimilation technique for reanalysis.
- Strategy and international cooperation for future reanalysis.

The conference considered not only global atmospheric reanalysis but also ocean and land reanalysis, mainly from the viewpoint of interaction with the atmosphere. It was attended by 260 scientists, 80 talks were given and there were 60 poster presentations. Extended abstracts and presentations will be made available from the WCRP website at www.wmo.int/pages/prog/wcrp.

Signing of the Co-operation Agreement between ECMWF and Latvia

MANFRED KLÖPPEL

On 18 January 2008, Mr Raimonds Vējonis, Minister of Environment of the Republic of Latvia, and Mr Dominique Marbouty, Director of ECMWF, signed a co-operation agreement at ECMWF's headquarters. Mr Andris Leitass, Director of the Latvian Environment, Geology and Meteorology Agency, attended the ceremony.

Minister Vējonis stated: "I take great pleasure in signing this co-operation agreement with the European Centre for Medium-Range Weather Forecasts, the world leader in numerical weather prediction. The information we receive from the Centre will be a great help to Latvian institutions as they strive to deliver top quality services to the general public. I am confident that in particular the Latvian Environment, Geology and Meteorology Agency will benefit immensely from this close co-operation."

Dominique Marbouty (Director of ECMWF) and Raimonds Vējonis (Minister of Environment of the Republic of Latvia) signing the co-operation agreement.

Mr Leitass said: "This co-operation agreement is highly significant for the Latvian Environment, Geology and Meteorology Agency. We are confident that closer collaboration with ECMWF will enable us to issue earlier advice on the likelihood of extreme weather, such as the storms we experienced recently in January 2007. We will be able to pass on the information we receive as a Co-operating State to both the public and the responsible authorities so that they can prepare for and respond to severe weather events more effectively. We welcome the opportunity to share knowledge and expertise with our colleagues at ECMWF and will use ECMWF's products to improve our forecasts and extend their range. We very much value this agreement and the benefits it will bring to the people of Latvia."

Mr Marbouty said: "ECMWF owes its reputation as world leader in the field of numerical weather prediction to close collaboration with the meteorological community. Governments are becoming increasingly aware of the need to improve the quality and accuracy of numerical weather prediction in order to obtain advance warning of severe weather events such as storms, heat waves and floods. I look forward to working closely with the Latvian Environment, Geology and Meteorology Agency and am pleased to offer the agency access to all our products, especially medium-range and seasonal weather forecasts."

The agreement will come into force when ECMWF is officially notified by the Latvian Government that the agreement has been ratified by Parliament.

To date Co-operation Agreements have been concluded with the Czech Republic, Croatia Estonia, Hungary, Iceland, Latvia, Lithuania, Montenegro, Morocco, Romania, Serbia, Slovakia and Slovenia.

ECMWF's contribution to the SMOS project

PATRICIA DE ROSNAY, MATTHIAS DRUSCH, THOMAS HOLMES, GIANPAOLO BALSAMO, KLAUS SCIPAL, ERIK ANDERSSON, PHILIPPE BOUGEAULT

Soil Moisture and Ocean Salinity (SMOS) is the second Earth Explorer Opportunity mission developed as part of the European Space Agency (ESA) Living Planet programme. The SMOS mission provides two-dimensional interferometric radiometer measurements of L-band (1.4 GHz) brightness temperatures from a satellite in polar orbit. At this frequency the atmosphere is almost transparent and surface emission is strongly related to soil moisture over continental surfaces and salinity over oceans – see www.esa.int/ esaLP/LPsmos.html.

SMOS is scheduled for launch in spring 2009. The key objectives of the SMOS mission are as follows.

- Improve our understanding of the global water cycle.
- Contribute to the improvement in weather and seasonal-climate forecasting.

ECMWF plays a major role in developing and implementing the use of SMOS brightness temperature data in NWP models. The contribution of ECMWF to the SMOS mission is two-fold.

- Development of a data monitoring system for the SMOS near-real-time product to provide a timely quality check for ESA and the SMOS calibration and validation teams.
- Assimilation of SMOS brightness temperature data in ECMWF's global NWP system through the Surface Data Assimilation System (SDAS) based on the Extended Kalman Filter. This system is currently being tested with the active microwave Metop/ASCAT surface soil moisture data.

The common assimilation approach for soil moisture data underlines the high level of synergy between active and passive microwave remote sensing between ESA's SMOS and EUMETSAT's Hydrological Satellite Application Facility (H-SAF).

One main component of the monitoring is the observation operator that transforms model fields of soil moisture and ocean salinity into observation equivalent brightness temperatures. To this end the CMEM (Community Microwave Emission Model) has been developed at

ECMWF; it is based on a state-of-the-art low-frequency passive microwave model. The structure of CMEM is highly modular in terms of both physical parametrizations for the multi-component surface emission (soil-vegetation-atmosphere and water bodies) and the input/output coding structure encompassing grib, ascii and netcdf formats.

CMEM is freely distributed to NWP Centres and to SMOS Validation and Retrieval Teams. A web interface has been developed which is accessible from the ECMWF web site by going to:

www.ecmwf.int/research/ESA_projects/SMOS/cmem/cmem_index.html

The figure illustrates CMEM results over West Africa produced within the African Monsoon Multidisciplinary Analysis (AMMA) Land Surface Model Inter-comparison Project (ALMIP). It shows the time-latitude diagrams obtained for 2006 over the Sahel region for observations from AMSR-E (Advanced Microwave Scanning Radiometer - Earth Observing System) on NASA's Aqua Satellite and the offline HTESSEL-CMEM simulated brightness temperatures. Dryer soil and higher vegetation water content result in higher brightness temperatures. A seasonal wet patch centred on 15°N and on Julian day 220 (early August) is clearly observed by AMSR-E. It corresponds to the monsoon season over Sahel and is characterized by a decrease of brightness temperature.

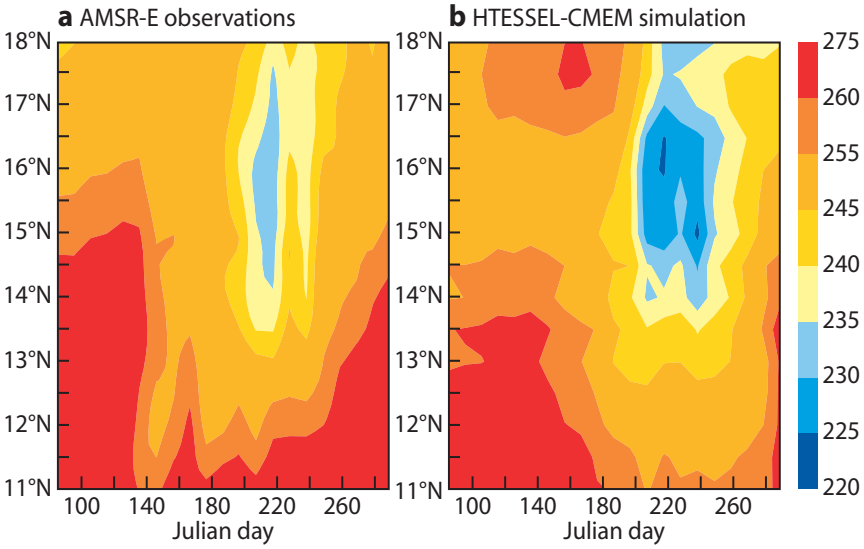

Time-latitude diagram for the year 2006 over the Sahel region (latitude 11°N to 18°N and longitude averaged from 10°W to 10°E) of the C-band horizontal brightness temperature with horizontal polarization at 6.9 GHz as (a) observed by the AMSR-E and (b) simulated by the ECMWF land surface model HTESSEL coupled to the CMEM microwave emission model developed by ECMWF to be used as the SMOS forward operator.

Seminar on the parametrization of subgrid physical processes

ELS KOOIJ-CONNALLY, ANTON BELJAARS, MARTIN MILLER

The 2008 ECMWF Seminar will run for four days from 1 to 4 September 2008. Invited and ECMWF expert speakers will provide an overview of the parametrization of subgrid physical processes and their interaction with the dynamics. The preliminary list of speakers and topics is as follows.

Processes		
Robin Hogan	University of Reading	Radiation parametrization
Adrian Tompkins	ICTP	Cloud parametrization
Peter Bechtold	ECMWF	Convection parametrization
Bjorn Stevens	UCLA	Boundary layer processes
Bart van den Hurk	KNMI	Land surface processes
Michael Schulz	LSCE	Aerosol modelling
Richard Forbes	ECMWF	Microphysics

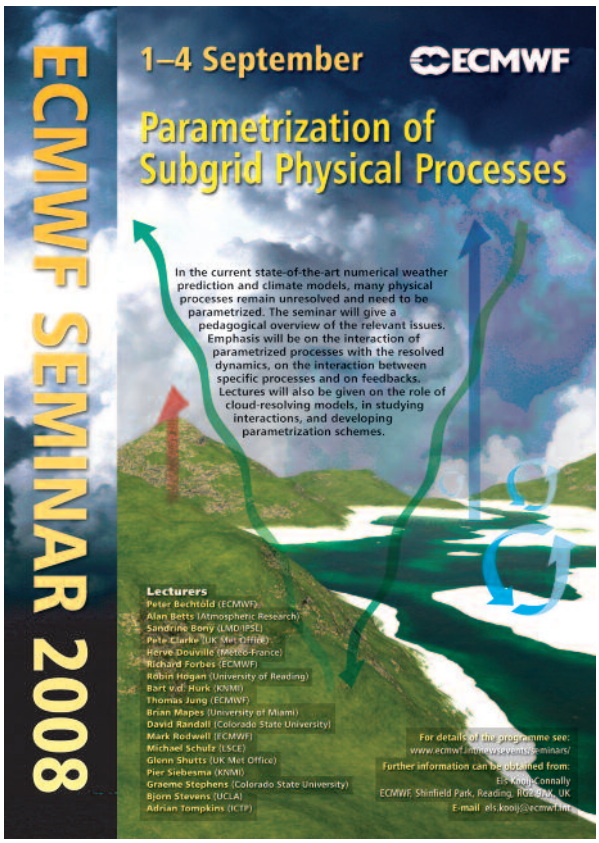

High resolution modelling		
Pier Siebesma	KNMI	Process studies in GCSS
Pete Clarke	University of Reading	Limited area modelling in CRM mode
David Randall	Colorado State University	Multi-modelling framework and parametrization
Interactions		
Sandrine Bony	LMD/IPSL	Cloud/radiation interactions
Brian Mapes	University of Miami	Tropical variability
Thomas Jung	ECMWF	Parametrized processes and atmospheric variability

Interactions		
Hervé Douville	Météo-France	Land surface versus ocean influence on atmosphere
Glenn Shutts	UK Met Office	Convection/dynamics interaction including stochastic approaches
Verification/validation		
Alan Betts	Atmospheric Research	Physical relations in observations and models
Graeme Stephens	Colorado State University	Cloud profiling with satellite data
Mark Rodwell	ECMWF	Model and process diagnostics

There is no registration fee for ECMWF Member States and Co-operating States. For registration and further information go to: www.ecmwf.int/newsevents/meetings/annual_seminar/2008/ or contact Els Kooij-Connally (els.kooij@ecmwf.int) or Anton Beljaars (anton.beljaars@ecmwf.int) or Martin Miller (martin.miller@ecmwf.int)

Annual bilateral meeting with EUMETSAT

JEAN-NOËL THÉPAUT

On 5 February 2008 the annual EUMETSAT-ECMWF bilateral meeting was held at ECMWF. This meeting gives the senior managers of both organisations the opportunity to:

- Exchange information of mutual interest between the two organisations.
- Review the status of various work packages and studies that are carried out in partnership between EUMETSAT and ECMWF.
- Secure common understanding for initiating future activities.

The highlight this year was of course ECMWF's swift exploitation of Metop-A data shortly after launch, especially for the two "new" instruments IASI and ASCAT. The Centre's future plans for assimilating cloud and rain-affected radiances were also discussed.

This meeting was also an opportunity for EUMETSAT to report to ECMWF about their future programmes, in particular JASON-follow-on, MTG (Meteosat Third Generation) and Post-EPS (EUMETSAT Polar System), together with their involvement in activities associated with GEO (Group on Earth Observations) and GMES (Global Monitoring for Environment and Security).

More information about EUMETSAT's plans can be found at www.eumetsat.int.

There is a co-operation agreement between ECMWF and EUMETSAT. In addition both organisations are members of the network of operational meteorological organisations responsible for implementing the European Meteorological Infrastructure (EMI). The network members deploy the operational infrastructures and resources required to provide Europe with a comprehensive meteorological system, including ground-based and space-based observations, and NWP models.

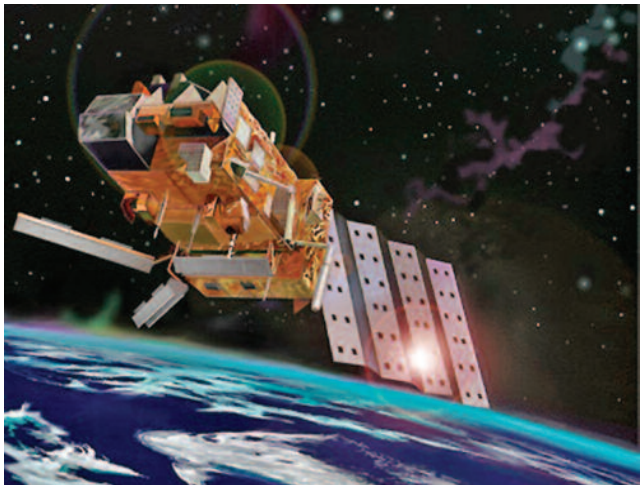

ECMWF is currently exploiting operationally five instruments from the EUMETSAT Metop-A instrument: AMSU-A, MHS, HIRS and IASI, which provide temperature and moisture information derived from microwave and infrared radiances, and ASCAT which provides surface wind vectors over sea. The assimilation of GRAS radio-occultation bending angles and GOME-2 total ozone information is under test at the time of writing.

ECMWF's 4D-Var data assimilation system – the genesis and ten years in operations

ERIK ANDERSSON, JEAN-NOËL THÉPAUT

ONE OF ECMWF's biggest-ever projects was the development of the variational data assimilation system. The project culminated with the operational implementation of 4D-Var on 25 November 1997. Recently we celebrated ten years of continuous operational production of 4D-Var analyses. In that time the system has matured into a high-performing, efficient algorithm that is capable of combining the information brought by the modern array of terrestrial and satellite observations. The resulting analyses provide the starting point (initial condition) for the ECMWF forecasts. In this short article we look back at the early years of development, and try to answer the question: on what basis was the decision taken to launch such an ambitious project, at the time?

The motivation

The 4D-Var algorithm is fundamentally tightly coupled with the forecast model – see Box A. This means that the software for assimilation, physics and numerics needs to be closely integrated. This was the impetus that initiated the coding of a new forecasting system for ECMWF: the Integrated Forecast System, the IFS. The chain of events was as follows.

- IFS/Arpege development started at the end of 1987.
- The IFS model was introduced on 2 March 1994 (Cy11r7) on the Cray C90 computer.
- 3D-Var became operational on 30 January 1996 (Cy14r3).
- 3D-Var was migrated from CRAY (shared memory) to Fujitsu VPP700 (distributed memory) on 19 September 1996 (Cy15r5).
- 4D-Var became operational on 25 November 1997 (Cy18r1).

We can see that the 4D-Var development work in itself took ten years to complete. A quick look at the plans as they were presented to the Scientific Advisory Committee (SAC) back in 1988 reveals that the amount of work required had initially been vastly underestimated. At that time, the plan spoke of the IFS model becoming operational in 1990, 3D-Var in 1991, and 4D-Var in 1993. Three years later, at the SAC in 1991, 4D-Var's huge hunger for computing power as well as the need for further software, science and algorithmic developments had become more fully understood. The completion date was then more accurately scheduled for 1995/1996.

There were two main motivations to launch this ambitious project. The first was general recognition that initial data (the analysis) is of critical importance for success in forecasting the medium range. However, from about 1986 there had been growing frustration with a couple of aspects of the then operational Optimum Interpolation (OI) assimilation scheme:

- It was difficult to produce a good analysis at the large horizontal scales, as OI by necessity was becoming more and more localized with higher observation density.

Box A

3D-Var and 4D-Var assimilation techniques

4D-Var is a four-dimensional variational data assimilation technique. It performs a statistical interpolation in space and time between a distribution of meteorological observations and an *a priori* estimate of the model state (the background). This is done in such a way that account is taken of the dynamics and physics of the forecast model to ensure the observations are used in a meteorologically consistent way.

The basic idea behind 4D-Var is illustrated by reference to the figure. In the case illustrated here, for a single parameter x the observations are compared with a short-range forecast from a previous analysis over a twelve-hour period. The model state at the initial time is then modified (by adding the analysis increment) to achieve a statistically good compromise x_a between the fit J_b to the previous forecast x_b and the fit J_o to all the observations within the assimilation window. J_b and J_o are referred to as cost functions.

The observations are compared to model fields at the correct time, but in 3D-Var the forecast model is not involved in propagating the analysis increment to the observation times. The 3D-Var analysis increment thus refers to the central time of the interval and it does not evolve. The 3D-Var algorithm is therefore computationally less demanding and less accurate than that for 4D-Var.

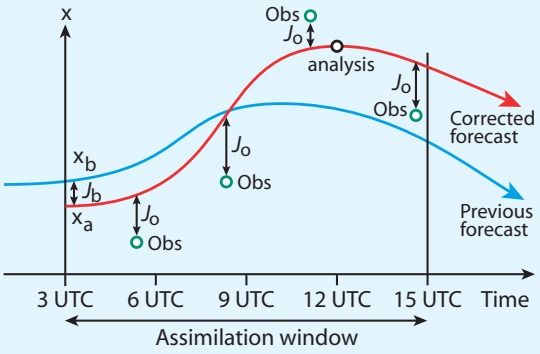

- There was only small impact from TOVS satellite data.

Initially (at the SAC meeting in 1986), the variational approach (*LeDimet & Talagrand*, 1986; *Lewis & Derber*, 1985) was seen as an effective means to address the first issue, and it was noted that, in addition, it had the prospect to introduce consistent use of the dynamics in assimilation (*Lorenc*, 1986, 1988). Philippe Courtier and Olivier Talagrand quickly set out to demonstrate these capabilities of 4D-Var with a vorticity equation model in 1986 and a shallow water model in 1987 (published in 1987 and 1990, respectively). These results were so significant that the ECMWF four-year plan in 1987 proclaimed:

> *"Advances in experimental application of 4D-Var techniques have reached a stage where it has become feasible to develop and evaluate such a scheme with a view to replacing the current intermittent OI scheme with a 4D-Var scheme in the early 1990s."*

The SAC commented a little more cautiously that they "*regarded the planned long-term development of variational techniques as an excellent, albeit speculative, research project*".

The second motivation, that variational methods would provide a solid foundation for the assimilation of satellite data, was understood one year later. New results from two separate studies had led Jean Pailleux and John Eyre to this realisation: Experimentation with so called 'physical retrievals' at the UK Met Office had demonstrated the benefit of using model fields as first guess for the retrieval of temperature and humidity profiles from the observed radiances. In addition the "PERIDOT" system at Météo-France had attempted to use radiances directly in OI. "*In March 1988 everything on this was clear in our minds*" according to Philippe Courtier. TOVS temperature and humidity retrievals were being used operationally in OI, but reports about small or sometimes negative impact forced ECMWF in May 1991 to withdraw the use of such data from the northern hemisphere and the tropics. An exasperated SAC took comfort in that "*direct use of radiances in a 3D-Var through a direct radiative transfer model and its adjoint is a natural and attractive solution*".

Towards an operational system

The group of scientists involved in coding the IFS had gradually grown from the initial two pioneers (Mats Hamrud and Philippe Courtier) to about ten. David Burridge (who was Head of Research) and Jean Pailleux (Head of Data Assimilation Section) had been enthusiastic supporters right from the outset. Tony Hollingsworth (Head of Data Division) had been a little more reluctant at first but became deeply involved following a set of convincing results obtained in 1991–1992 (e.g. *Rabier et al.*, 1993; *Thépaut et al.*, 1993; *Andersson et al.*, 1994). These studies had demonstrated that 4D-Var could (a) generate well-balanced fields, (b) create flow-dependent, vertically sloping corrections from single-level observations, and (c) induce wind-field information from a time-sequence of humidity-sensitive satellite radiance observations. The 'variational team' of developers were now busy building all the elements needed for a full-scale 4D-Var which included:

- A forecast model and its adjoint.
- The observation operators linking the observed variables to the model quantities; code to compute the observation cost function J_o and its gradient.
- The first-guess operator, to incorporate information from recent analyses; code to compute the first-guess cost function J_b and its gradient.
- Balance operators to ensure the appropriate relationship between mass and wind.
- General minimisation algorithm, to seek the analysis as the minimum of the cost function J_o+J_b.
- A suitable solution algorithm that can take advantage of the computing power available on multi-processor computing platforms.

The computing cost of 4D-Var was always a concern. It became clear that it would be prohibitively expensive, even taking into account the planned computer upgrade in 1996, to solve the full system. It was clear that significant cost-saving devices had to be developed. The breakthrough came by adopting the so-called incremental approach (published in 1994 by Courtier et al. who was influenced by the approach of John Derber from NOAA/NCEP, Washington), which enabled very significant trade-off opportunities between cost-savings and accuracy. Once the Fujitsu computer became available in September 1996, the performance of incremental 4D-Var was thoroughly evaluated and was soon shown to outperform 3D-Var (*Rabier et al.*, 1997; 1998a).

Before this, the variational system in the form of 3D-Var needed to prove its worth with respect to the operational, and by this stage finely tuned, OI scheme. At first there was no immediate time pressure, but as the arrival of the Fujitsu computer was drawing nearer, a decision had to be made whether to (a) invest considerable manpower to adapt the OI codes to this distributed memory parallel computer or (b) rely on the already parallelized 3D-Var codes and take a bet on its eventual performance. It was decided not to migrate OI. Shortly thereafter it was (fortunately) possible to show that 3D-Var could outperform OI by using additional new data such as scatterometer near-surface winds and satellite radiance data for the first time, and by producing less noisy analyses (*Courtier et al.*, 1998; *Rabier et al.*, 1998b; *Andersson et al.*, 1998). Having ensured these results, a great deal of technical work still remained to facilitate the operational implementation of 4D-Var. This included developing efficient observation processing, code parallelisation, optimisation of codes and algorithms and design of UNIX scripts in close collaboration between the Research and Operations Departments.

In *ECMWF Newsletter No. 78* there was an article by François Bouttier and Florence Rabier to proudly announce the successful implementation of 4D-Var on 25 November 1997. Here are some quotations from that article.

"This is the first ever operational application of the 4D-Var technique successfully applied to a high-resolution assimilation and forecast system."

"This was made possible by more than 10 years of scientific and technical developments in and around ECMWF's IFS as well as the availability of a powerful new computer system organized around a Fujitsu VPP700 with 116 processors."

"This is an impressive yet young assimilation system that offers an exceptional scope for future improvements."

In the article some results were presented from the extensive pre-operational validation of 4D-Var. Figure 1 shows the impact on the 500 hPa geopotential height of going from 3D-Var to 4D-Var with everything else being kept identical. These results show that there is an improvement in forecast accuracy when using 4D-Var to provide the initial conditions (analyses) for the forecasts.

The promise of 'exceptional scope for future improvements' was not an exaggeration. The list of accomplishments that have actually materialized in the past ten years is too long and varied to summarize here. However, the articles that have appeared in the *ECMWF Newsletter* give a clear indication of the way 4D-Var has developed – see Box B.

A visual impression of the progress can be seen by comparing the plots shown in Figure 2. It shows the magnitude of analysis increments, i.e. the amount of work done by the assimilation system, in terms of 500 hPa height for the month of October in four different years: 1994 (OI), 1997 (3D-Var), 1998 (4D-Var) and 2007 (recent 4D-Var). The panels show a clear reduction in the magnitude of increments, which can be interpreted as a reduction in errors (increased accuracy) in the data assimilation process. This reflects improvements in model accuracy, assimilation methods, and the vast increase of available satellite data.

What next?

Satellite data with high density and increasing computer power make it possible to explore the benefits of higher-resolution assimilation on a global scale. The performance of T1279 (15 km) assimilation with analysis increments at up to T399 (50 km) resolution will be assessed within the coming year.

The potential benefits of longer-window 4D-Var assimilation, beyond the current 12 hours, are being evaluated within a simulation test-bed with a quasi-geostrophic model. This tests the performance of an extension to 4D-Var that accounts for model error – the so-called weak-constraint 4D-Var.

The use of data assimilation ensembles is another important area for current research. It is planned that in the near future this will facilitate every analysis field being provided with a reliable estimate of its accuracy (uncertainty). Apart from its inherent value, this will also

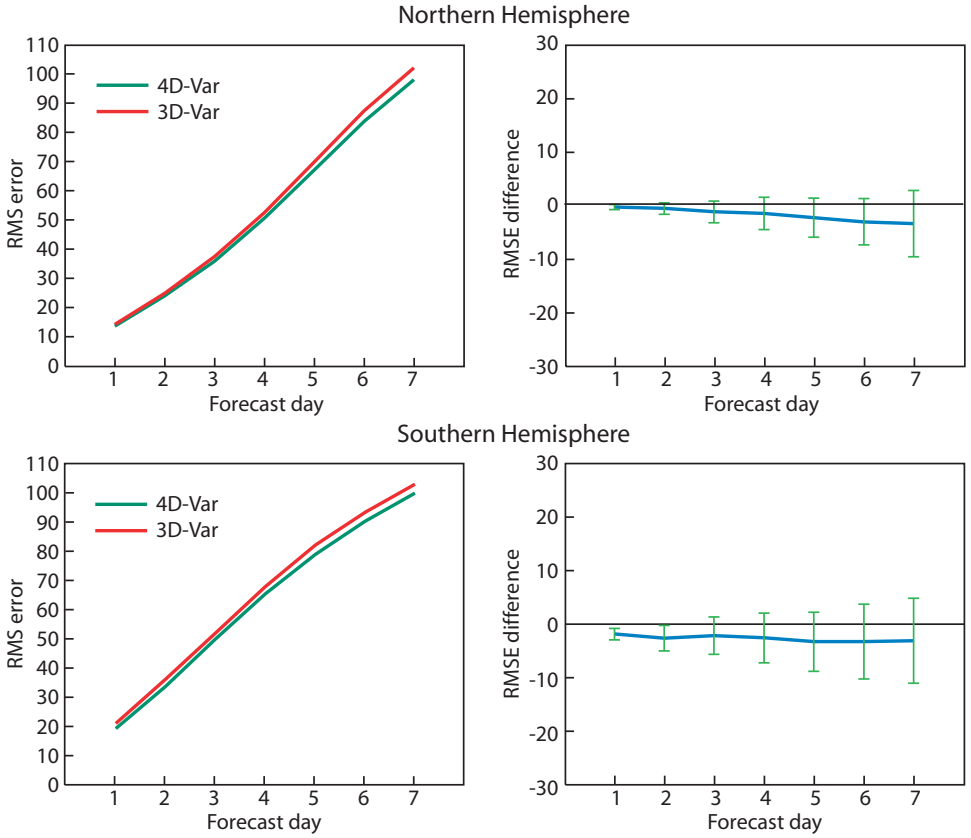

Figure 1 Comparison of RMS error for a set of forecasts started from 3D-Var and 4D-Var analyses (left) and the corresponding difference in the RMS error between the two sets of forecasts with 95% confidence intervals (right) for the northern hemisphere extratropics (top) and southern hemisphere extratropics (bottom). (From *Bouttier & Rabier*, 1998, *ECMWF Newsletter No. 78*).

Box B

Key articles about variational data assimilation techniques and data impact that have appeared in the ECMWF Newsletter

- Operational implementation of 4D-Var, *Winter 1997/98, 78, 2–5*
- Recent improvements to 4D-Var, *Autumn 1998, 81, 2–7*
- Raw TOVS/ATOVS radiances in the 4D-Var system, *Spring 1999, 83, 2–7*
- Assimilation of meteorological data for commercial aircraft, *Autumn 2002, 95, 9–14*
- Assimilation of high-resolution satellite data, *Spring 2003, 97, 6–12*
- ERA-40: ECMWF's 45-year reanalysis of the global atmosphere and surface conditions 1957–2002, *Summer/Autumn 2004, 101, 2–21*
- CO_2 from space: estimating atmospheric CO_2 within the ECMWF data assimilation system, *Summer 2005, 104, 14–18*
- New observations in the ECMWF assimilation system: satellite limb measurements, *Autumn 2005, 105, 13–17*
- "Wavelet J_b" – A new way to model the statistics of background errors, *Winter 2005/06, 106, 23–28*
- A variational approach to satellite bias correction, *Spring 2006, 107, 18–23*
- Analysis and forecast impact of humidity observations, *Autumn 2006, 109, 11–15*
- Assimilation of cloud and rain observations from space, *Winter 2006/07, 110, 12–19*
- Operational assimilation of GPS radio occultation measurements at ECMWF, *Spring 2007, 111, 6–11*
- Evaluation of the impact of the space component of the Global Observing System through Observing System Experiments, *Autumn 2007, 113, 16–28*

be valuable as an input to the Ensemble Prediction System (EPS) whose aim it is to predict the reliability of today's forecast. It is envisaged that 5 to 10 lower-resolution 4D-Var assimilations will be run in parallel, each one with differently perturbed observation inputs. The information from the ensemble will also be used in the assimilation system itself to give varying weights to observations depending on today's situation. This will be particularly beneficial for the analysis of intense and extreme weather events.

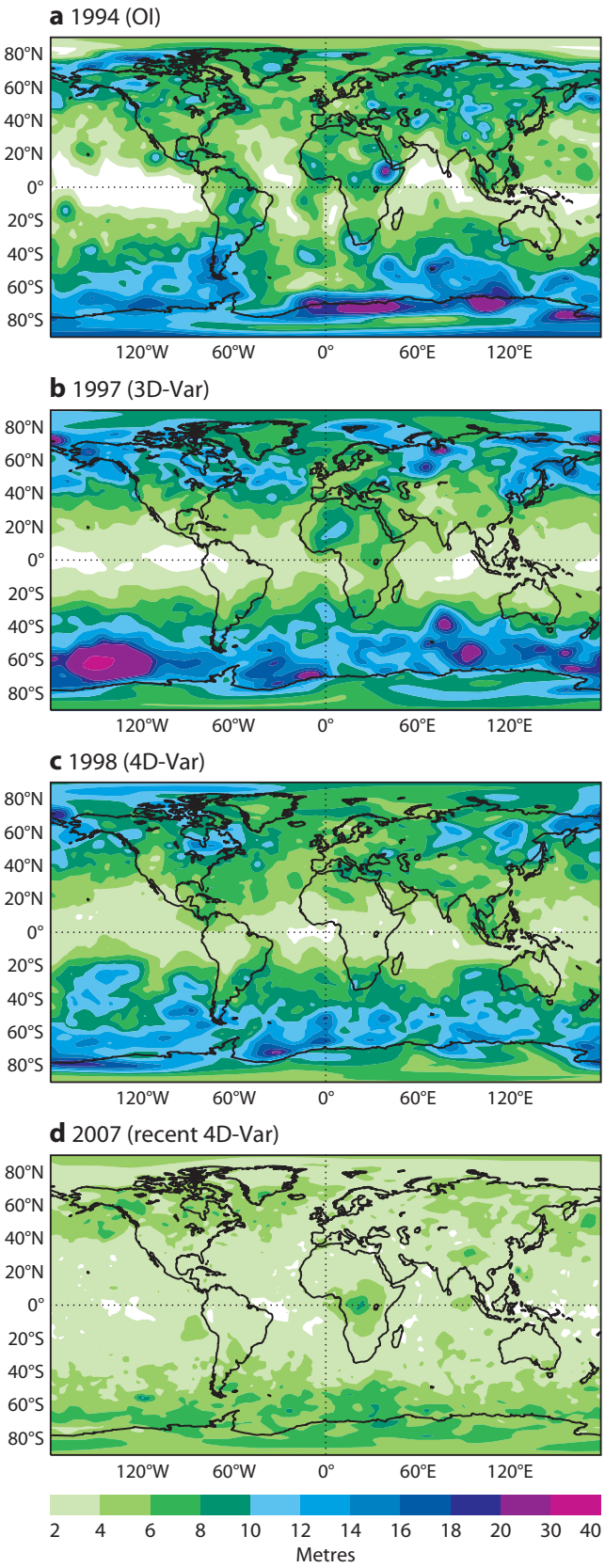

Figure 2 RMS of analysis increments in terms of 500 hPa geopotential height in ECMWF's operational assimilation system for the month of October for (a) 1994 (OI), (b) 1997 (3D-Var), (c) 1998 (4D-Var) and (d) 2007 (recent 4D-Var). Where observations are available, these results reflect the assimilation accuracy which depends on the accuracy of the observations, the forecast model and the assimilation system.

FURTHER READING

Andersson, E., J. Pailleux, J.-N. Thépaut, J. Eyre, A.P. McNally, G. Kelly & P. Courtier, 1994: Use of cloud-cleared radiances in three/four-dimensional variational data assimilation. *Q. J. R. Meteorol. Soc.*, **120**, 627–653.

Andersson, E., J. Haseler, P. Undén, P. Courtier, G. Kelly,

D. Vasiljević, **C. Branković**, **C. Cardinali**, **C. Gaffard**, **A. Hollingsworth**, **C. Jakob**, **P. Janssen**, **E. Klinker**, **A. Lanzinger**, **M. Miller**, **F. Rabier**, **A. Simmons**, **B. Strauss**, **J.-N. Thépaut** & **P. Viterbo**, 1998: The ECMWF implementation of three dimensional variational assimilation (3D-Var). III: Experimental results. *Q. J. R. Meteorol. Soc.*, **124**, 1831–1860.

Courtier, **P.**, **J.-N. Thépaut** & **A. Hollingsworth**, 1994: A strategy for operational implementation of 4D-Var, using an incremental approach. *Q. J. R. Meteorol. Soc.*, **120**, 1367–1388.

Courtier, **P.** & **O. Talagrand**, 1987: Variational assimilation of meteorological observations with the adjoint vorticity equation. II: Numerical results. *Q. J. R. Meteorol. Soc.*, **113**, 1329–1347.

Courtier, **P.** & **O. Talagrand**, 1990: Variational assimilation of meteorological observations with the direct and adjoint shallow-water equations. *Tellus*, **42**, 531–549.

Courtier, **P.**, **E. Andersson**, **W. Heckley**, **J. Pailleux**, **D. Vasiljević**, **M. Hamrud**, **A. Hollingsworth**, **F. Rabier** & **M. Fisher**, 1998: The ECMWF implementation of three-dimensional variational assimilation (3D-Var). I: Formulation. *Q. J. R. Meteorol. Soc.*, **124**, 1783–1807.

LeDimet, **F.** & **O. Talagrand**, 1986. Variational algorithms for analysis and assimilation of meteorological observations. *Tellus*, **38A**, 97–110.

Lewis, **J.M.** & **J.C. Derber**, 1985: The use of adjoint equations to solve a variational adjustment problem with advective constraints. *Tellus*, **37**, 309–327.

Lorenc, **A.C.**, 1986: Analysis methods for numerical weather prediction. *Q. J. R. Meteorol. Soc.*, **112**, 1177–1194.

Lorenc, **A.C.**, 1988: Optimal nonlinear objective analysis. *Q. J. R. Meteorol. Soc.*, **114**, 205–240.

Rabier, **F.P. Courtier**, **J. Pailleux**, **O. Talagrand** & **D. Vasiljević**, 1993: A comparison between four-dimensional variational assimilation and simplified sequential assimilation relying on three-dimensional variational analysis. *Q. J. R. Meteorol. Soc.*, **119**, 845–880.

Rabier, **F.**, **J-F. Mahfouf**, **M. Fisher**, **H. Järvinen**, **A.J. Simmons**, **E. Andersson**, **F. Bouttier**, **P. Courtier**, **M. Hamrud**, **J. Haseler**, **A. Hollingsworth**, **L. Isaksen**, **E. Klinker**, **S. Saarinen**, **C. Temperton**, **J.-N. Thépaut**, **P. Undén** & **D. Vasiljević**, 1997: Recent experimentation on 4D-Var and first results from a Simplified Kalman Filter. *ECMWF Tech. Memo No. 240.*

Rabier, **F.**, **J.-N. Thépaut** & **P. Courtier**, 1998a: Extended assimilation and forecast experiments with a four-dimensional variational assimilation system. *Q. J. R. Meteorol. Soc.*, **124**, 1861–1887.

Rabier, **F.**, **A. McNally**, **E. Andersson**, **P. Courtier**, **P. Undén**, **J. Eyre**, **A. Hollingsworth** & **F. Bouttier**, 1998b: The ECMWF implementation of three dimensional variational assimilation (3D-Var). II: Structure functions. *Q. J. R. Meteorol. Soc.*, **124**, 1809–1829.

Talagrand, **O.** & **P. Courtier**, 1987: Variational assimilation of meteorological observations with the adjoint vorticity equation. I: Theory. *Q. J. R. Meteorol. Soc.*, **113**, 1311–1328.

Thépaut, **J.-N.**, **R. Hoffman** & **P. Courtier**, 1993: Interactions of dynamics and observations in a four-dimensional variational assimilation. *Mon. Wea. Rev.*, **121**, 3393–3414.

Towards a climate data assimilation system: status update of ERA-Interim

SAKARI UPPALA, DICK DEE, SHINYA KOBAYASHI, PAUL BERRISFORD, ADRIAN SIMMONS

THE PROCESS of reanalysis involves using observations from past decades in a state-of-the-art forecasting system that is more sophisticated than that available when the observations were made. This process provides a set of high quality global analyses which have been used for a wide variety of applications in sectors such as agriculture, water management, air quality and health.

The Reanalysis Section of ECMWF has in the past produced three major reanalyses: FGGE, ERA-15 (*ECMWF Newsletter No 73*) and ERA-40 (*ECMWF Newsletter No 101*). The last of these consisted of a set of global analyses describing the state of the atmosphere and land and ocean-wave conditions from mid-1957 to mid-2002. Now progress is being made in producing 'ERA-Interim'. This is a reanalysis of the atmospheric state covering the period from 1989 until real time, using a 12-hour 4D-Var data assimilation system as described in *ECMWF Newsletter No 110*. The plans are to continuously update ERA-Interim in near-real-time when it reaches present.

Here some comparisons will be made between ERA-40 and ERA-Interim, and occasionally reference will be made to two other sets of reanalyses:

- JRA-25 produced by the Japanese Meteorological Agency (JMA) and the Central Research Institute of Electric Power Industry (CRIEPI).
- NCEP-DOE reanalysis 2 produced by the National Centers for Environmental Prediction and the National Center for Atmospheric Research in the USA.

As the second half of 2003 is now being analysed, ERA-Interim has progressed beyond the end of ERA-40. After completion of the first four years it was decided to revise the configuration of the system, as discussed in *ECMWF Newsletter No. 111*, and to rerun the initial segment. Other shorter reruns for later periods have been completed as needed for technical reasons.

The first ten years, 1989–1998, of the validated ERA-Interim analysis daily products, comprising the merged production run and the reruns, can now be accessed by MARS users (`expver=1`, `class=ei`). Also available are the

twice daily ten-day forecasts and monthly means. The ERA-Interim archive is more extensive than that for ERA-40, e.g the number of pressure levels is increased from ERA-40's 23 to 37 levels and additional cloud parameters are included. It is expected that the next five years of ERA-Interim, 1999–2003 will be released after validation around June 2008 and that the production will catch up with real time during the second half of this year. ERA-Interim products are also publicly available on the ECMWF Data Server, at a 1.5° resolution, including several products that were not available for ERA-40.

The ERA-Interim website will provide information on the current status and latest developments. Near the end of the year ERA-Interim will be running as a Climate Data Assimilation System, which will open new opportunities for climate monitoring. A subset of the current reanalysis monitoring information, together with some additional climate monitoring indices recommended by WMO, will be included on the ERA-Interim web site. Details will be decided later as what can be provided will depend on available resources.

ERA-Interim quality aspects

Based on internal evaluations and comparisons with other reanalyses, the quality of ERA-Interim products is generally good and its long-term homogeneity has improved considerably over that of ERA-40. Internal validation of the ocean wave height analysis produced with ERA-Interim also indicates a higher degree of homogeneity. Verification against independent buoy measurements shows rms errors that are stable and much smaller than in ERA-40. Also there is reduced 10-metre wind speed bias over extratropical ocean areas in the northern hemisphere.

While it is not possible to state exactly how each new component of the ERA-Interim data assimilation system contributes to these improvements, we can, in broad terms, state the following.

- 4D-Var with a 12-hour window makes better use of asynoptic observations than the 6-hour 3D-Var FGAT used in ERA-40, especially for the "relatively sparse" HIRS, MSU and the stratospheric SSU radiances in the early 1990s.
- The upgraded moisture analysis together with improved model physics have resulted in smaller humidity increments, lower precipitation and reduced spindown during the model integration relative to ERA-40.
- Compared to the static bias corrections used in ERA-40, the new variational bias correction scheme (VarBC) is better able to maintain consistency among different components of the observing system. This facilitates the extraction of the true signal present in the data, and helps to maintain time continuity by reducing analysis increments (e.g. in the stratosphere).

New satellite data types improving the analysis quality

ERA-Interim will make use of data from the increasing number of new instruments on satellites from 2003 onwards as discussed by Graeme Kelly and Jean-Noël Thépaut in *ECMWF Newsletter No. 113*. In particular 4D-Var and VarBC will improve the extraction of information from data provided by high-resolution instruments. Nevertheless, specially designed observing system experiments may be needed to help interpret climate signals in the ERA-Interim time series.

The transition from a stratospheric analysis dominated by SSU radiance data to one primarily controlled by AMSU-A occurred in August 1998. Prior to the transition, SSU channel 3 radiances (with peak sensitivity at 1 hPa) were used without bias correction in order to prevent a drift of the assimilation towards the model climate in the upper stratosphere. With the introduction of AMSU-A in August 1998 it was decided to switch to using AMSU-A channel-14 radiance data (also peaking

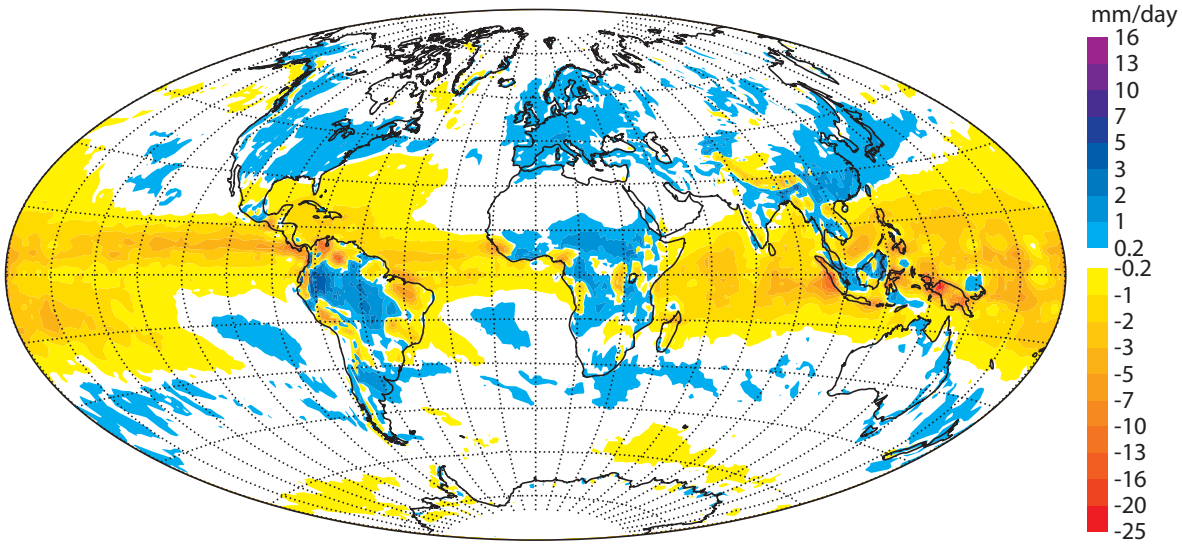

Figure 1 The difference of total precipitation between ERA-Interim and ERA-40 for 1989–1998. Units: mm day^{-1}.

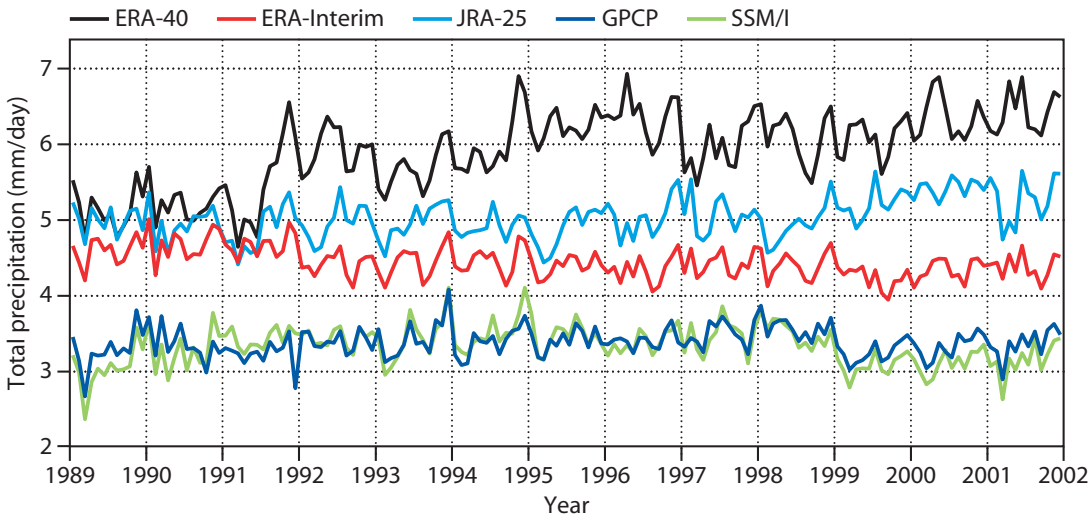

Figure 2 Time series of monthly mean total precipitation rate averaged over tropical oceans from the ERA-40, ERA-Interim and JRA-25 reanalyses, from SSM/I retrievals and from GPCP. Units: mm day^{-1}.

at 1 hPa) without bias correction, and to allow VarBC to correct SSU channel 3 in order to maintain consistency between the two sensors. Since the constraints provided by the two sensors are qualitatively different, this transition produced a noticeable but unavoidable shift in the upper-stratospheric temperature analysis. This has resulted in a jump in temperature at levels higher than 10 hPa in mid-1998, as also occurred in ERA-40. Fundamentally, in the absence of additional high-quality observations, there is no way to further improve the fidelity of the upper-stratospheric climate signal without improving the assimilating model.

ERA-Interim has started to benefit from GPS radio occultation (GPS-RO) data reprocessed by UCAR from June 2001 onwards; for details of the operational use of these data see Sean Healy's article in *ECMWF Newsletter No. 111*. It has been demonstrated (by Shinya Kobayashi, not shown here) that the use of GPS data results in a further reduction of the residual oscillations in the mean vertical temperature observation-background structures that are not well-resolved by AMSU-A observations.

Hydrological cycle

Several of the problems found in ERA-40 have been eliminated or significantly reduced in ERA-Interim, most notably the excessive precipitation over the tropical oceans from the early 1990s onwards. The mean total precipitation over the tropical oceans for the period 1989–1998 (Figure 1) shows an overall reduction. Over tropical land areas and in the extratropics the ERA-Interim precipitation is slightly higher than in ERA-40. Figure 2 shows that over tropical oceans total precipitation in ERA-Interim is substantially lower than in ERA-40 as well as being somewhat lower than the JRA-25 precipitation. However, ERA-Interim precipitation still exceeds estimates from the Global Precipitation Climatology Project (GPCP). Until 1997 both JRA-25 and ERA-Interim are in relatively close agreement, but from then on JRA-25 indicates a small upward trend in precipitation. A small decrease in precipitation in ERA-Interim occurs in 1992, probably due to an increase in SSM/I rain-affected radiances used in the analysis.

A major part of the explanation for the improved

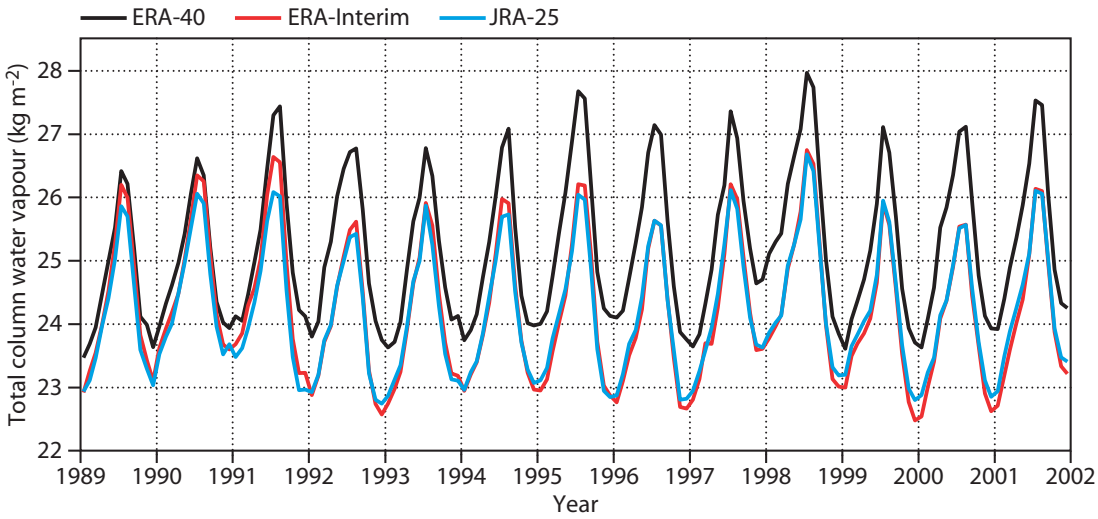

Figure 3 Global total column water vapour in ERA-40, ERA-Interim and JRA-25. Units: kg m^{-2}.

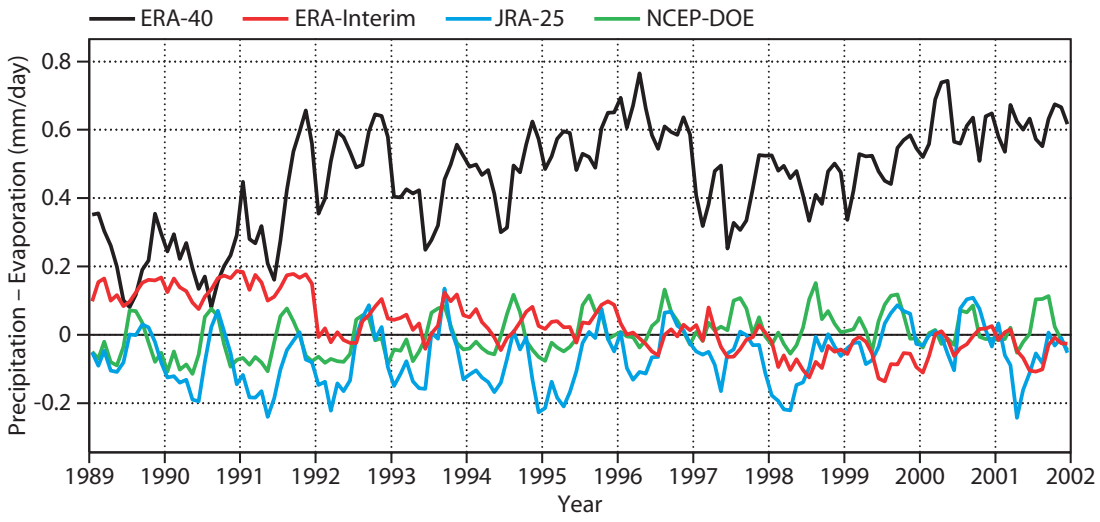

Figure 4 Global precipitation minus evaporation in ERA-40, ERA-Interim, JRA-25 and NCEP-DOE reanalysis 2. Units: mm day^{-1}.

precipitation in ERA-Interim results from both the improved moisture analysis and the model physics. The global total column water vapour in ERA-Interim is now significantly lower than in ERA-40. ERA-Interim and JRA-25 total column water vapour show very good agreement (Figure 3). Over the tropical oceans the total column water vapour from ERA-Interim is also closer to the SSM/I values produced by Remote Sensing Systems than ERA-40 (not shown).

The excessive precipitation in ERA-40 resulted in a large positive bias in the hydrological precipitation minus evaporation (P-E) balance (Figure 4). In ERA-Interim precipitation remains slightly higher than evaporation until 1991, but from then on the balance is close to zero. The JRA-25 balance is slightly negative until 1995 and is very good from then on. The NCEP-DOE reanalysis 2 has a very good P-E balance throughout.

There are strong indications that the Brewer-Dobson circulation, which is too strong in ERA-40, is more reasonable in ERA-Interim. For example, the annual cycle of specific humidity in the tropical lower stratosphere is much smaller than in ERA-40, due to reduced vertical transport across the tropopause. Preliminary diagnostic studies of 'age of air' have shown that ERA-Interim provides a much improved dataset for driving models of stratospheric chemical transport and stratosphere-troposphere exchange.

Variational radiance bias correction during the first ten years

A major problem with the use of observations for climate analysis is the presence of biases. Of particular importance is the effect on the estimation of climate signals of changes in these biases, their sampling frequencies, and details of the analysis techniques. This problem also exists in atmospheric reanalyses; they combine many different types of observations together with information from sophisticated models in order to produce accurate and dynamically consistent estimates of global atmospheric parameters.

In spite of best efforts to remove all systematic errors at the source, some residual biases inevitably remain. Their presence can be readily detected in a reanalysis system by monitoring the data against a common reference. The data assimilation then provides a final opportunity to correct the biases in the data, and possibly in the model as well, based on the consensus of all information presented to the analysis system. This idea, along with the practical challenge of dealing with a heterogeneous and evolving observing system, has led to the development of automated bias correction schemes embedded in the analysis component of the data assimilation system.

Questions about the long-term stability of the VarBC were raised at the *Workshop on Bias Estimation and Correction* held at ECMWF in November 2005. Do we have enough unbiased observations to anchor the system and will the variational bias corrections remain bounded? In this regard static bias corrections were considered safer even if suboptimal, but it was recognised that they are also dependent on special characteristics of the period during which the bias corrections were estimated. For example, the Pinatubo eruption in 1991 affected subsequent bias corrections of radiances in ERA-40. This in turn was partly responsible for the excessive and gradually increasing tropical precipitation.

Variational bias correction provides an automatic inter-calibration of the observing system in the context of the forecast model combined with all available observations. This results in bias corrections that improve the consistency of the information entering the analysis. Figure 5 shows bias corrections produced during the first ten years of ERA-Interim, in this case for radiance data from MSU channel 2 on NOAA-10, NOAA-11, NOAA-12 and NOAA-14 satellites. The corrections account for systematic errors in the data (e.g. due to calibration issues) but also for errors in the fast radiative transfer model used to simulate the data (e.g. due to inaccurate spectroscopy). However, there is the possibility that these corrections may also falsely correct the data for

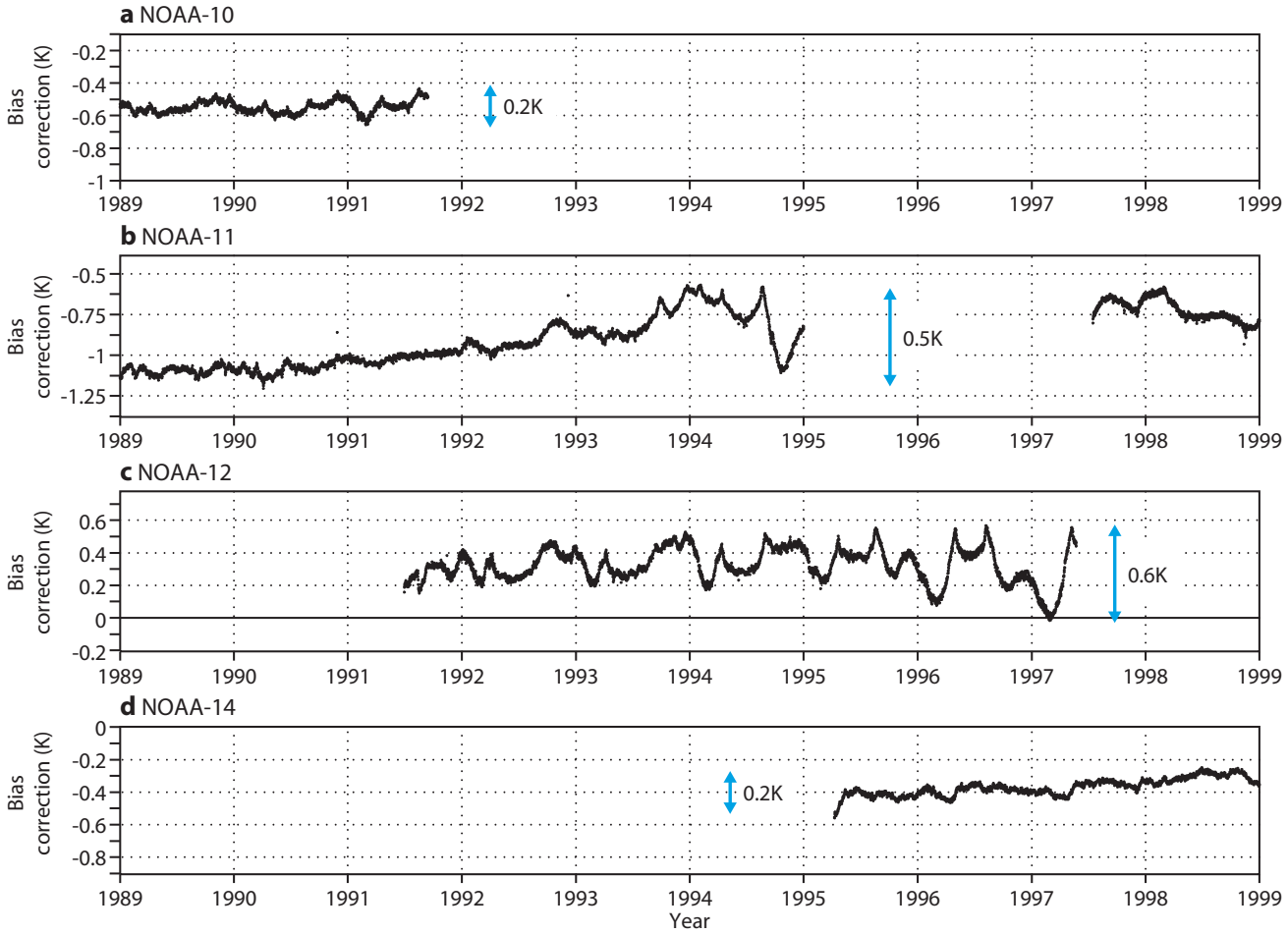

Figure 5 Global mean bias corrections for MSU channel 2 radiances from (a) NOAA-10, (b) NOAA-11, (c) NOAA-12 and (d) NOAA-14 in ERA-Interim.

errors in the background which are due to forecast model bias, especially where observations are sparse (such as in the stratosphere).

The range of corrections produced by VarBC is rather small, and the slow trend detected in the NOAA-11 bias most likely corresponds to a drift of the instrument calibration. The variations in the correction patterns for the overlapping satellites (e.g. in 1996 for NOAA-14 and NOAA-12) may be due to actual differences between individual instruments or, alternatively, could reflect different exposures of the instruments to short wave radiation. There are strong indications that variational bias correction of radiance data is generally beneficial to the quality of the ERA-Interim reanalysis. For example, the vertical consistency of the temperature analysis, as well as the fit to radiosonde data in the polar regions, is much improved compared to ERA-40. A wealth of information will be available on the details of bias corrections that needs to be evaluated in collaboration with satellite data producers and radiance transfer modellers.

Improving the consistency between SSU and AMSU in ERA-Interim

Stratospheric temperature analyses are dominated by satellite data and therefore strongly affected by biases present in these data and/or in the radiative transfer models used to model them. In ERA-40, two problematic periods were identified in the stratospheric temperature analysis after 1979. One is the early 1980s when the observations from the Stratospheric Sounding Unit (SSU) had significant biases due to leakage of gas from the pressure modulation cell. The other is from the late 1990s to early 2000s when observations from SSU and the Advanced Microwave Sounding Unit A (AMSU-A) overlapped. In ERA-40, the static bias correction system was unable to resolve the significant discrepancy between the observed SSU and AMSU-A radiances and those computed by the Radiative Transfer model for TOVS (RTTOV) – see Figure 6. This led to blacklisting of the SSU top channel after AMSU-A observations became available, causing a second jump in temperatures above 10 hPa in mid-1999.

For better use of SSU and AMSU-A observations in reanalysis, the biases in these observations have been investigated using co-located observations produced by the Simultaneous Nadir Overpass (SNO) technique. This technique utilizes simultaneous observations at the orbital intersections over polar regions and provides reliable estimates for the inter-satellite biases with little ambiguity. The biases estimated by this method were used for verification of the radiative transfer model-

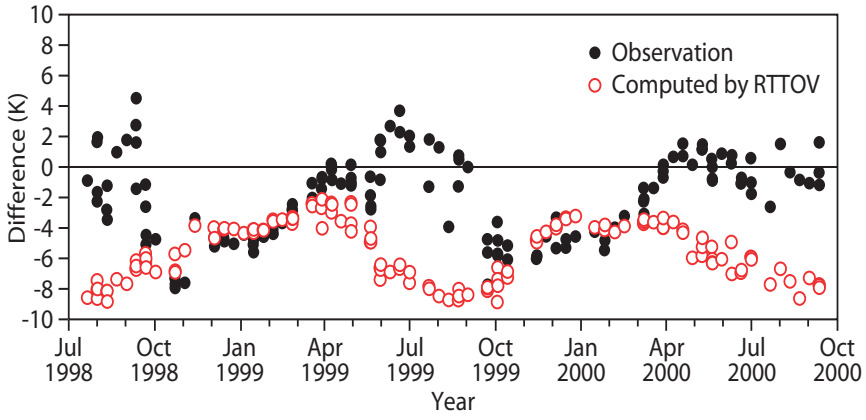

Figure 6 Differences in the observed radiances between SSU3 on NOAA-11 and AMSU-A14 on NOAA-15 over Antarctica compared to differences computed by the standard RTTOV. The difference computed by RTTOV is inconsistent with the observations in the polar winter.

ling, and it was found that the biases in the SSU observations can be simulated by taking into account the gas leak from the pressure modulation cell. It was also found that the principal cause of the discrepancy between SSU and AMSU-A was the inaccurate modelling of the Zeeman effect in the computation of the AMSU-A radiances – Figure 7.

Accordingly, new regression coefficients have been computed for RTTOV using a revised line-by-line model, and experiments were carried out to test the impact of the new RTTOV. The control assimilation using the old RTTOV tends to create spurious peaks around model levels 6 and 10 (2 and 5 hPa respectively) when the strong polar vortex develops in winter. This is because the weighting function for AMSU-A channel 14 in the old RTTOV is located too high; this results in too warm radiance simulations when the mesosphere is warmer than the stratosphere. Such a situation occurs in polar regions in winter. Using the new RTTOV these spurious peaks have been reduced and the vertical temperature structure varies more smoothly with seasons. The monthly averaged zonal mean temperatures also demonstrate the significant reduction of the spurious peaks in the polar regions.

The ERA-Interim stratospheric analysis from 1998 onwards already benefits from the more accurate modelling of AMSU-A. The better modelling of SSU and AMSU-A radiances is expected to increase significantly the time consistency of all future stratospheric temperature analyses.

Forecast performance

Ten-day forecasts have been run twice daily from both the ERA-40 and ERA-Interim analyses. We can see a substantial improvement in forecast skill of ERA-40 over ECMWF operations for 1989–1990. ERA-Interim in turn improves substantially on ERA-40, especially in the southern hemisphere. The ability of 4D-Var to use the satellite data more effectively is a key factor in the larger improvement in the southern hemisphere. Even during 1999–2001, when operations already used 4D-Var and a higher resolution T511 assimilating model, the ERA-Interim forecasts perform better than operations and more so again in the southern hemisphere. Other improvements to the model and the analysis together with the variational radiance bias correction contribute to this. By comparing the performance between 1989–1990 and 1999–2001 in both hemispheres (see Figure 8) we conclude that ERA-Interim forecasts have a more uniform quality in time and space than forecasts from ERA-40, implying a more homogeneous analysis and product quality in ERA-Interim.

Future outlook

The ERA-Interim reanalysis at ECMWF is the latest iteration of a process which combines developments in modelling, data-analysis techniques and computing power together with new data rescue efforts and experience gained from previous reanalyses to produce a succession of reanalyses of increasing quality. ERA-Interim benefits from many analysis and model

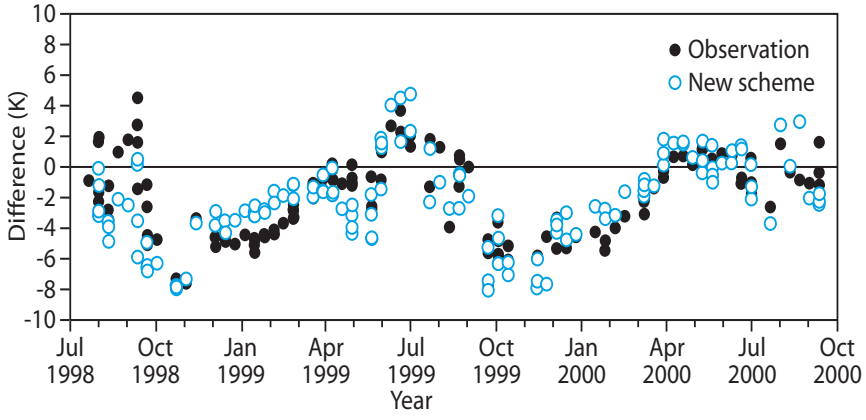

Figure 7 Differences in the observed radiances between SSU3 on NOAA-11 and AMSU-A14 on NOAA-15 over Antarctica compared to differences computed with a new scheme consisting of the standard RTTOV for SSU and a line-by-line model without the Zeeman effect for AMSU-A. The new scheme is in better agreement with the observations than if the standard RTTOV is used for AMSU-A.

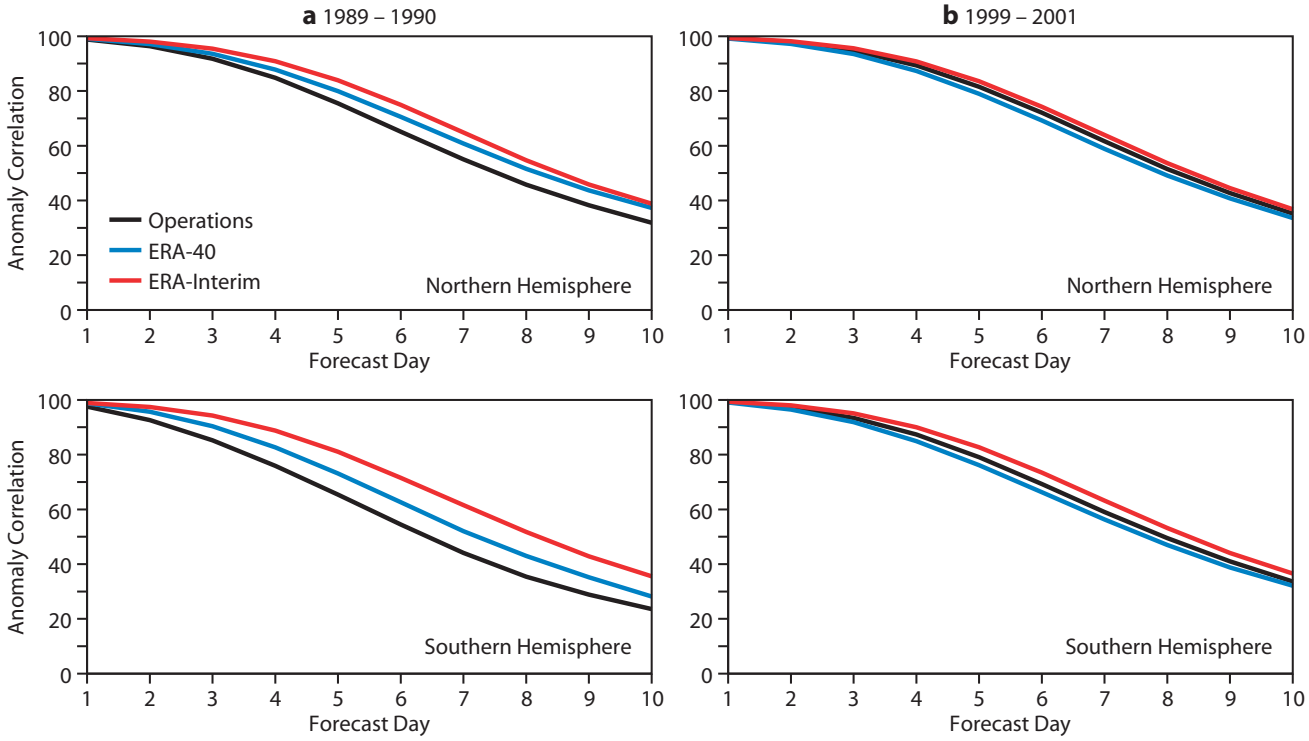

Figure 8 Mean anomaly correlation of 500 hPa geopotential for ERA-Interim, ERA-40 and original operations for (a) 1989–1990 and (b) 1999–2001. Top panels: extratropical northern hemisphere. Bottom panels: extratropical southern hemisphere.

improvements made since ERA-40 was produced, particularly in the ability to make good use of satellite radiances. After three decades of NWP development and continuous feedback from the scientific community, reanalyses are now approaching the qualities required for climate-change studies. Also, the hydrological cycle, surface fluxes and surface parameters together with the boundary layer quantities have improved over the sensitive and data sparse polar areas. Comparisons with stratospheric datasets show that we can now have good confidence in reanalyses up to 10 hPa through the years when satellite observations are available.

As seen from the news item about the *Third International Conference on Reanalysis* on page 3 of this edition of the *ECMWF Newsletter*, new reanalysis activities have now been funded in the US and Japan and are firmly established. It is urgent that similar support be re-established in Europe. To achieve this, ECMWF has engaged in extensive consultations with a number of European organizations and will aggressively seek funding under the European Commission Research and Development Framework Programmes and other sources.

Several important improvements are on the horizon. Together with the use of higher resolution models and improved analysis methods, the data assimilation can be better configured for reanalysis purposes. There are exciting developments in the use of cloud- and rain-affected radiance data for reanalysis. Active coupling of the atmospheric, ocean, land and ice components will become possible in the coming years. Collaborative work on improved observational input and boundary forcing data, the ongoing homogenization work on radiances and conventional data, and the increased availability of reprocessed satellite data will further advance the role of reanalyses in climate-change assessments and other applications. For the data-sparse historical periods, modern analysis schemes such as 4D-Var have demonstrated their ability, when properly tuned, to transfer information from data-dense to data-sparse areas. Therefore the concept of a century-long reanalysis is realistic and needs to be considered as a key goal for future reanalysis activities.

FURTHER READING

Gibson, **R.**, **P. Kållberg** & **S. Uppala**, 1996: The ECMWF Re-Analysis (ERA) Project. ECMWF *Newsletter No. 73*, 7–17.

Healy, **S.**, 2007: Operational assimilation of GPS radio occultation measurements at ECMWF. *ECMWF Newsletter No. 111*, 6–11.

Kelly, **G.** & **J.-N. Thépaut**, 2007: Evaluation of the impact of the space component of the Global Observing System through Observing System Experiments. *ECMWF Newsletter No. 113*, 16–28.

Simmons, **A.**, **S. Uppala**, **D. Dee** & **S. Kobayashi**, 2007: ERA-Interim: New ECMWF reanalysis products from 1989 onwards. *ECMWF Newsletter No. 110*, 25–25.

Simmons, **A.**, **S. Uppala** & **D. Dee**, 2007: Update on ERA-Interim. *ECMWF Newsletter No. 111*, 5.

Uppala, **S.**, **P. Kållberg**, **A. Hernandez**, **S. Saarinen**, **M. Fiorino**, **Xu Li**, **N. Sokka**, **U. Andrae** & **V. Bechtold**, 2004: ERA-40: ECMWF 45-year reanalysis of the global atmosphere and surface conditions 1957–2002. *ECMWF Newsletter No. 101*, 2–21.

ECMWF's contribution to AMMA

ANNA AGUSTÍ-PANAREDA, ANTON BELJAARS

THE AFRICAN Monsoon Multidisciplinary Analysis (AMMA) is an international project whose main focus is to improve the prediction of the West African Monsoon and its socio-economic impact on West African nations, as well as improving our understanding of fundamental scientific issues, such as the monsoon variability on diurnal, intra-seasonal, inter-annual and decadal scales.

Based on a French initiative, AMMA was built by an international scientific group and is currently funded by a large number of agencies, especially from France, UK, USA and Africa. It has been the beneficiary of a major financial contribution from the European Community's Sixth Framework Research Programme. This funding has allowed ECMWF to have a consultant to work full-time on the AMMA project. Detailed information on scientific coordination and funding is available on the AMMA International web site at:

www.amma-international.org.

Between 400 and 500 scientists from more than 25 countries, representing more than 140 agencies and institutions, are involved in AMMA. A network of African scientists linked to AMMA has been established to consolidate existing collaborations in Africa.

Purpose of AMMA and ECMWF's role

The West African Monsoon (WAM) provides most of the rainfall for West African countries, in particular those in the region of the Sahel with an agriculturally-based economy which is very much dependent on rain-fed crops. Sahel had long-lasting drought leading to widespread crop failure and famine in the 1980s and 1990s. Thus, predicting the rainfall season is crucial for farmers and aid planning. The WAM also encompasses very interesting meteorological phenomena. During the wet monsoon season the region has often been depicted as a natural laboratory for convection. About 40% of Atlantic tropical cyclones originate from mesoscale convective systems (MCS) embedded in synoptic-scale African Easterly Waves (AEWs). These MCS are also important for the troposphere-stratosphere exchange through deep convection.

The study of the complex interaction of all monsoon components on different spatial and time-scales (e.g. the continental Intertropical Convergence Zone (ITCZ), the African Easterly Jet (AEJ), the AEWs, the Saharan Air Layer (SAL), convection and land-surface processes) is one of the main scientific aims of AMMA. Other topics of interest are the important role of atmosphere and land-surface coupling and soil moisture, and the global impact of dust transport within the SAL and aerosols from biomass combustion. For more information on the aims and organization of the AMMA project see *Redelsperger et al.* (2006) and http://amma.mediasfrance.org/index.

Due to the complex physical interaction between different components of the WAM, and the lack of data available in the West African region, forecasting the WAM and precipitation in particular remains a challenge. This is reflected in systematic errors in the short-range, medium-range and seasonal forecasts. In order to improve our understanding and the forecast of the monsoon season it is important to have access to observations, in particular radiosonde observations which are currently the only means of providing comprehensive vertical thermodynamic and wind profiles in the troposphere. The poor status of the meteorological observing system in West Africa, due to lack of infrastructure and telecommunication problems, means that the number of observations that reach the Global Telecommunications System (GTS) is very low. This has a direct impact on the quality of the analyses and forecasts.

AMMA scientists have been working with operational agencies in Africa to reactivate silent radiosonde stations, renovate unreliable stations and install new stations in regions of particular climatic importance. During the AMMA field experiment in 2006 there was the monitoring of 26 stations (Figure 1). From those, 21 stations were active from June to September 2006 and some 7,000 soundings could be made (Figure 2). This represented the greatest density of radiosondes ever launched in the region; even greater than during GATE (GARP Atlantic Tropical Experiment) in 1974.

Our activities related to AMMA are strongly embedded in ECMWF's core activity of data assimilation and medium-range weather forecasting. Many people in various sections at ECMWF have directly or indirectly contributed. There is also a strong link with other partners in the AMMA project, not least because many partners make use of ECMWF analyses for their studies.

The main activities at ECMWF have been:

- Monitoring the radiosonde network in West Africa.
- Developing a radiosonde humidity bias correction scheme.
- Evaluating the medium-range forecasts for West Africa.
- Performing a special AMMA reanalysis and data impact studies.

There are also supporting activities such as:

- Placing real-time forecast plots for AMMA participants on the web, aimed at supporting forecasters in the West African region, in particular forecasters from the African Centre of Meteorological Application for Development (ACMAD) in Niamey, Niger.

Anna Agustí-Panareda is supported by the European Union project AMMA.

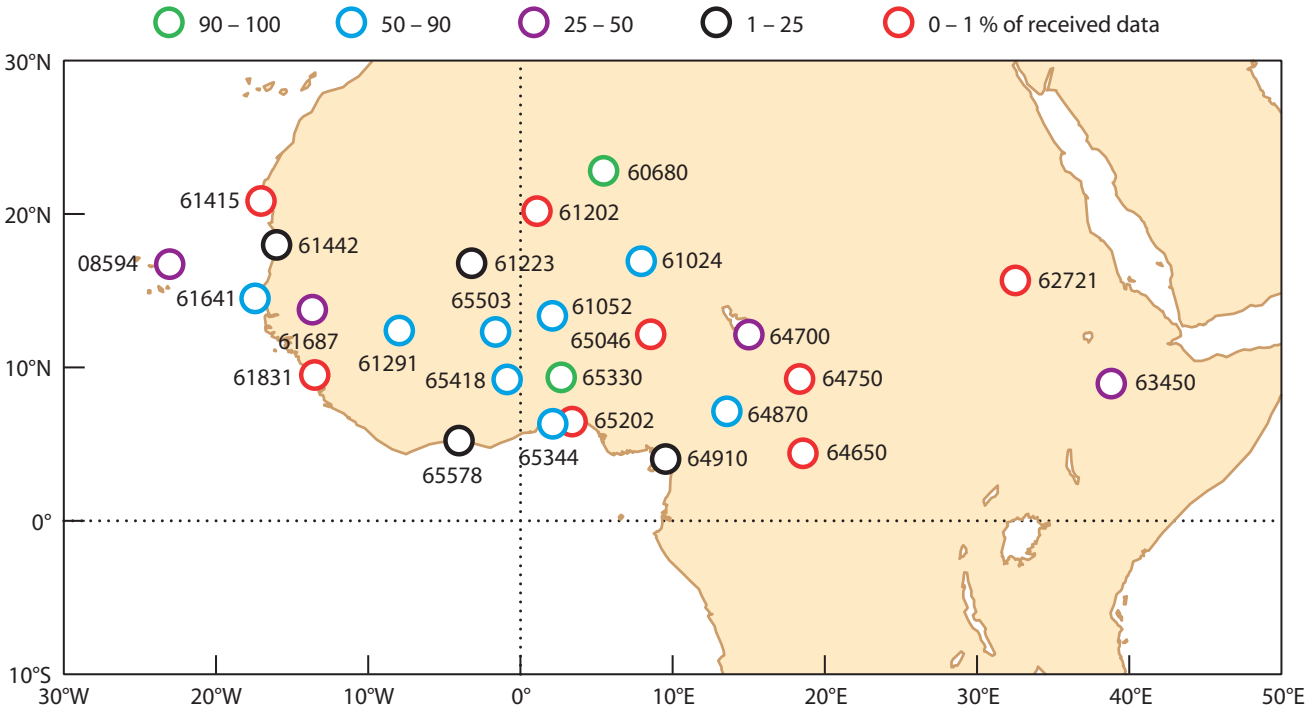

Figure 1 Radiosonde stations monitored in the AMMA project based on 700 hPa temperatures from the 00 and 12 UTC soundings for August 2006 which was during the AMMA Special Observing Period in 2006. Colours indicate the percentage of data received at ECMWF mainly via the GTS. Additional radisonde TEMP reports were also received via email.

- Providing model output to the AMMA Model Intercomparison Project (AMMA-MIP).

Finally, collaboration with other projects including ARM, THORPEX and ENSEMBLES has led to the exchange of valuable observations (e.g. ARM mobile facility and driftsondes) and model output from the seasonal forecast models.

Monitoring the radiosonde network in West Africa

Failure in data reception over Africa can be due to communication problems which can often be resolved if there is a timely report of reception failure. Thus, one of the most critical aspects of monitoring is to find out which stations are reporting to the GTS and which stations are not. At ECMWF, data reception from radiosondes is monitored by producing a monthly table with information on radiosonde TEMP messages received each day. All the monthly tables from January 2005 onwards are available on the website at:

www.ecmwf.int/amma/d/ammatab.

From March 2006, alarm bells and summaries of the data reception have been issued by email to the radiosonde core group responsible for contacting the relevant station operators. There are three types of emails: daily check, three-day check and weekly summary.

- **Daily check**. This is an alarm bell issued when more than half of the stations considered to be reliable are not reporting. In that case, it is likely that the reception failure is due to a general communication problem in the GTS hub.
- **Three-day check**. This is an alarm bell for individual stations that have not reported for more than three days, indicating a possible local problem with a particular station.
- **Weekly check**. This contains information on the number of soundings received, planned and missing, as well as the percentage of success in data reception.

The monitoring tables can help to assess (a) the continuity of radiosonde datasets, (b) the frequency of soundings and (c) whether the complete information on the soundings has been received. In the pre-AMMA period most stations were only launching one sound-

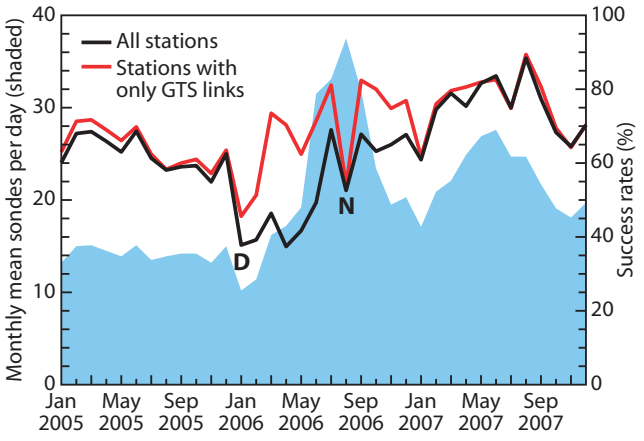

Figure 2 Shaded area: Numbers of soundings (monthly mean sondes per day) acquired operationally by ECMWF from the AMMA network from January 2005 to November 2007. Black line: Percentage success rate of data reception for the 21 primary stations in the network. Red line: Percentage success rate excluding the 4 stations with no direct GTS link that used satellite and email transmission. 'D' identifies the effects of a GTS failure at Dakar, while 'N' denotes lightning damage at Niamey which interrupted transmission for several stations (from *Parker et al.*, 2008).

ing per day, but during the AMMA period most stations had two soundings per day and a subset of stations had four soundings per day. During 20–29 June 2006 and 1–15 August 2006 the frequency of soundings increased to 8 per day at 6 stations along a north-south transect from the Guinea coast to the desert. Details of the AMMA effort on the radiosonde network in West Africa are presented in *Parker et al.* (2008).

The quality of the data was assessed by computing statistics of departures between the observations with respect to the model short-range forecast and the model analysis. Tephigrams and monthly vertical statistics are available in near real time for all 21 AMMA radiosonde stations (see www.ecmwf.int/products/forecasts/d/charts/monitoring/amma/). The monitoring of the departures between observations and model shows the following.

- There is up to 20% negative bias in the relative humidity between the observations and the first guess during the monsoon season over the Sahel below 700 hPa. This is partly due to a dry bias in the Vaisala RS80 radiosondes and partly due to an overestimation of model relative humidity. The statistics for MODEM radiosondes also show a dry bias at low-levels, as well as a larger moist bias around 500 hPa.
- The winds at the level of the African Easterly Jet (AEJ), which is at about 700 hPa, tend to deviate anticlockwise by 20° in the model first guess during the monsoon season in the Sahel. On average during August the AEJ is oriented from east to west in the observations, which means the 700 hPa winds in the ECMWF model tend to have a stronger northerly component than the observations over the Sahel.
- Stations launching balloons to only measure wind profiles produce very noisy soundings, many reporting data at very few levels. Therefore, many such stations in northwest Africa have been blacklisted.

Radiosonde humidity bias correction in the AMMA region

Almost half of the radiosondes assimilated were Vaisala RS80 which are known to have a substantial dry bias at both lower and upper troposphere (*Wang et al.*, 2002). This is an important issue as dry radiosonde humidity bias can have a detrimental impact on NWP models, in particular on cloud cover and precipitation (*Lorenc et al.*, 1996). The dry bias also affects the ECMWF analysis increments of specific humidity which are negative around radiosonde stations. This could lead to the southward shift of the ITCZ over Africa in the ECMWF short-range forecast which has too little precipitation over the Sahel. All this has motivated the development and application of a radiosonde humidity bias correction.

Four main types of radiosondes were used operationally during the AMMA field experiment with six different WMO code types: Vaisala RS80 and RS92, VIZ and MODEMs. From the 21 radiosonde stations that were active from May to September 2006, 9 of them used Vaisala RS80 sondes, 3 used a mixture of Vaisala RS80 and RS92, 3 used Vaisala RS92, 5 used MODEM sondes and 1 used VIZ sondes.

Creating the new humidity bias correction scheme

Previous studies have used a variety of empirically and physically-based methods of radiosonde humidity bias correction for specific radiosonde sensor types using independent reference data from research instruments during field and laboratory experiments. We have developed an empirically-based method that can work operationally and globally for any radiosonde type by using the ECMWF short-range forecast as an intermediary dataset for computing biases. The main reasons for developing a new correction scheme operationally and for the future AMMA reanalysis are:

- Many radiosonde types have been used in the AMMA field experiment and not all of them are well documented.
- Operationally not all the additional metadata required to apply the existing humidity bias correction schemes is available.
- ECMWF analyses compare well with independent Total Column Water Vapour (TCWV) derived from Global Positioning System (GPS) data (*Bock et al.*, 2007).

The bias correction coefficients are based on the difference between the bias of the sonde type to be corrected and the bias of a reference sonde at nighttime. Such a scheme has been recently implemented operationally to correct the radiosonde humidity and temperature bias in ECMWF IFS cycle 32r3 (see *Bechtold et al.*, 2008). The scheme is developed further for the West African region in view of the future AMMA reanalysis by considering the dependency of the humidity bias on the value of the observed humidity. Previous studies have shown that humidity biases associated with radiosonde observations depend on the observed relative humidity (RH), as well as sonde type, solar elevation, temperature, age of radiosonde and pressure. Over the Sahel, the variation of RH bias with the observed RH is particularly strong due to the pronounced seasonal cycle. Scatter plots of short-range forecasts – used as first guess in the data assimilation – versus observed values also reveal that the RH bias varies with observed values as shown in Figure 3(a). Thus, this refined bias correction is computed for all sonde types used in the AMMA field experiment within the geographical area from 5°S to 35°N and 25°W to 40°E using data from January 2005 to July 2007.

Relative humidity biases vary with sonde type, solar elevation and pressure level. Thus, the humidity bias for each of these categories is computed separately. In order to compute the bias we have adopted the technique of equiprobability transform also known as Cumulative Distribution Function (CDF) matching. The observed RH is transformed from its original CDF to another CDF which here is given by the model short-range forecast of RH. The bias is thus found by plotting quantile-quantile (QQ) plots obtained by matching the

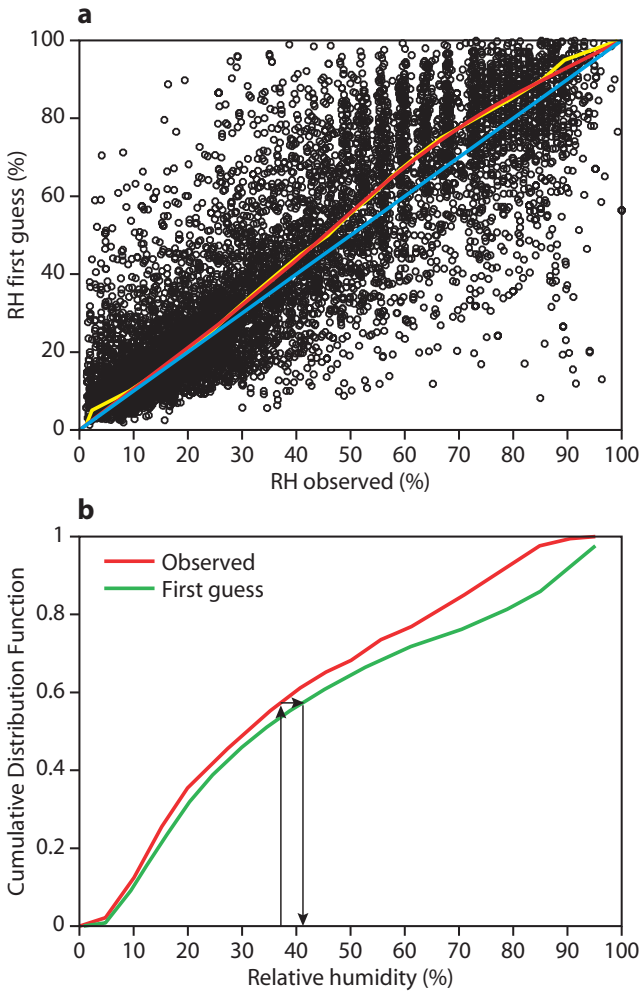

Figure 3 (a) Scatter plot of first guess versus observed relative humidity (%) for Vaisala RS80 Digicora I, II radiosondes at 925 hPa and for positive solar elevations. The coloured curves show the identity line (blue), the bias obtained from Cumulative Distribution Function (CDF) matching (yellow) and the best fit using four sine waves (red). (b) Cumulative distribution function for observations (red) and first guess (green). Arrows illustrate the CDF matching technique described in the text.

CDF of the observations and CDF of the model first guess. Figure 3(b) illustrates this. The bias correction is computed by subtracting the bias function of the reference sonde from the bias function associated with the observed sounding. The reference sonde used is the Vaisala RS92 at night-time, i.e. the same as in the operational radiosonde bias correction scheme. Vaisala RS92 sondes are one of the most accurate operational radiosondes and are now widely used.

Evaluating the new humidity bias correction scheme

In order to evaluate the new radiosonde bias correction scheme, two analysis experiments at resolution T511 (~40 km) and 91 vertical levels have been performed using the ECMWF IFS Cy32r3.

- The control experiment has no humidity bias correction; it uses only the old temperature bias correction.
- The bias correction experiment has the new operational radiosonde temperature and humidity bias correction as well the new AMMA bias correction procedure.

Comparison of observation biases with respect to first guess and analysis for the two experiments with and without humidity bias correction are shown in Figure 4 for Vaisala RS80 sondes at Dakar. The observed RH bias with respect to the model is greatly reduced after applying the humidity bias correction. The negative analysis increments – shown by the difference between the dotted and solid lines – are also greatly reduced. Thus, the drying effect of the observed RH on the humidity analysis is much smaller. As expected, the bias correction generally reduces the bias at low-levels more than at upper-levels, due to the upper-level dry bias associated with Vaisala RS92 at night-time which is not corrected here. The impact of radiosonde RH bias correction on NWP analysis and forecast is also significant.

By reducing the dry bias of the AMMA radiosonde stations, the TCWV in the analysis increases by between 1 and 4 kg m^{-2} (Figure 5). The increase in moisture is mainly located around the Vaisala RS80 stations. These stations are in the vicinity of the steep meridional moisture gradient over the northern Sahel region. Thus, the dry bias can also have an impact on the location and magnitude of this gradient. The humidity bias correction has a larger impact on TCWV during daytime (12 UTC) when the dry bias associated with solar heating is largest. In particular, stations using MODEM radiosondes have an increase of moisture during daytime but not during night-time. This is because MODEMs have a dry bias at low-levels during the day and a moist bias at mid-levels during night-time.

A significant impact is also found on simulated infrared brightness temperatures from channel 10.8 μm derived from analysis fields from the two experiments (not shown).

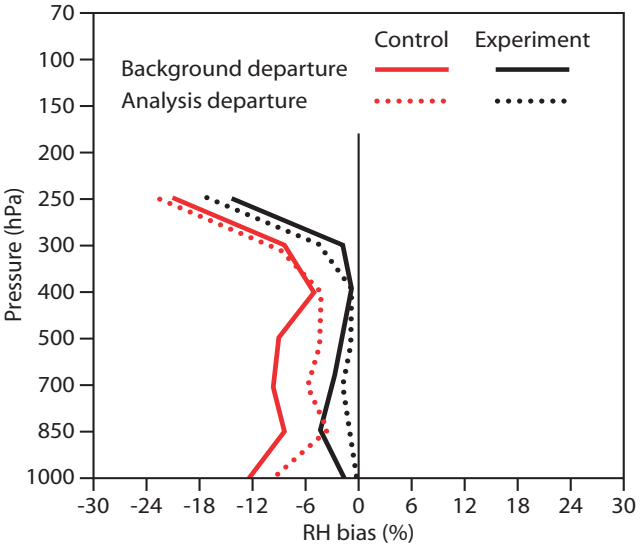

Figure 4 Bias of the relative humidity background departure (observations minus first guess, solid lines) and analysis departure (observations minus analysis, dotted lines) accumulated over July 2006 comparing the control experiment (red) and the radiosonde bias correction experiment (black) at Dakar radiosonde station (14.44°N, 17.30°W) using Vaisala RS80 radiosondes.

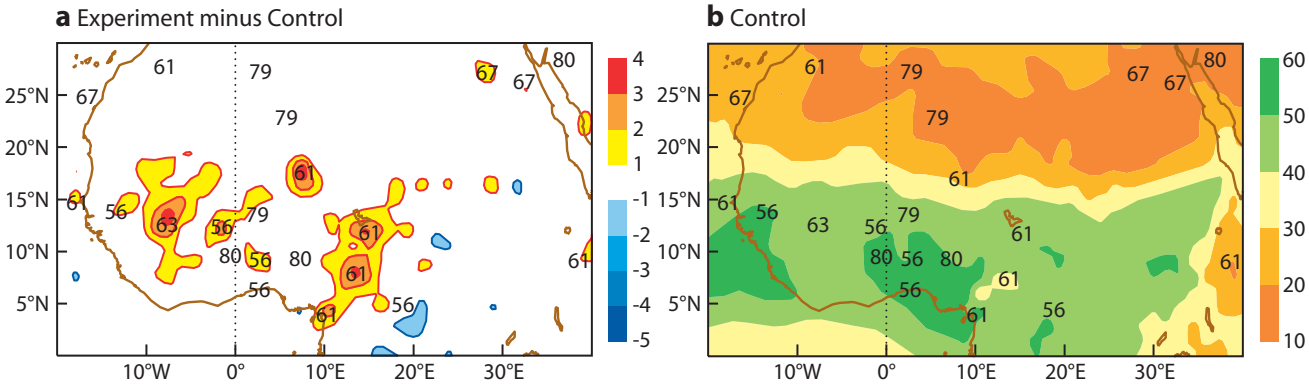

Figure 5 Mean total column water vapour (kg m^{-2}) from 14 to 23 July 2006 from analysis experiments: (a) Difference between radiosonde humidity bias correction experiment and control experiment at 12 UTC. (b) Control experiment at 12 UTC. Numbers depict the radiosonde type (61, 63 and 67 are Vaisala RS80; 79 and 80 are Vaisala RS92; 56 is MODEM; 49 is VIZ).

In the bias correction experiment there is an increase in cold cloud tops over the region of the Gulf of Guinea and Cameroon highlands, as well as an increase of lower-level clouds in the regions around N'Djamena (12.08°N, 15.02°E) and around Bamako (12.32°N and 7.57°E).

Figure 6 shows the impact on different diagnostics linked to convection for the model gridpoint nearest to Bamako. The humidity bias correction leads to a mean increase in Convective Available Potential Energy (CAPE) of 446.62 J kg^{-1} and a mean decrease in Convective Inhibition (CIN) of 25 J kg^{-1}. The impact of the humidity bias correction on CAPE and CIN is consistent with previous studies performed by correcting TOGA-COARE radiosonde data in the West Pacific warm pool.

In the areas around Bamako (12.32°N, 7.57°W) and N'Djamena (12.08°N, 15.02°E) there is also a precipitation increase of 2 mm/day in the short-range forecast (T+12 to T+36) in the bias correction experiment (not shown). Overall there is an increase in the precipitation over Sahel between 10°N and 15°N consistent with CAPE and CIN changes. However, the magnitude of the mean precipitation is still too low over this region in the forecast compared to the satellite-derived precipitation.

Evaluation of the medium-range forecast in West Africa

The onset of the West African monsoon is commonly defined as the shift in the band of precipitation and cloud associated with the ITCZ from the coast of Guinea (5°N) to around 10°N. This occurs sometime between end of June and beginning of July. Before the onset there is an intensification of the Saharan heat low at around 25°N and the establishment of the African Easterly Jet (AEJ) in the region around 15°N. Synoptic-scale African Easterly Waves (AEWs) develop through barotropic and baroclinic instabilities associated with the AEJ. The AEWs provide forcing for the development of Mesoscale Convective Systems. These four key components of the West African monsoon have been evaluated in the medium-range weather forecast using IFS cycles Cy30r1 (up to 11 September 2006) and Cy31r1 (from 12 September 2006) which were operational during the monsoon season in 2006. Forecasts at day 1 and day 5 illustrate the problems with the short-range and medium-range respectively. In IFS Cy30r1 and Cy31r1 the radiosonde humidity bias was not corrected.

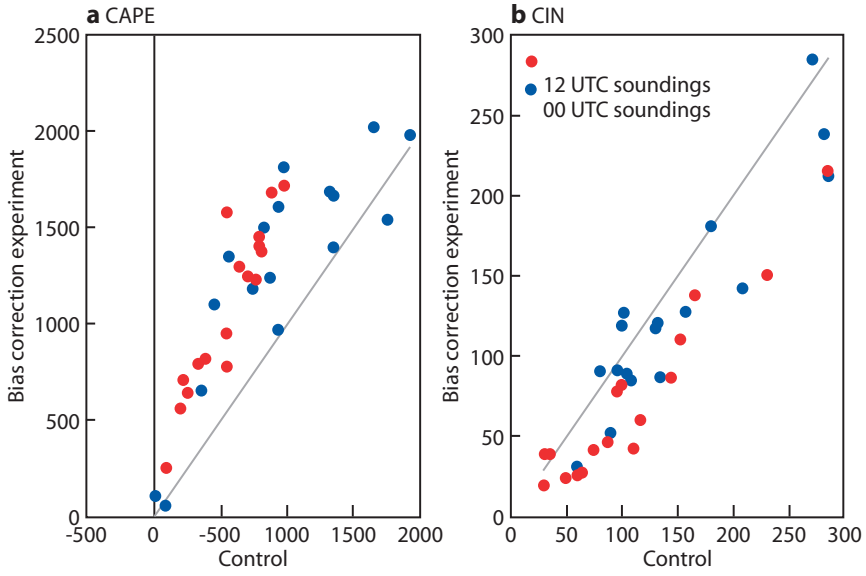

Figure 6 Scatterplots of (a) positive Convective Available Potential Energy (CAPE, J kg^{-1}) and (b) Convective Inhibition (CIN, J kg^{-1}) at Bamako (12.32°N, 7.57°W) from 2 to 18 July 2006 for the bias correction experiment versus the control experiment. Red dots depict 12 UTC soundings and blue dots 00 UTC soundings.

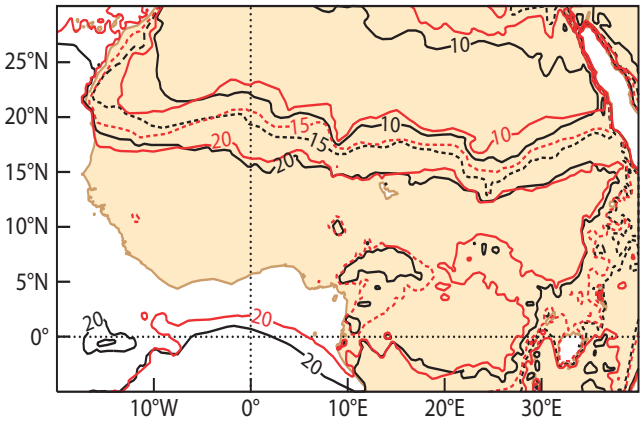

Figure 7 Mean 2-metre dew point temperature for August 2006 at 12 UTC from the analysis (black contours) and five-day forecast (red contours). Contours are plotted for 10°C, 15°C and 20°C to depict the intertropical front (ITF). Note that for forecasting purposes the location of the ITF is commonly defined by the 15°C contour (dash line).

Heat low

The heat low is the key driver to the advection of moisture inland by the low-level southwesterly monsoon flow just before the onset of the wet monsoon season. This results in the movement of the large-scale moisture and temperature gradient (also known as the intertropical front or ITF) to around 20°N. During the forecast the heat low tends to intensify, leading to a progressive strengthening of the monsoon low-level south-westerly flow in the forecast with respect to the analysis over land (north of 5°N) and a weakening over the ocean south of 5°N. As a result, the ITF tends to shift northwards (Figure 7). The gradient associated with the ITF is also weakened during the forecast as shown by the spreading of the 2-metre dew point temperature contours.

Intertropical Convergence Zone (ITCZ)

The mean precipitation band associated with the ITCZ in the short-range forecast during the peak of the monsoon season (August 2006) is located around 8°N whereas SYNOP stations indicate the maximum precipitation values are further north at around 12°N. This is confirmed by plotting a time series of an index for the latitude of the ITCZ for different forecast ranges. Figure 8 shows that the short-range forecast (e.g. day 1) is not able to shift the precipitation band from 5°N to 10°N during the monsoon onset. An apparent improvement with the forecast range (e.g. day 5) is due to the model drifting the ITCZ further north in association with the over-intensification of the heat low in the forecast.

African Easterly Jet (AEJ)

A simple index of the AEJ strength shows the decrease in the speed of the jet with forecast range (Figure 9). This is consistent with the weakening of the gradient associated with the ITF as shown in Figure 7.

African Easterly Waves (AEWs)

The AEWs have been evaluated in collaboration with the Met Office, Météo-France and NCEP (National Centers for Environmental Prediction) using diagnostics based on the curvature vorticity at 700 hPa. This effort has been coordinated by Gareth Berry and Chris Thorncroft from University of Albany. Curvature vorticity describes the vorticity associated with AEWs and shear vorticity that associated with the AEJ. Figure10 shows the propagation of the long-lived wave troughs as positive curvature vorticity anomalies in the operational ECMWF analysis. The analyses of the other meteorological centres compare well with the timing of wave troughs. The forecast accuracy with respect to analysis decreases rapidly at day 2 (Figure 11). The western region around 15°W has always a better forecast than the region around 15°E up to day 4. After day 3 the root mean square errors become as large as the magnitude of the 700 hPa curvature vorticity in the analysis, and thus, the forecast ceases to be useful. The rapid deterioration of the forecast of AEWs is probably linked to the lack of Mesoscale Convective Systems in the region during the forecast.

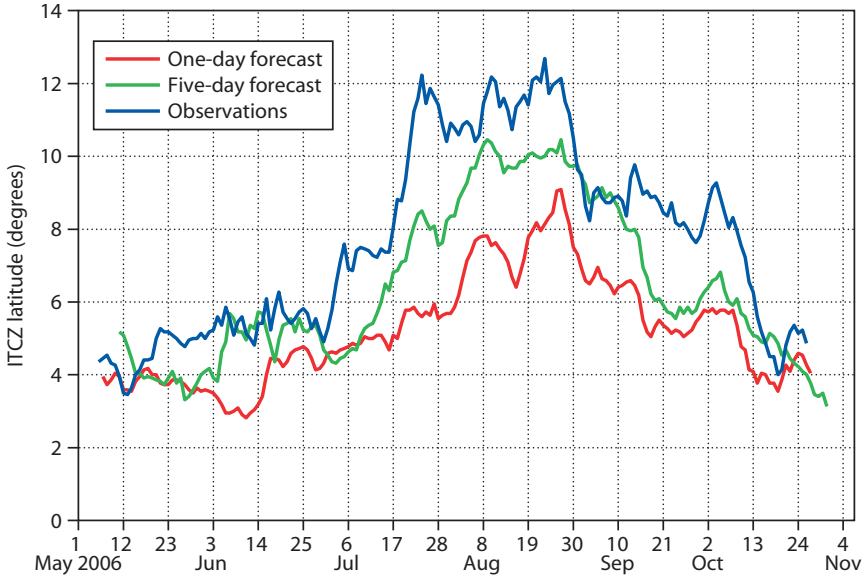

Figure 8 Time series of the ITCZ latitude computed as the latitude of the maximum zonally averaged precipitation between 10°W and 10°E for the one-day forecast, five-day forecast and observations based on the satellite estimated precipitation merged with raingauge data from the Famine Early Warning System (*Courtesy of CPC, NCEP, NOAA*).

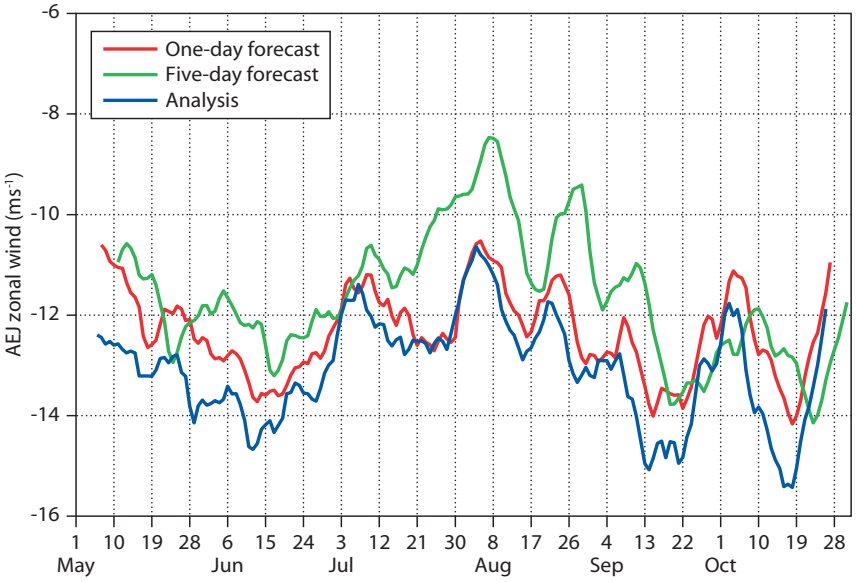

Figure 9 Time series of the zonal wind associated with the AEJ for the one-day forecast, five-day forecast and analysis. The AEJ zonal wind is computed as the maximum zonally averaged easterly zonal wind at 700 hPa between 10°W and 10°E.

These are very important in triggering the AEWs in the eastern region and modulating their lifecycle.

These errors reported in IFS Cy30r1 and Cy31r1 also affected the operational forecasts in 2007 with Cy32r2. However, a significant improvement occurred in the systematic error of the ITCZ location with cycle Cy32r3. This new cycle, which is currently operational, features an improved precipitation forecast in the short-range over the tropics (see *Bechtold et al.*, 2008) and in particular over West Africa where the mean precipitation band associated with the ITCZ is shifted northward by approximately 1 degree.

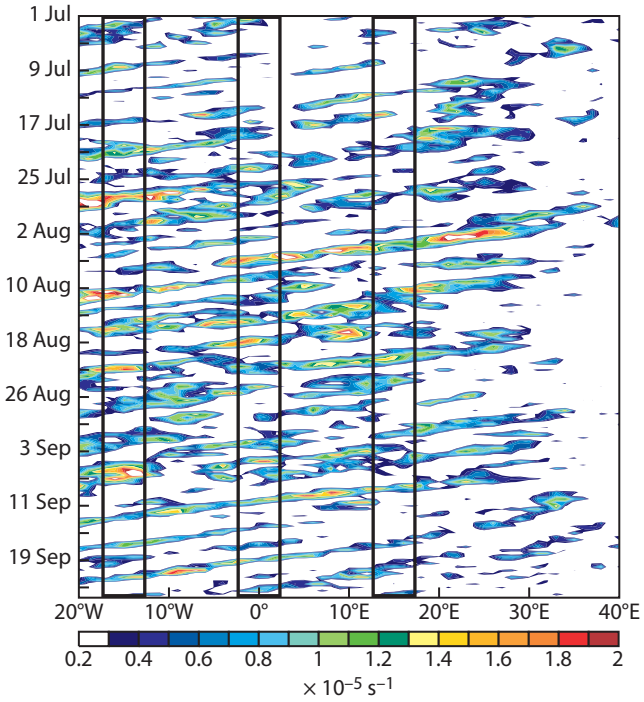

Figure 10 Hovmöller longitude-time diagram of curvature vorticity at 700 hPa from analyses averaged within a band between 5°N to 15°N showing synoptic African easterly wave activity from 1 July to 25 September 2007. For clarity only positive values are shown which depict the trough of the waves. The boxes around 15°W, 0°E and 15°E with a 5° width depict the different longitude bands for which the RMS error has been computed in Figure 11.

The AMMA reanalysis

The AMMA project has dedicated a large effort to enhance the West African radiosonde network in 2006 with special observing periods (SOPs) covering the different phases of the wet monsoon. This effort has been hampered by persistent communication problems, which resulted in valuable radiosonde data not reaching the GTS. Consequently this missing data was not included in the operational analysis at ECMWF as well as other operational centres. Even the data that reached the GTS very often contained many missing values due to problems encountered during the automatic encoding process. In addition to radiosonde data, many dropsondes were deployed from research aircrafts and gondolas during the SOPs which could not be used in the analysis either. Therefore, it was recognised by the AMMA community that a special AMMA reanalysis was necessary to include this unique dataset in a region which generally suffers from data scarcity.

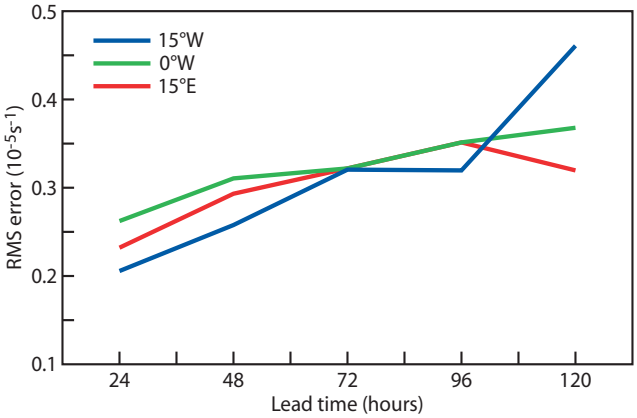

Figure 11 Root mean square errors of 700 hPa curvature vorticity from forecast at different ranges with respect to analysis for the three boxes indicated in Figure 10.

Another advantage of performing a reanalysis is the availability of a new IFS cycle (Cy32r3) with improved physics and a new radiosonde temperature and humidity bias correction scheme (see *Bechtold et al.*, 2008). Given the improvement to the systematic error that affects the short-range precipitation forecast over West Africa, Cy32r3 is particularly well-suited for the AMMA reanalysis. The reanalysis is currently running with T511 resolution and 91 vertical levels and it will span the wet monsoon period from 1 May to 30 September 2006. The humidity radiosonde bias correction developed for the AMMA radiosonde data described earlier in this article is also applied to the reanalysis.

In the reanalysis all the sounding data collected in the AMMA database are used. Details are given in Box A.

In order to test the impact of the extra AMMA soundings, a control experiment will be run with a data-poor scenario for the month of August (i.e. the month with more observations) using the same IFS cycle and resolution as the AMMA reanalysis. In this control experiment, only the radiosonde stations that were reporting reliably in 2005 will be used (i.e. pre-AMMA scenario).

Summary of progress, further activities and plans for the future

Evaluation of the short-range forecast shows a systematic error in the location of the main precipitation band associated with the ITCZ over continental West Africa by approximately 4° to the south during the wet monsoon period. An improvement of this systematic error has been detected with the changes in the vertical diffusion, convection parameterizations, hydrology as well as the radiosonde humidity bias correction introduced in IFS Cy32r3. This has been further improved by developing a refined radiosonde humidity bias correction for the West Africa region which takes into account the variation of the radiosonde humidity bias with the observed humidity.

Results from analysis experiments show how the correction of radiosonde humidity bias is particularly important in the West African region due to its impact on the development of convection. This new radiosonde humidity bias correction for the AMMA region is applied using IFS Cy32r3 in the AMMA reanalysis for the 2006 West African wet monsoon season during the AMMA observational campaign. This is expected to benefit a wide number of AMMA-related studies that make use of the reanalysis, in particular those focusing on the water cycle.

Another important advance for the West African region is the development of new seasonal products at ECMWF. These products provide information on probability distribution of rainfall and near surface temperature anomalies over the West African region. PRESAO, a Regional Climate Outlook Forum activity dedicated to West Africa and coordinated by ACMAD, makes regular use of those products. Monsoon indices, based on the large-scale distribution of observed rainfall anomalies, have been recently developed for both the West African and South Asian regions. The forecast skill of those indices has been estimated by looking at the seasonal forecast performance in the past 25 years and is available on the web at:

www.ecmwf.int/products/forecasts/d/charts/seasonal/forecast/seasonal_range_forecast/group

Although model errors affect the rainfall variability over the tropical lands, with the monsoon indices the predictive skill over land can be improved by exploiting teleconnections with adjacent ocean regions.

Despite significant improvements in the systematic error of precipitation over West Africa, there is still a lack of convection over the Sahel in the model. Comparison of high-resolution radiosonde data and model analysis/forecast at Niamey (Niger) show significant differences in the boundary layer moisture distribution which are likely due to the mixing being too strong in the model boundary layer. This issue is currently being investigated by the Physical Aspects Section at ECMWF. Other ongoing work to improve the medium-range and seasonal forecasts also includes the use of a better representation of land surface initial conditions, specially in

Box A

Sounding data collected in the AMMA database

The sounding data collected in the AMMA database includes:

- 6,063 high resolution radiosondes/dropsondes collected from 21 stations, 3 research vessels and 2 research aircrafts. These have been thinned from about 2,500 to approximately 300 vertical levels.
- Radiosondes launched from operational stations, research stations and research vessels obtained via the GTS. The radiosonde data from West Africa typically contains 70 to 100 levels. These data are only used when there is no corresponding high-resolution data available.
- 101 dropsondes from research aircrafts obtained via the GTS.
- 110 dropsondes from gondolas, also known as driftsondes.
- 7,317 pilot balloons that only measure wind profiles obtained via the GTS.

The development and deployment of the driftsonde system was a collaborative effort between the Earth Observing Laboratory (EOL/NCAR) and the French Space Agency (CNES) as part of the SOP3 period to investigate the development of tropical cyclogenesis downstream of Africa. It is the first time they will be assimilated in an analysis experiment. Preliminary comparisons with operational analysis show a good agreement.

terms of soil moisture obtained from off-line land surface models using observed precipitation and radiation forcing and from remote sensing (see the news item about the SMOS project on page 5 of this edition of the *ECMWF Newsletter*). In addition it is expected that the assimilation of more satellite data (e.g. TRMM or SSM/I microwave brightness temperatures sensitive to clouds and precipitation) might improve the quality of moisture analyses and precipitation forecasts.

The success of the work done at ECMWF on the AMMA project strongly relies on external collaboration with many AMMA partners.

- Collaboration with Jean-Blaise Ngamini from ASECNA, Doug Parker from University of Leeds and Adreas Fink from University of Cologne on the radiosonde monitoring has been invaluable.
- The visit of André Kamga from ACMAD in 2006 provided advice on model evaluation and the development of forecast products for West Africa.
- The development of the AMMA radiosonde bias correction and model evaluation has benefited from discussions and exchange of diagnostics, data and information with Mathieu Nuret, Françoise Guichard and Jean-Philippe Lafore from Météo-France.
- The verification of the AMMA radiosonde humidity bias correction method performed in the reanalysis is currently in progress using GPS which provides a fully independent observational dataset of TCWV. The comparison of GPS/model TCWV is being performed by Olivier Bock from IPSL.
- Collaboration with Dave Parsons, Junghong Wang and Kate Young from NCAR on the use of driftsonde data has also made possible the use of a new type of dataset in the AMMA reanalysis.

The commitment and expertise of the wide variety of collaborators has helped ensure the success of the project. Also this collaboration has laid the foundation for further developments which will bring benefits to the people of West Africa and the wider meteorological community.

FURTHER READING

Bechtold, P., M. Köhler, T. Jung, M. Leutbecher, M. Rodwell & F. Vitart, 2008: Advances in simulating atmospheric variability with IFS cycle 32r3. *ECMWF Newsletter No. 114*, 29–38.

Bock, O., M.-N. Bouin, A. Walpersdorf, J.-P. Lafore, S. Janicot, F. Guichard & A. Agustí-Panareda, 2007: Comparison of ground-based GPS precipitable water vapour to independent observations and NWP model reanalyses over Africa. *Q. J. R. Meteorol. Soc.*, **133**, 2022–2027.

Lorenc, A.C., D. Barker, R.S. Bell, B. Macpherson & A.J. Maycock, 1996: On the use of radiosonde humidity observations in mid-latitude NWP. *Meteorol. Atmos. Phys.*, **60**, 3–17.

Parker, D.J., A. Fink, S. Janicot, J.-B. Ngamini, M. Douglas, E. Afiesimama, A. Agustí-Panareda, A. Beljaars, F. Dide, A. Diedhiou, T. Lebel, J. Polcher, J.-L. Redelsperger, C. Thorncroft & G.A. Wilson, 2008: The AMMA radiosonde programme and its implications for the future of atmospheric monitoring over Africa. *Bull. Am. Meteorol. Soc.* (in press).

Redelsperger, J.-L., C.D. Thorncroft, A. Diedhiou, T. Lebel, D.J. Parker & J. Polcher, 2006: African Monsoon Multidisciplinary Analysis: An international research project and field campaign. *Bull. Am. Meteorol. Soc.*, **87**, 1739–1746.

Wang, J., H.L., Cole, D.J. Carlson, E.R. Miller & K. Beierle, 2002: Corrections of humidity measurement error from the Vaisala RS80 radiosonde – application to TOGA-COARE data. *J. Atmos. Oceanic Technol.*, **19**, 981–1002.

Coupled ocean-atmosphere medium-range forecasts: the MERSEA experience

ALBERTO TROCCOLI, DAVID ANDERSON, KRISTIAN MOGENSEN, GERALD VAN DER GRIJN, NICOLAS FERRY, GILLES GARRIC

IT IS common practice at ECMWF, and other weather forecasting centres, to use atmospheric models with fixed boundary conditions over the ocean to produce medium-range weather forecasts. Yet there is evidence that the atmosphere can, on occasion, substantially affect the sea surface temperature (SST), and that SST changes could possibly influence the atmosphere. Here we investigate the impact of allowing the SST to evolve throughout the forecast, rather than using fixed SST, by using an ocean model coupled to the atmospheric model. In order to allow maximum interaction between the two media, we will use an ocean model at a resolution comparable to or better than that of the atmospheric model.

Particular attention is given to assessing the impact of using a coupled atmosphere-ocean model on forecasts of tropical cyclones as these are likely to be influenced by an evolving SST. Integrations at such high resolutions are computationally extremely demanding and so only a limited number of cases has been considered.

Although the work was primarily a proof of concept, we obtained some interesting results. The influence of the two selected tropical cyclones on the ocean is well

AFFILIATIONS

Alberto Troccoli*, **David Anderson**, **Kristian Mogensen**, **Gerald Van der Grijn**, ECMWF, Reading, UK

Nicolas Ferry, **Gilles Garric**, Mercator Océan, Toulouse, France

* Supported by the European Union project MERSEA (AIP3-CT-2003-502885)

reproduced, with a realistic evolution of the cool trail of SST in the wake of the cyclones. There is certainly scope for improving the interaction between the atmospheric model and its lower boundary, and a few pointers for further investigation have been suggested. Overall, we show how the coupling of a high-resolution ocean model to a weather-forecasting atmospheric model can be beneficial to features such as SST evolution and possibly cyclone tracks even at relatively short timescales.

It is worth noting that coupling the operational atmospheric model used for the medium-range forecasts to an ocean model from day zero is an objective of the ECMWF 10-year strategy (2006–2015). The present study offers a contribution towards this goal.

This work was carried out under the EU project MERSEA (www.mersea.eu.org), the main objective of which is to provide an integrated service of global and regional ocean monitoring and forecasting to intermediate users and policy makers. Such services would support safe and efficient offshore activities, environmental management, security, and sustainable use of marine resources.

Description of the medium-range coupled forecast system

The coupled model used for the medium-range forecast experiments consists of two main configurations, which differ from each other in the resolution of the atmospheric model. Both use the atmospheric model of the ECMWF Integrated Forecast System (IFS) at Cy31r1. The resolutions are:

- T399 (~50 km horizontal resolution), 62 vertical levels, for the Ensemble Prediction System (EPS) integrations.
- T799 (~25 km horizontal resolution), 91 vertical levels, for the deterministic integrations.

These resolutions match those of the operational EPS and deterministic systems.

The ocean general circulation model is OPA/NEMO version 9.0, ORCA025 grid (¼° horizontal resolution), with 50 vertical levels. Coupling between the ocean and the atmosphere is via the OASIS coupler (version 3) and carried out every hour: the atmosphere is driven by SST and sea-ice, with the ocean being driven by heat, momentum and moisture fluxes. Solar radiation, needed to calculate the effect of penetrative radiation within the upper layers of the ocean, is passed separately from the other heat fluxes.

The ECMWF global wave model (WAM cycle 4) on a 0.5° regular grid with wave spectral resolution of 30 frequencies and 24 directions is also coupled to the atmospheric component. Although it does not interact directly with the ocean model, it influences the stress used to drive the ocean model through the Charnock parameter. It is worth noting that the use of such a high-resolution coupled model with comparable resolution in the atmosphere and ocean required extensive technical work. The ocean analyses are provided by Mercator Océan (*Drevillon et al.*, 2007).

Because the atmospheric model cycle used in these experiments is slightly different to the one used operationally in February 2007, additional uncoupled experiments using the same atmospheric configuration as in the coupled model have also been run. This allowed a clean comparison of forecasts made using coupled versus uncoupled models. The current operational EPS consists of 51 ensemble members. For computational reasons, the ensemble size in the EPS experiments described here is restricted to 15. The ensemble members of the EPS differ from each other in their atmospheric initial conditions (by employing singular vectors) and the use of stochastic physics during the integrations. Unlike monthly and seasonal forecasts made with a coupled model, this investigation only needs a limited analysis period; a full reanalysis to calibrate the forecast results is not needed as the model drift should be small.

Case studies

The ocean analyses at a quarter degree resolution come from the MERSEA-1/4°v2 system. We have chosen case studies for two tropical cyclones in the Indian Ocean, FAVIO and GAMEDE. These are two of the strongest tropical storms in the Indian Ocean in 2007. Both occurred in the vicinity of La Réunion/Madagascar with FAVIO subsequently making a landfall in Mozambique.

- The first signs of what would become FAVIO were noticeable at around 12 February 2007, but the deepest low pressure was not attained until 21 February when it reached 930 hPa.
- GAMEDE developed around 20 February 2007, when FAVIO was still active, albeit about two thousand kilometres to the east. It peaked on 26 February with a core pressure of about 935 hPa.

Coupled forecasts starting from 14 February 2007 and 21 February 2007 have been performed.

It would have been interesting to consider the effect of ocean-atmosphere coupling on Atlantic hurricanes or Pacific typhoons and tropical cyclones, but this was not possible as the Mercator operational ocean analyses are only available for dates after 3 January 2007. Our work for the MERSEA project had to be completed before the summer of 2007, thus excluding the 2007 tropical cyclone season in the northern hemisphere.

Global sea surface temperature evolution

We first assess the evolution of the global SST in the deterministic case (T799/ORCA025) to evaluate the ability of the coupled model to reproduce the main features of the observed SST. Figure 1(a) shows the difference between the SST reproduced by the coupled model at day 5 and its initial condition (i.e. the SST at day 0) for 14 February 2007. When compared with the equivalent observed difference (Figure 1(b)), one can see that the main features are represented fairly well by the model. For example, the large-scale differences in the subtropics/mid-latitudes of the southern hemi-

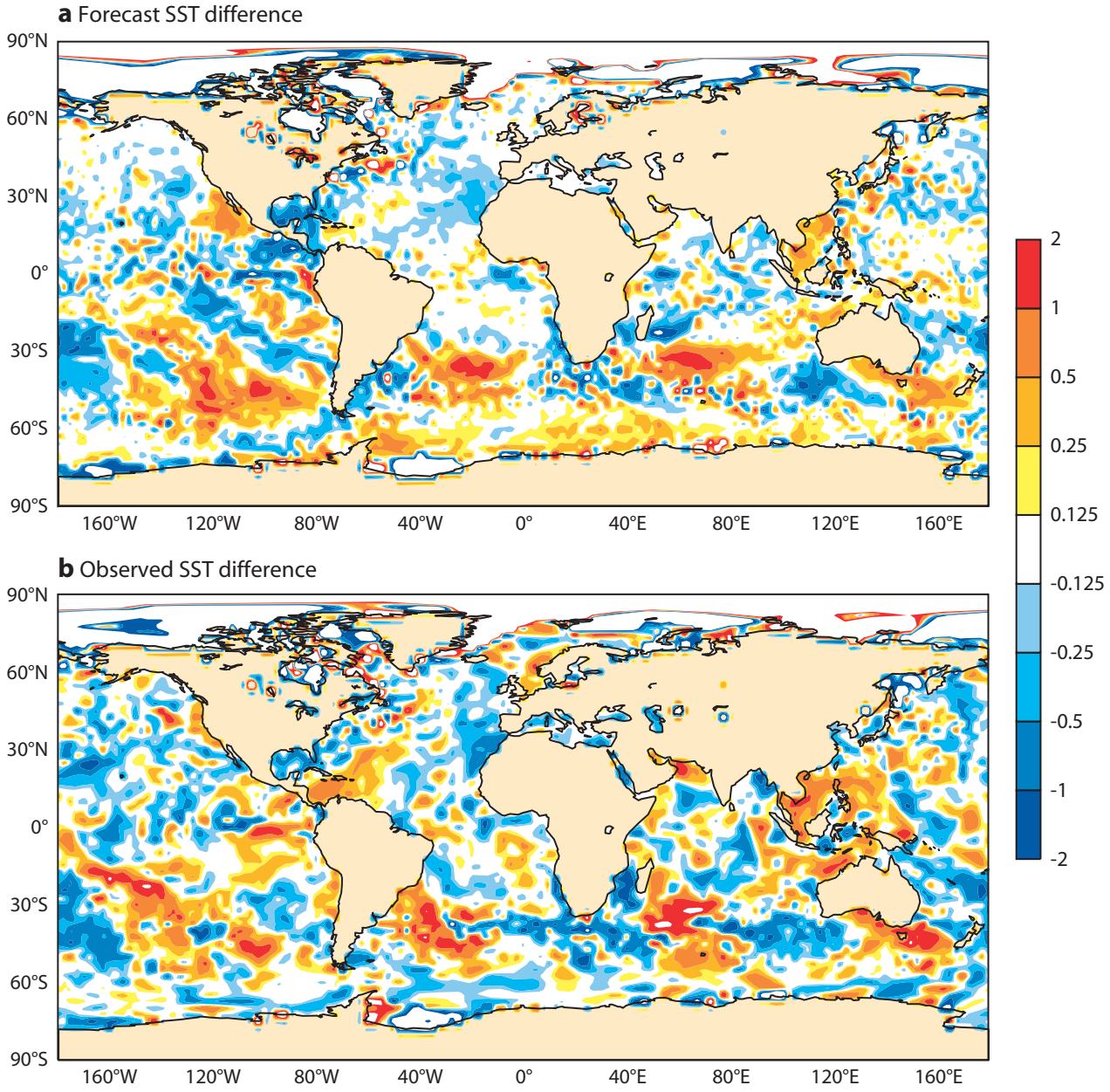

Figure 1 Sea surface temperature difference between day 5 and day 0 for (a) the coupled integration (ORCA025/T799) started on 14 February 2007 and (b) the Real Time Global (RTG) observations. SST differences range from –2 °C to 2 °C.

sphere in all three oceans and, more specifically, the large-scale positive difference between about 20°S and 60°S in the Pacific Ocean. The negative difference in the North Atlantic, east of Spain/North Africa, is also reproduced well, though the amplitude is not as large as that observed. Clearly not all the simulated features are satisfactorily reproduced but the results look promising when compared to the current approach of keeping the SST fixed throughout the forecast.

The SST analyses are themselves not without error. Comparison is later made with the OSTIA (Operational Sea Surface Temperature and Sea Ice Analysis) product which shows substantial differences from the Real Time Global (RTG) SST product used operationally at ECMWF (*Gemmill et al.*, 2007) as in Figure 1(b).

Tropical cyclones simulation using the deterministic model

The tracks of the two tropical cyclones we have chosen to study are shown in Figure 2 for FAVIO and GAMEDE. The colour of the dots represents the type of synoptic feature according to the World Meteorological Organization (WMO) convention (see the caption; note that this scale is different from the 5-grade Saffir Simpson scale). As can be seen from the plots, both FAVIO and GAMEDE reached hurricane strength. As remarked earlier, FAVIO just crossed the southern tip of Madagascar before making landfall over Mozambique.

The observed pressure values at the core of FAVIO and GAMEDE as a function of time are shown in Figure 3. The deepest pressure has been highlighted in black,

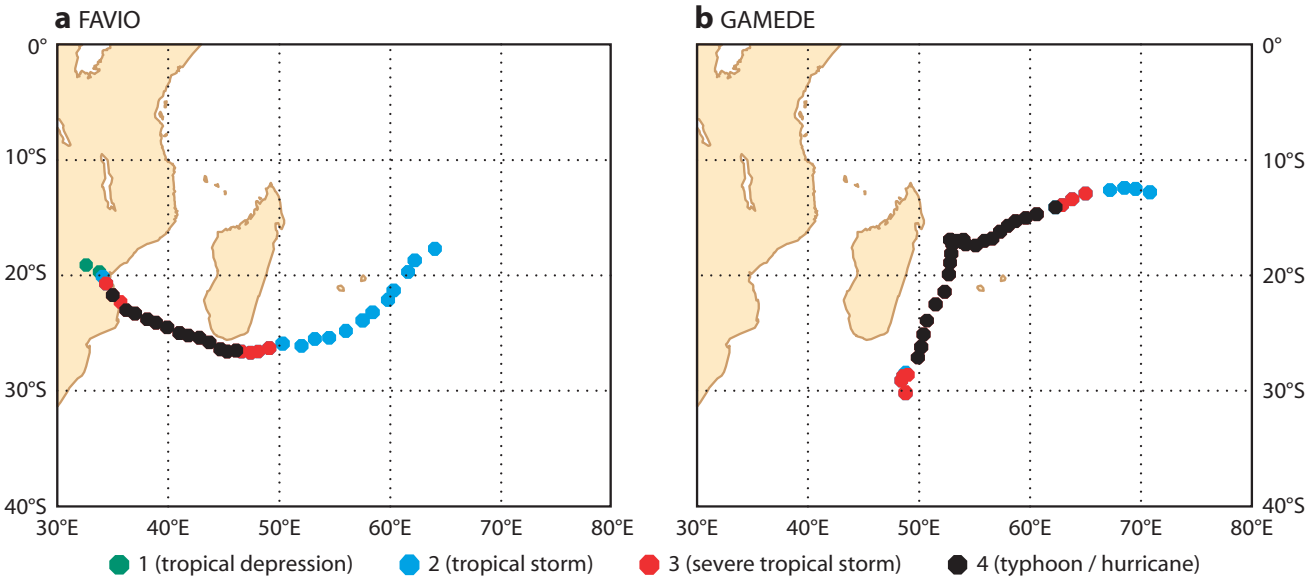

Figure 2 Observed track of tropical cyclones (a) FAVIO (15 to 23 February 2007) and (b) GAMEDE (21 February to 4 March 2007). The colour of the dots indicates the intensity of the cyclones based on 6-hourly observations: green = tropical depression, blue = tropical storm, red = severe tropical storm, black = typhoon/hurricane.

whereas the day 5 considered in this article is shown in red (for GAMEDE day 5 coincides with the day of the deepest core pressure).

Figure 4(a) shows the SST difference between day 5 and day 0 for the coupled simulation. The mean sea level pressure at day 5 is superimposed. Not only does the coupled model reproduce well tropical cyclone FAVIO with a 5-day lead time (see the low pressure off the coast of Madagascar), it also simulates the cool trail of the cyclone in what looks like a realistic way (i.e. the negative SST differences east of the cyclone core). Of particular interest is the cold wake to the east of FAVIO seen in Figure 4(a). This is not seen in the RTG SST analysis used operationally at ECMWF (Figure 4(d)), where the SSTs at day 5 are warmer than at day 0. However, in the delayed mode OSTIA high-resolution SST product (*Stark et al.*, 2007), a cold wake is clearly visible (Figure 5). The differences are smaller in the case of GAMEDE but it too shows a cold wake, well predicted by the coupled model (not shown).

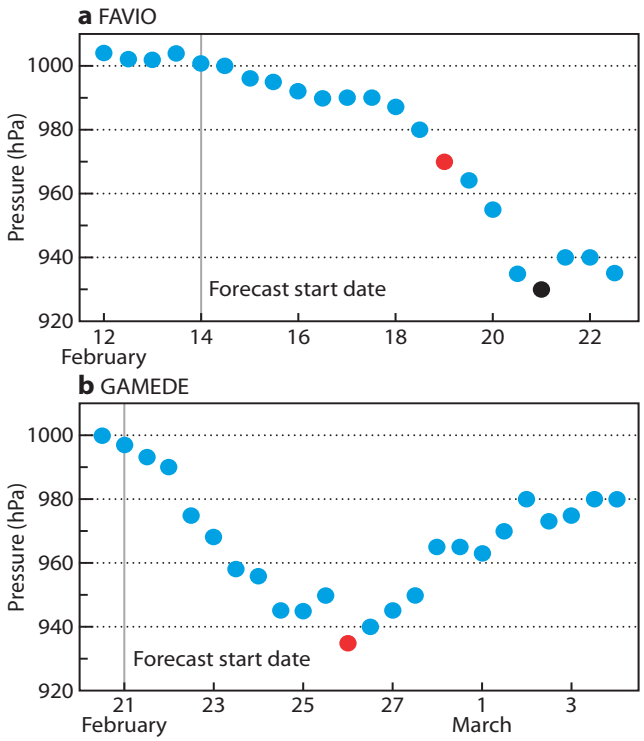

Figure 3 Time evolution of the observed core pressure for tropical cyclones (a) FAVIO and (b) GAMEDE. The red circle indicates the day 5 forecast lead-time whereas the black circle is the lowest recorded pressure (for GAMEDE red and black are superimposed).

The cold wake is not quite in the same position as in the model simulation because the tropical cyclone track is displaced slightly to the north. This is true of all forecasts shown in Figure 4: coupling has not had a significant impact on the cyclone track. The uncoupled (i.e. atmospheric-only) simulation is also able to reproduce the deep low pressure of FAVIO even if the SST remains unchanged throughout the integration. Similarly, the operational model captures well the low pressure (Figure 4(c)).

The analysis for 19 February in Figure 4(d), however, shows very little sign of the cyclone. This behaviour appears counter-intuitive as one would expect the analysis to be the closest to reality. The reason for the poor representation of the cyclone in the analysis is the broad structure functions used to produce the analysis. Other factors such as the wrong position of the cyclone in the first guess, due to shortage of data, and the low resolution used in the inner loops of the analysis may also contribute (*Isaksen & Janssen*, 2004). Nonetheless, the information of the presence of the cyclone in the circulation of the atmosphere is normally present in the three-dimensional analysis to some extent, which is why the forecasts are able to produce realistic cyclones.

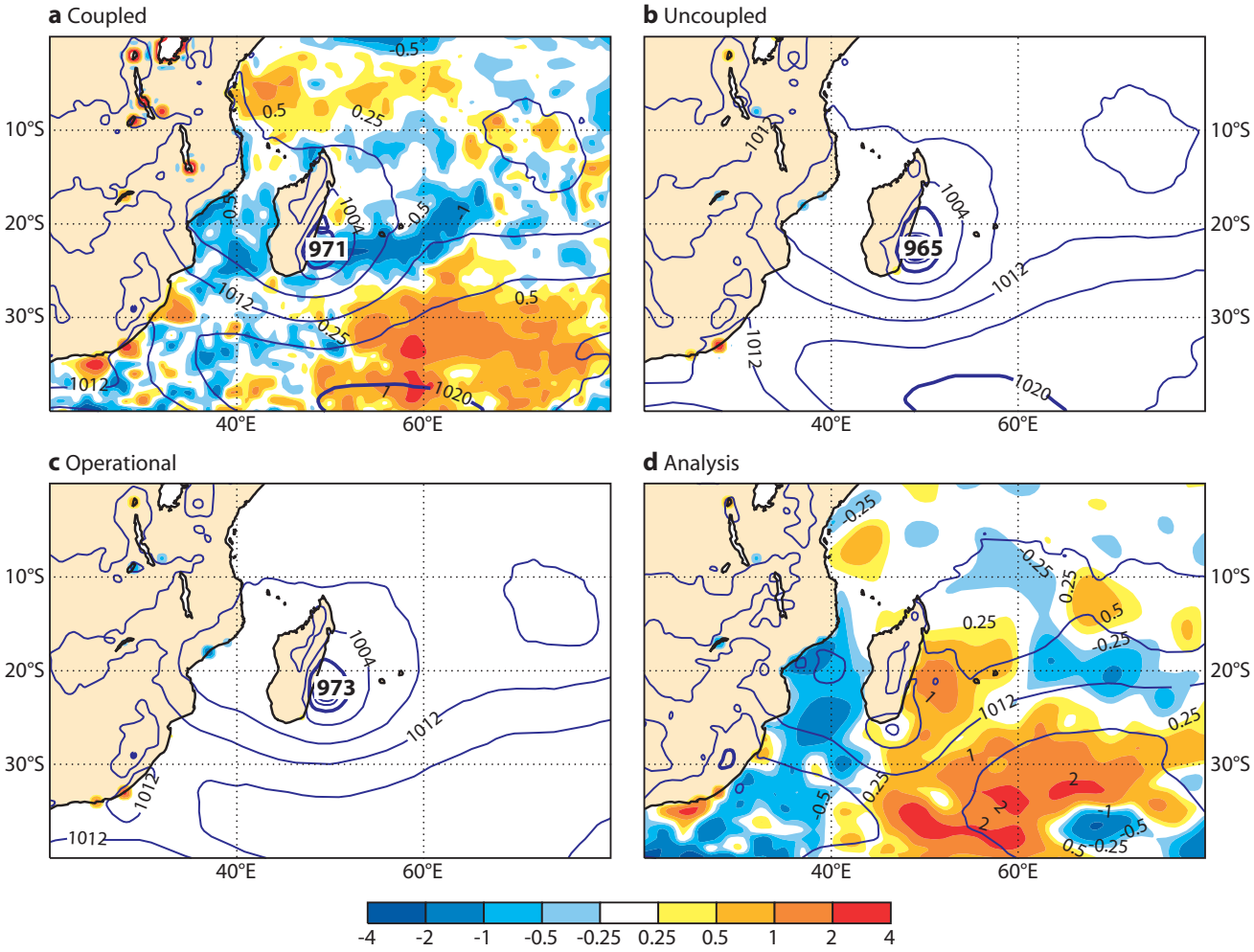

Figure 4 Sea surface temperature difference between day 5 and day 0 for (a) coupled integration (ORCA025/T799) starting on 14 February 2007 – the FAVIO case, (b) uncoupled integration, (c) operational ECMWF forecast (similar to the uncoupled but with a model version slightly different, and (d) ECMWF analysis at 00 UTC on 19 February 2007. SST differences range from –4°C to 4°C. The isobars of mean sea level pressure (MSLP) at day 5 are superimposed with a 4 hPa spacing. There is little evidence of the tropical cyclone in this analysis, probably as a result of the broad structure functions used in the analysis but also because the first guess cyclone may be in slightly wrong position due to shortage of data and because of the lower resolution (T255) of part of the analysis system (the inner loop).

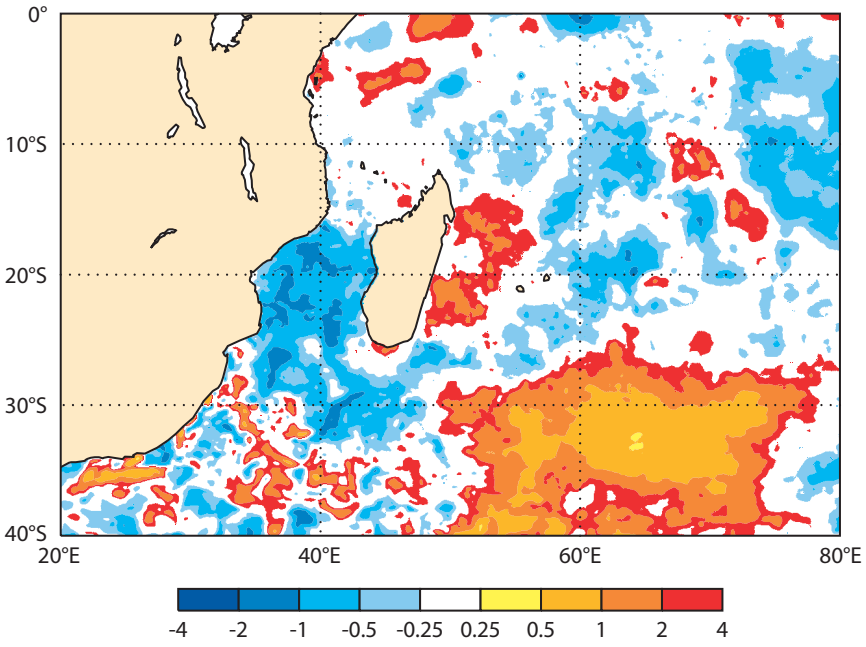

Figure 5 OSTIA high-resolution SST product for the difference between 19 February 2007 and 14 February 2007 (as in Figure 4(d)). Note the cooling along the cyclone track (c.f. Figure 2(a)).

The core pressure of FAVIO for 19 February 2007 for the four cases presented in Figure 4, as well as for the directly observed value, are shown in Table 1. As can be seen, all three forecasts are close to the observed value.

In the case of tropical cyclone GAMEDE the coupled simulation is also quite successful. In fact, the negative SST anomalies, resulting from the interaction between the cyclone and the ocean, are well reproduced (compare Figures 6(a) and 6(d)). The intensity of the cyclone is also reasonably well represented but, even if visually very intense, the core pressure does not reach the very low value observed of 935 hPa (see Table 1). However, given errors in the positioning and strength of the cyclone in the initial conditions, model imperfections and the limited (even if very high) resolution for cyclone simulations, the value of 966 hPa in the coupled integration is encouraging.

Both the uncoupled integrations reproduce well the low pressure of GAMEDE, with the uncoupled run shown in Figure 6(b) reaching a lower core pressure (961 hPa) than the (uncoupled) operational forecast in Figure 6(c) (967 hPa). The uncoupled (non-operational) run simulates in both cases a lower core pressure than the coupled case as will be confirmed with the EPS experiments later. The reason seems to be related to the lower SST in the coupled case. Thus, even if this is closer to the observed SST than in the uncoupled case, there seems to be some deficiency in the interaction between the atmosphere and the ocean, with the lower SST inhibiting growth in the model cyclone. The lower SST in the coupled case may well be the correct response; it is just that the cyclone is too weak in the uncoupled case and the coupling makes it weaker, as it should.

Experiment	Core pressure (hPa)	
	FAVIO	GAMEDE
Coupled (ORCA025/T799)	970	966
Uncoupled (T799)	968	961
Operational (T799)	972	967
Analysis	1004	963
Observed	970	935

Table 1 Core pressure of FAVIO at 00:00 UTC on 19 February 2007 and GAMEDE at 00:00 UTC on 26 February 2007 for three integrations, plus analysed and observed values.

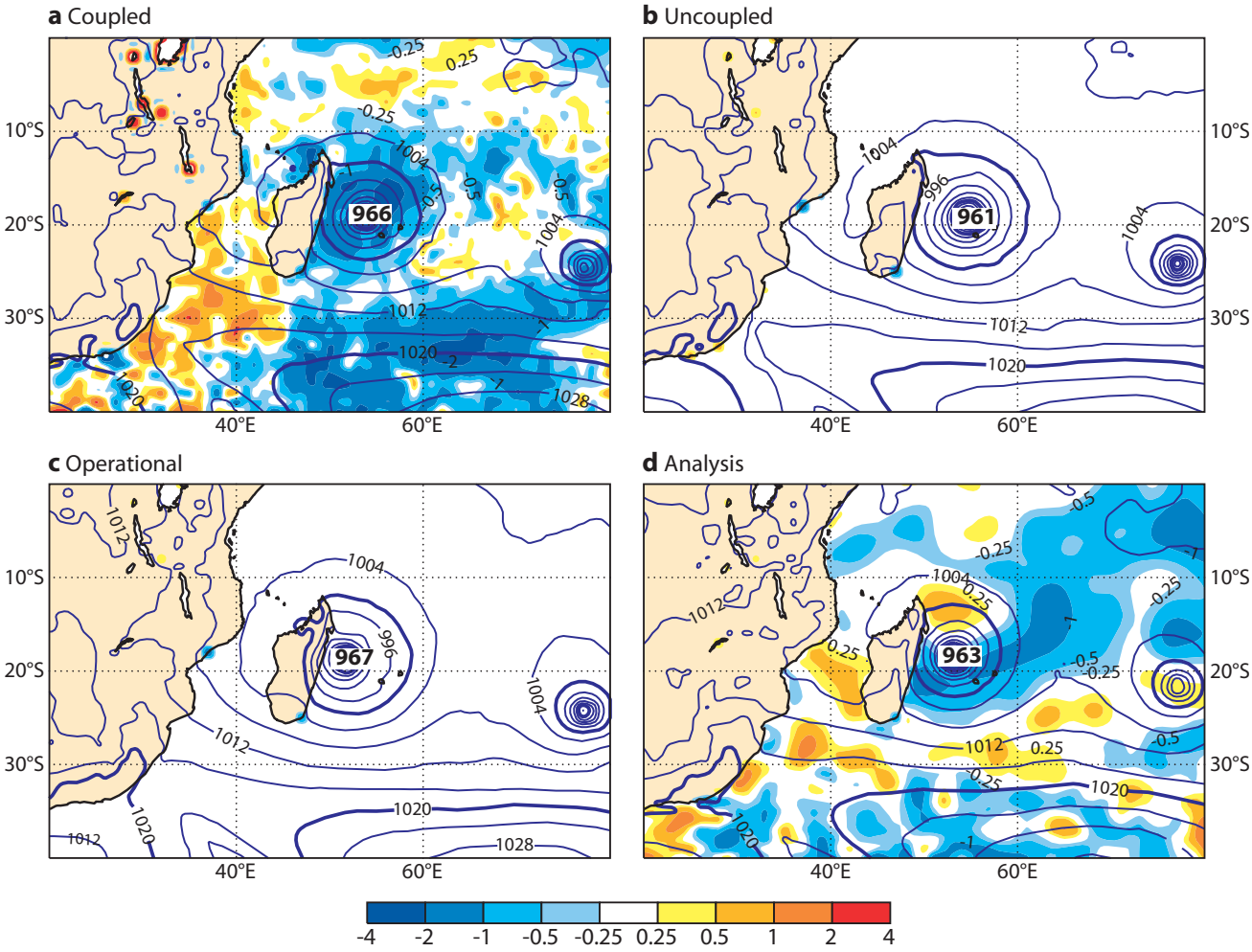

Figure 6 As in Figure 4 but for forecasts starting on 21 February 2007 – the GAMEDE case. In this case the MSLP analysis better captures the tropical cyclone, possibly due to its larger spatial scale than in the case of tropical cyclone FAVIO.

Sea surface temperature versus 2-metre temperature

In order to understand better the link between the surface and the upper atmosphere we now look at the temperature on a level just above the surface, i.e. the 2-metre temperature. Given the large differences in SST which develop during the first five days of integration (up to 4°C either way), one might expect similar differences in the 2-metre temperature field. This is not so clear, however, as can be seen from Figure 7. Despite the SST being fixed in the two uncoupled runs (Figures 7(b) and 7(c)) large differences develop in the 2-metre temperature field nevertheless. However, these differences are very similar to those in the coupled integration (Figure 7(a)). One exception is the cyclone track wake where the coupled model is able to produce the observed cool temperatures (Figure 7(d)).

A plausible explanation for the fact that the 2-metre temperature field does not seem to be influenced much by the SST is that the heat budget, which ultimately needs to be balanced, is little affected by the sensible heat (determined by the difference in temperature between the surface and that at a higher level, as well as by the wind speed) and is instead controlled more by the latent heat. Another explanation might be that the atmospheric model has been tuned to function with fixed SST and therefore the coupling with varying SST may not be as strong as it ought to be.

Tropical cyclones simulation in the coupled EPS

The same two cases of tropical cyclones have been run with a lower-resolution coupled model (T399 instead of T799) but for an ensemble of size of 15. Different diagnostics to those shown thus far are applied for this probabilistic approach.

Figure 8 shows the EPS Lagrangian meteogram for FAVIO. The meteogram is a diagnostic tool developed as part of the ECMWF operational tropical cyclone tracking software. This diagnostic highlights the EPS distributions of tropical cyclone core pressure and 10-metre wind speed as a function of time, along with the number of EPS members predicting the event.

Two main features can be noted from Figure 8. The first is that there is a difference in spread (the bars) in the coupled (left) and uncoupled (right) cases, with the latter having a larger spread than the former, especially in the cyclone core pressure (bottom panels). The same is true for GAMEDE (not shown). A larger number of cases would be needed to test its significance. If it was

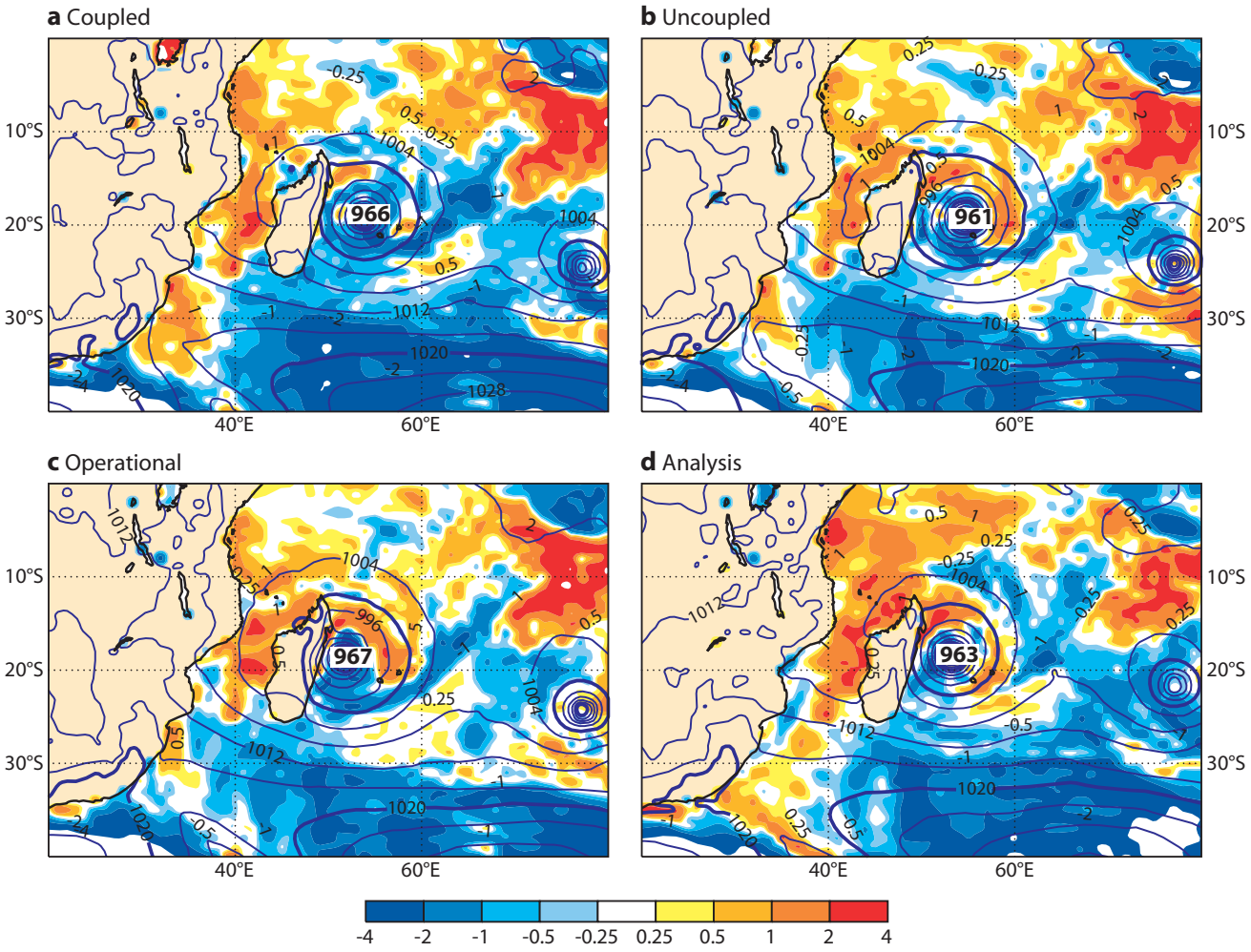

Figure 7 As Figure 6 but for 2-metre temperature instead of SST.

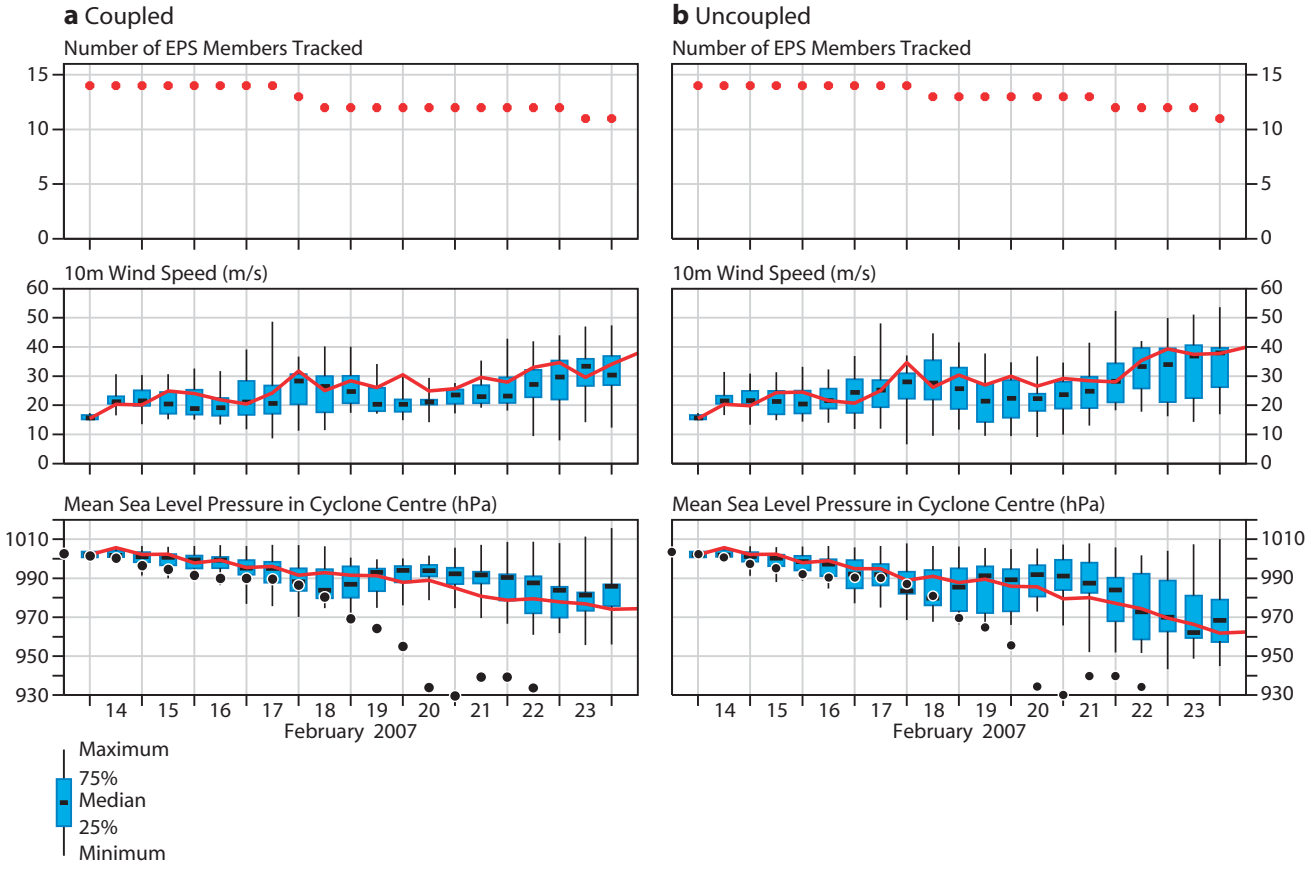

Figure 8 EPS Lagrangian meteograms for (a) the coupled ORCA025-T399 model and (b) the uncoupled T399 model for the FAVIO case starting at 00 UTC on 14 February 2007. Top panel: number of EPS members predicting the event. Middle panel: 10-metre wind speed. Bottom panel: mean sea level pressure in cyclone centre. The line represents the evolution of the member number 1 (control run) and the box-and-whiskers the spread of the remaining 14 members. The EPS distribution is determined in a 7×7 degree box centred on the tropical cyclone location. The black dots on the bottom panels are the observed values of the cyclone pressure.

significant, the reason for this difference would require further investigation but two initial hypothesis would be: (a) the presence of negative feedbacks in the radiation/cloud balances which would be more pronounced in the coupled case because of the lower SSTs and (b) the way in which the initial perturbations (via singular vectors) are calculated as they are currently tuned with a system which keeps SSTs fixed.

The second feature is that beyond day 5 neither coupled nor uncoupled forecasts are able to reproduce the very low observed core pressures for FAVIO (see the black dots in bottom panels of Figure 8), even if the uncoupled integrations reach slightly lower values than the coupled forecasts because of the lower SSTs in the latter integrations (it is a general feature of the EPS that the core pressure of tropical cyclones is systematically not low enough: according to Martin Leutbecher (ECMWF) this is a resolution-related issue). The same deficiency in the core pressure, even if to a lesser extent, is found for the GAMEDE case (not shown). However, up to day 5 both integrations simulate the observed core pressure well: the observations are within the spread and the spread is not very large. Note also that the deterministic integration (T799) reproduces the core pressure at day 5 much better than the corresponding T399 control run (compare Table 1 with the line in the bottom panels of Figure 8 on 19 February at 00 UTC). For instance, in the coupled case the core pressure in the T399 control is above 990 hPa whereas in the T799 it is 970 hPa (the same as observed!).

Lastly, we consider the strike probability maps based on the first 10 days of the integrations. The strike probability is based on the number of EPS members that predict the tropical cyclone. Figure 9 shows such a map for the FAVIO tropical cyclone in the coupled and uncoupled integrations. Both show that, albeit small, there is some probability that FAVIO makes a landfall over Mozambique with a lead-time of 10 days: a remarkable result. A sample of 15 members is not very large but the strike probability maps indicate that the coupled integration has a slightly higher probability that FAVIO makes a landfall (the purple over Mozambique). Interestingly, only one member, compared to two in the uncoupled integration, veers south of Madagascar.

What next?

A high-resolution ocean model has been coupled to the atmospheric model used for medium-range weather forecasts at ECMWF. Such a coupled model has been tested on two tropical cyclone case studies.

Encouragingly, the coupled model shows a physically reasonable behaviour in the evolution of the global

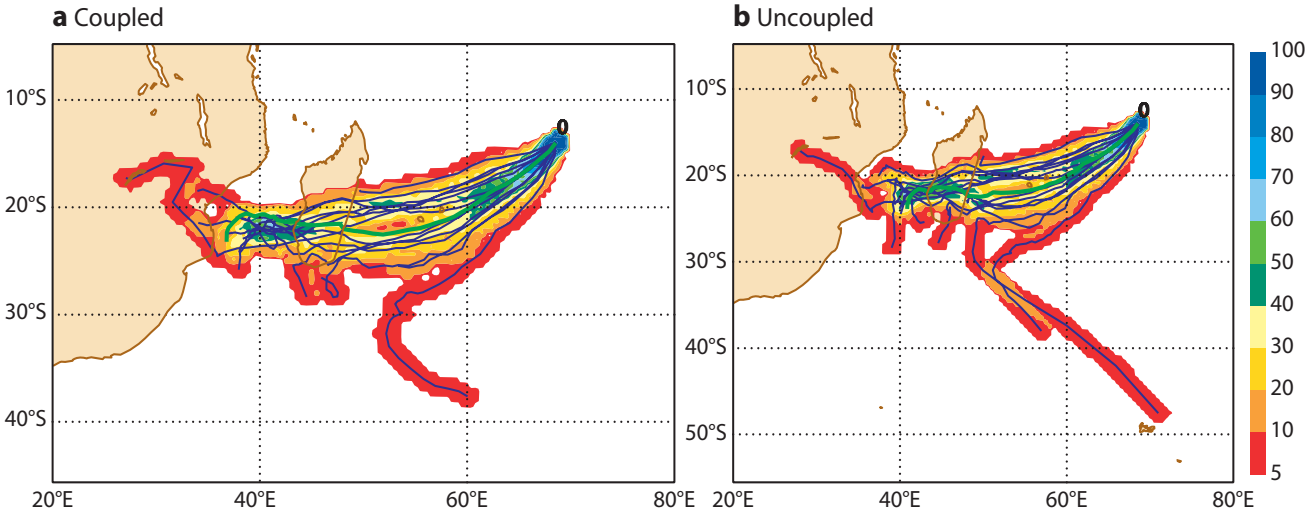

Figure 9 Strike probability maps for the FAVIO case in (a) coupled and (b) uncoupled integrations starting at 00 UTC on 14 February 2007. The strike probability is based on the number of EPS members that predict the tropical cyclone and is defined as the probability that a tropical cyclone will pass within a 120 km radius from a given location at anytime during the next 240 hours. The time dimension is thus eliminated, which allows for a quick assessment of high-risk areas regardless of the exact timing.

sea surface temperature (SST). The two tropical cyclones are nicely reproduced by the coupled model. However, despite the well simulated SSTs, differences with analogous uncoupled integrations for which SST is held fixed throughout the integrations are generally not striking, at least in terms of minimum pressure and winds. It has been argued that a possible explanation is that the IFS Cycle of the atmospheric model used in the study has been tuned to function with fixed SST and therefore the coupling with varying SST may not be as realistic as it ought to be. Indeed, no specific tuning of the coupling has been attempted. Other possible causes have been discussed as well.

Now that such a coupled model has been implemented it could be used for similar case studies, Atlantic hurricanes for example. Work is already under way to study the behaviour of this coupled model on the simulation of the intra-seasonal oscillation.

FURTHER READING

Drévillon, **M.**, **L. Crosnier**, **N. Ferry**, **E. Greiner** & **PSY3V2 Team**, 2007: The new ¼° Mercator-Ocean global multivariate analysis and forecasting system: Tropical oceans outlook. *Mercator Ocean Quarterly Newsletter No. 26*, 9–18 (www.mercator.eu.org/documents/lettre/lettre_26_en.pdf).

Gemmill, **W.**, **B. Katz** & **X. Li**, 2007: Daily Real-Time Global Sea Surface Temperature – High Resolution Analysis at *NOAA/NCEP. NOAA/NWS/NCEP/MMAB Office*, 39 pp.

Isaksen, **L.** & **P.A.E.M. Janssen**, 2004: Impact of ERS scatterometer winds in ECMWF's assimilation system, *Q. J. R. Meteorol. Soc.*, **130**, 1793–1814.

Stark, **J.D.**, **C.J. Donlon**, **M.J. Martin** & **M.E. McCulloch**, 2007: OSTIA: An operational, high resolution, real time, global sea surface temperature analysis system. In *Proc. of Oceans '07 IEEE – Marine Challenges: Coastline to Deep Sea*, 18–21 June 2007, Aberdeen, Scotland (http://ghrsst-pp.metoffice.com/pages/latest_analysis/ostia.html).

Merging VarEPS with the monthly forecasting system: a first step towards seamless prediction

FRÉDÉRIC VITART, AXEL BONET, MAGDALENA BALMASEDA, GIANPAOLO BALSAMO, JEAN-RAYMOND BIDLOT, ROBERTO BUIZZA, MANUEL FUENTES, ALFRED HOFSTADLER, FRANCO MOLTENI, TIM PALMER

An integrated medium-range and monthly forecasting system became operational at ECMWF on 11 March 2008. This merges the Variable Resolution Ensemble Prediction System (VarEPS) with the monthly forecasting system. The new system is referred to as VarEPS-Monthly.

An ensemble monthly forecasting system has been operational at ECMWF since October 2004 (*Vitart*, 2005). This system was run separately from the medium-range ensemble prediction system (EPS): for example, it had a lower resolution but used a coupled ocean-atmosphere model instead of just an atmosphere model. When the monthly forecasting system was set up, it was too costly to extend the EPS integrations to the monthly time-scale and to produce the re-forecasts that are necessary to calibrate those forecasts.

In November 2006, the EPS was upgraded to the 15-day Variable Resolution Ensemble Prediction System

(VarEPS, see *Buizza et al.*, 2007). The VarEPS approach allows changes to be made to the atmospheric horizontal resolution during the model integration, and since its implementation it has been running with the following configuration:

- From day 0 to day 10: T399L62 resolution, uncoupled (hereafter referred as leg 1)
- From day 10 to day 15: T255L62 resolution, uncoupled (hereafter referred as leg 2)

Built upon the variable-resolution approach used with the 15-day VarEPS, the extension of the EPS integration to the monthly time-scale becomes feasible at a reasonable cost. Merging monthly forecasting with the 15-day VarEPS has several advantages:

- Resources are saved by not having to run separately the first 15 days of the monthly forecasting system.
- The re-forecasts produced to calibrate the monthly forecasting system will be available to calibrate medium-range forecasts.
- The monthly forecasting skill may benefit from the higher resolution in the first 10 days of the forecasts.
- User's access/retrieval to the ECMWF forecasts is simplified.

The only drawback of the merging is that the combined 32-day VarEPS-Monthly ensemble system will be uncoupled from day 0 to day 10, as will be discussed in more details in the next section.

In this article, the merged 32-day VarEPS-Monthly ensemble system will be referred to as VarEPS-Monthly and the previous monthly forecasting system will be referred to as MOFC.

The rest of this article will contain sections dealing with the following.

- Description of the merged VarEPS-Monthly forecasting system along with a comparison with the current monthly forecasting system.
- Comparison of the probabilistic scores obtained over a large number of cases with VarEPS-Monthly and MOFC.
- Comparison of the performance of VarEPS-Monthly and MOFC for some cases of extreme weather.
- Explanation of the rationale behind the coupling of the atmospheric model to an ocean model during the VarEPS-Monthly integrations.

The article will end with a summary of the benefits of the new system.

Description of the VarEPS-Monthly ensemble system

Figure 1 gives a description of MOFC and the new VarEPS-Monthly forecasting system.

VarEPS-Monthly is an extension of VarEPS to 32 days once a week (every Thursday at 00 UTC). The atmospheric resolution will be higher than in MOFC:

- Day 0 to 10 (leg 1): T399L62
- Day 10 to 32 (leg 2): T255L62

Ideally, the atmospheric model should be coupled to the ocean from days 0 to 32, but for technical reasons the T399 atmospheric and the ocean models cannot be

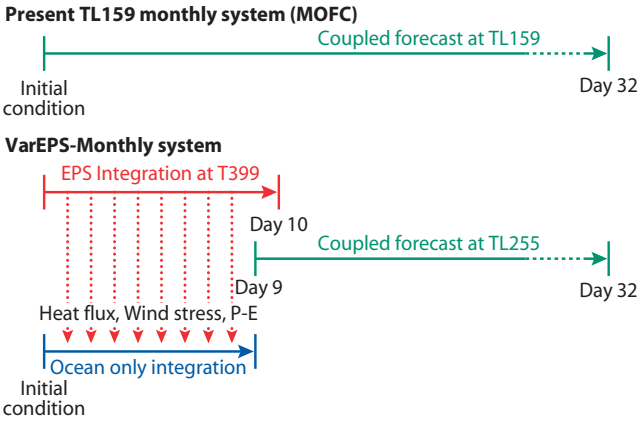

Figure 1 Description of MOFC and the new VarEPS-Monthly forecasting system. VarEPS-Monthly has a higher horizontal resolution than the old system, but the 10 first days of the integrations are uncoupled unlike in MOFC where the ocean-atmosphere coupling starts at day 0. The coupled integrations start at day 9 instead of day 10 in order to reduce the shock of the change of model resolution from T399 to T255 (see *Buizza et al.*, 2007 for more details).

coupled during the first 10 days. Therefore the coupled ocean-atmosphere integrations will start at the same time as the T255 integrations at day 9 (there is an overlap of one day between the two legs to reduce the impact of the change of resolution on the fields that are more sensitive to the truncation from the high to the low resolution). Coupling from day 0 will be possible when the next version of the ocean system (NEMO) is implemented in the near future.

The first leg of the VarEPS-Monthly forecasting system will therefore be uncoupled for the time being. However, the atmospheric model will be forced by *persisted SST anomalies* from day 0 to day 10 in the new configuration instead of *persisted SSTs*. The advantage of using persisted SST anomalies is discussed later.

In addition to the merging with the monthly forecasting system, the following changes will be introduced to VarEPS:

- All the VarEPS forecasts starting at 00 UTC (including those who are not extended to 32 days) will be coupled after day 10.
- All the VarEPS forecasts starting at 12 UTC will remain uncoupled after day 10, but forced by persisted SST anomalies instead of persisted SSTs as in the first leg.

The VarEPS system will introduce an additional difference between the 00 UTC and 12 UTC integrations since the ocean-atmosphere coupling is only applied to the 00 UTC runs. Ideally the coupling at day 10 should be also applied to the 12 UTC integrations, since it is beneficial in the tropics (see below). However, for technical reasons, this would be difficult to implement with the current ocean model. It will be implemented when the new ocean model is operational.

The ocean component is the same as the one used for seasonal forecasting and MOFC – the Hamburg Ocean Primitive Equation (HOPE) model. This ocean model has lower horizontal resolution in the extrat-

ropics, but higher resolution in the equatorial region in order to resolve ocean baroclinic waves and processes that are tightly trapped in the equator. The ocean model has 29 vertical levels, and the ocean and atmosphere communicate through the Ocean Atmosphere Sea Ice Soil (OASIS) coupler. The coupling frequency is 3 hourly whereas it was hourly in the previous system. This is because in the previous system both oceanic and atmospheric models had a 1 hour time step. Now the T255 integrations have a time step of 45 minutes, which means that the oceanic and atmospheric models are in phase every 3 hours.

The ocean initial conditions come from the Near Real Time (NRT) component of the operational ocean analysis system (*Balmaseda et al.*, 2007). During the first leg, the ocean model is forced by the fluxes provided by each atmosphere-only integration, but the atmosphere is not sensitive to the ocean model state. The persisted anomaly SST product used to force the atmosphere is also used to constrain the SST of the ocean model.

VarEPS-Monthly consists of 51 forecasts run from slightly different initial conditions. The 50 perturbed forecasts are generated by perturbing both the atmosphere and ocean initial conditions. The atmospheric perturbations are the same as those applied to the medium-range ensemble forecasts: singular vectors to perturb the atmospheric initial conditions and stochastic perturbations during the model integrations. The oceanic initial conditions include a control and four perturbed ocean analyses: the perturbed ocean analyses are produced by adding randomly chosen patterns (computed by taking the difference between different wind analyses) to the wind forcing as in MOFC. However, unlike MOFC, perturbations in the initial conditions of SSTs are not applied since the ocean model is integrated for the first nine days in uncoupled mode, forced by the fluxes produced by each ensemble member. Since the total ensemble size is 51, each of 5 ocean assimilations is used as the initial condition of 10 or 11 (for the control assimilation) ensemble members.

A problem with long-term integrations is that the model mean climate begins to be different from the analysis climate. As for MOFC and seasonal forecasting, the effect of the drift on the model calculations is estimated from integrations of the model in previous years (the re-forecasts). The drift is removed from the model solution during the post-processing. In MOFC, the re-forecasts consist of a five-member ensemble of 32-day coupled integrations, starting on the same day and month as the real-time forecast for each of the past 12 years. For instance, re-forecasts corresponding to 3 January 2008 consist of five-ensemble member integrations starting on 3 January 1996, 3 January 1997.... 3 January 2007 with the same resolution and model cycle as the real-time forecasts. In VarEPS-Monthly, the set of re-forecasts has been extended to 18 years. The ensemble size remains at five.

As for MOFC, the monthly forecasting products from VarEPS-Monthly are mainly based on weekly mean anomalies, since the monthly forecasting system does not have much skill to predict daily variability beyond day 10. The 7-day periods correspond to days 5–11, days 12–18, days 19–25 and days 26–32. They have been chosen so that they correspond to Monday to Sunday calendar weeks (the 32-day integrations start on Thursdays at 00 UTC).

The MARS archiving of the 32-day forecasts has been revised and the VarEPS-Monthly archiving is consistent with the VarEPS archiving. This should make the access and retrievals of ECMWF data simpler. A description of the MARS archiving of this new system can be found at:

www.ecmwf.int/research/monthly_forecasting/mofc-mars_veps.html

Current users of the monthly forecasting system are advised to view the differences between the old and new MARS retrieval commands at:

www.ecmwf.int/research/monthly_forecasting/differences.html

Table 1 summarizes the key differences between the old and the new systems.

Comparison of the general performances of VarEPS-Monthly and MOFC

VarEPS-Monthly has been tested in research mode to compare its skill to MOFC. The general comparison is based on five-member ensembles run of VarEPS-Monthly and MOFC with IFS cycle 31r2 (hereafter referred to as Cy31r2) starting on 1 January, 1 April, 1 June and 1 October for 1991 to 2003 (52 cases in total). With this experimental setting, the model biases with both config-

Initial time	Forecast days	Old	New
00 UTC	0–10	Leg1	Leg1–SST
	10–15	Leg2	Leg2–coupled
	0–32 (only Thu)	Monthly	—
	15–32 (only Thu)	—	Leg2–coupled
12 UTC	0–10	Leg1	Leg1–SST
	10–15	Leg2	Leg2–SST

Leg1	T399L62 with persisted SST
Leg2	T255L62 with persisted SST
Monthly	T159L62 with coupled ocean model
Leg1–SST	T399L62 with persisted SST anomalies
Leg2–SST	T255L62 with persisted SST anomalies
Leg2–coupled	T255L62 with coupled ocean model

Table 1 Key characteristics of the old and the new ensemble systems.

urations can be compared along with the probabilistic scores calculated in cross-validations. A relatively small ensemble size (5 members as opposed to the 51 used for the real-time forecasts) means that some of the probabilistic scores are lower than in the real-time forecasts. However the goal here is to compare VarEPS-Monthly with MOFC. The overall skill of the 51-member ensemble MOFC real-time forecasts is documented in *Vitart* (2004).

Model Bias

The mean annual bias has been computed from the 52 realizations of five-member ensemble integrations for VarEPS-Monthly and MOFC. Figures 2 and 3 show the biases in geopotential height at 500 hPa and precipitation for days 26–32 (last week of the forecast). The biases of precipitation look quite similar, but the biases in geopotential height at 500 hPa are reduced in VarEPS-Monthly, although the patterns remain broadly the same.

Probabilistic Scores

Figure 4 shows the ROC (Relative Operating Characteristic) diagrams of the probability that 2-metre temperature is in the upper tercile for days 5–11, 12–18 and 19–32. The ROC Scores obtained with VarEPS-Monthly are slightly increased with respect to those obtained with MOFC.

- For days 5–11, the ROC Score is 0.81 with VarEPS-Monthly instead of 0.80 with MOFC.
- For days 12–18, the ROC Score is 0.63 with VarEPS-Monthly instead of 0.61 with MOFC.
- For days 19–32, the ROC Score is 0.57 with VarEPS-Monthly instead of 0.55 with MOFC.

Similar improvements can be seen when looking at reliability diagrams and the Brier Skill Scores (not shown).

The improvements in ROC Score and Brier Skill Score translate into a higher potential economic value with VarEPS-Monthly than with MOFC. Figure 5(a) shows the Economic Value as a function of the Cost/Loss Ratio for the northern extratropics for days 12–18. According to the Wilcoxon-Mann-Whitney test, the difference is statistically significant within the 10% level of confidence for days 5–11 and days 12–18.

Overall, results indicate that the increase of atmospheric horizontal resolution from MOFC to VarEPS-Monthly slightly improves the performances of VarEPS-Monthly at all time ranges over the northern extratropics. The same conclusion is valid for the probability of 2-metre temperature in the lower tercile, and for other variables such as precipitation, surface temperature or mean sea level pressure. Similar results are also obtained over the southern extratropics.

Unlike in the extratropics, the probabilistic scores tend to be slightly higher with MOFC than with VarEPS-Monthly in the tropics. This is illustrated by the Economic Value as a function of the Cost/Loss Ratio

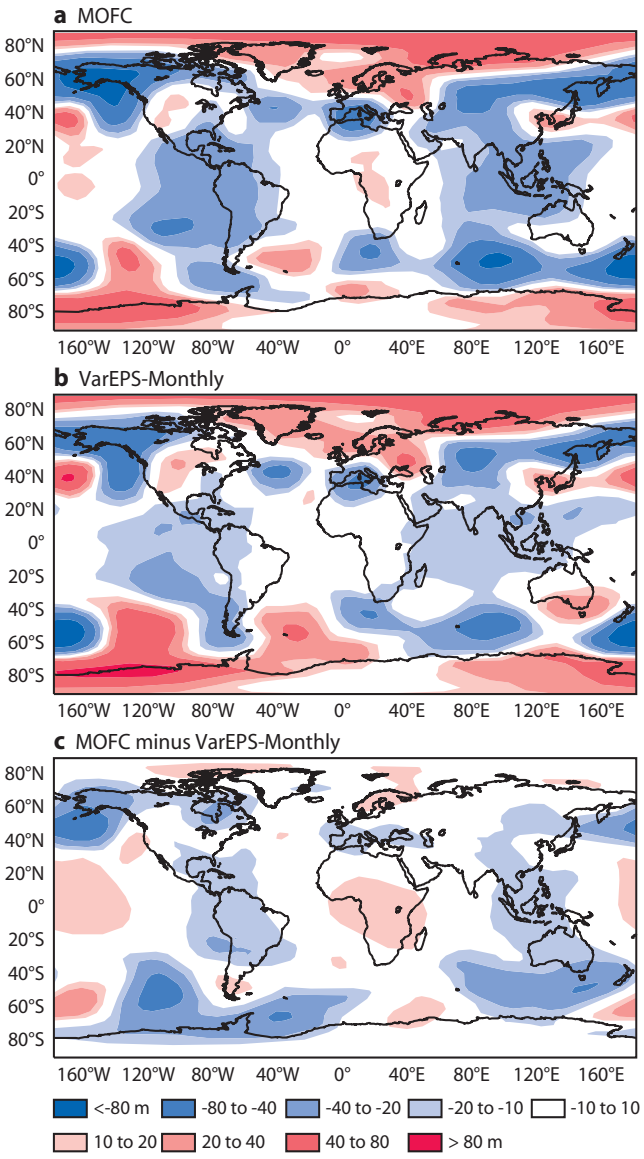

Figure 2 Bias in geopotential height at 500 hPa relative to ERA-40 calculated for (a) MOFC and (b) VarEPS-Monthly. (c) The difference of bias between MOFC and VarEPS-Monthly.

shown in Figure 5(b). A possible explanation is that in the tropics the ocean-atmosphere coupling may play a more important role than the increase of resolution. The penultimate section will show that this is at least the case for the Madden-Julian Oscillation (MJO). It is expected, therefore, that the quality exhibited by MOFC will be regained when the new ocean model allows coupling from the start of the VarEPS-Monthly forecasts.

A few case studies of extreme events

The previous section showed that VarEPS-Monthly displays slightly better scores overall in the extratropics than MOFC. However, the sharp increase in resolution from MOFC to VarEPS-Monthly is expected to be beneficial mostly for the prediction of extreme events. We now discuss two specific cases of extreme events over Europe: the heat wave over Europe in summer 2003 and the unusually wet summer 2007 over England.

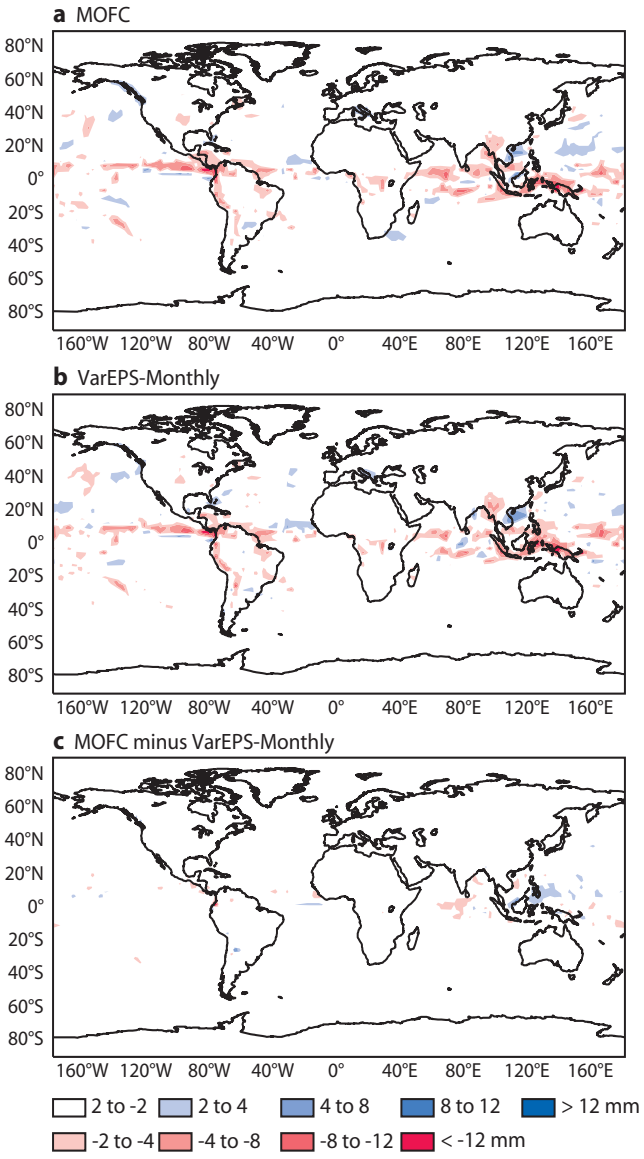

Figure 3 As Figure 1 but for total precipitation.

The heat wave over Europe in summer 2003

The heat wave in summer 2003 killed about 35,000 people in Europe, and is therefore a particularly important case for monthly forecasting. Here we will focus on the calendar week 2–9 August, when the 2-metre temperature anomalies were the highest, with weekly mean 2-metre temperature anomalies exceeding 6°C over some areas (Figure 6(a)).

The MOFC system, which was not operational, was running routinely at that time. Its performance in predicting the 2003 heat wave is discussed in *Vitart* (2005). Overall the ensemble mean anomalies for 2–9 August were above normal up to three weeks in advance. Figure 6(b) shows the ensemble mean anomalies of the 2-metre temperature for days 12–18 of the MOFC forecast starting on 23 July 2003 and verifying on 3–9 August. At this time range the model predicted a significant shift in the ensemble distribution, and the ensemble mean displays an anomaly larger than 2°C

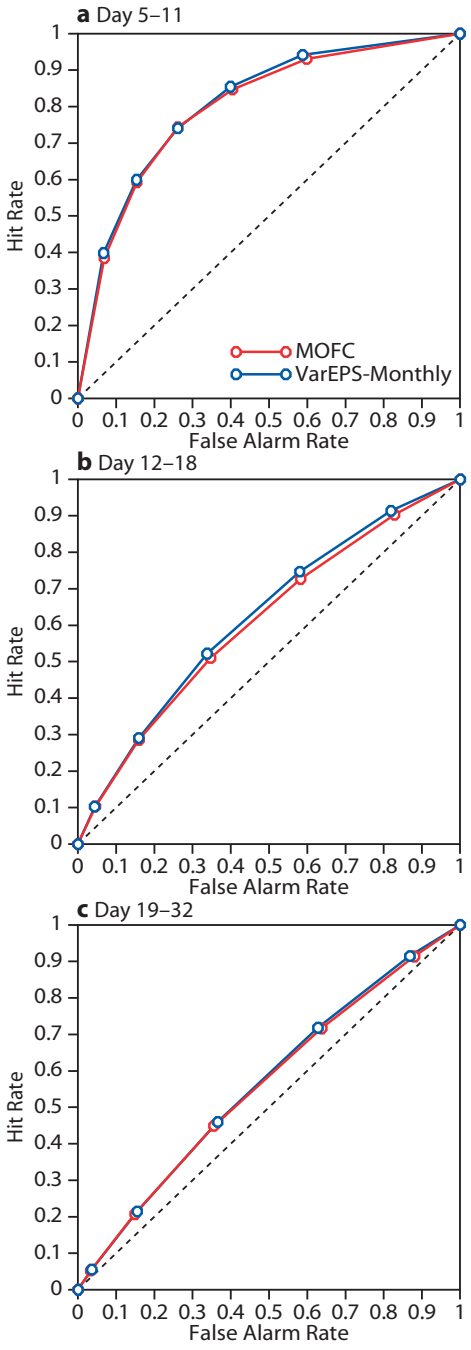

Figure 4 ROC diagram of the probability that 2-metre temperature averaged over (a) days 5–11, (b) days 12–18 and (c) days 19–32 is in the upper tercile over the northern extratropics for MOFC and VarEPS. Only land points are scored.

over most of France and Germany. Although a few ensemble members displayed a 2-metre temperature anomaly larger than 4°C, none of them produced a heat wave as intense as that observed.

Would the VarEPS-Monthly system have produced a better warning for this extreme event than the MOFC system? To answer this question, a 51-member ensemble of VarEPS-Monthly integrations with IFS Cy31r2 was run from 23 July 2003 with the same atmospheric and oceanic initial conditions as the pre-operational MOFC system, along with a five-member ensemble starting on

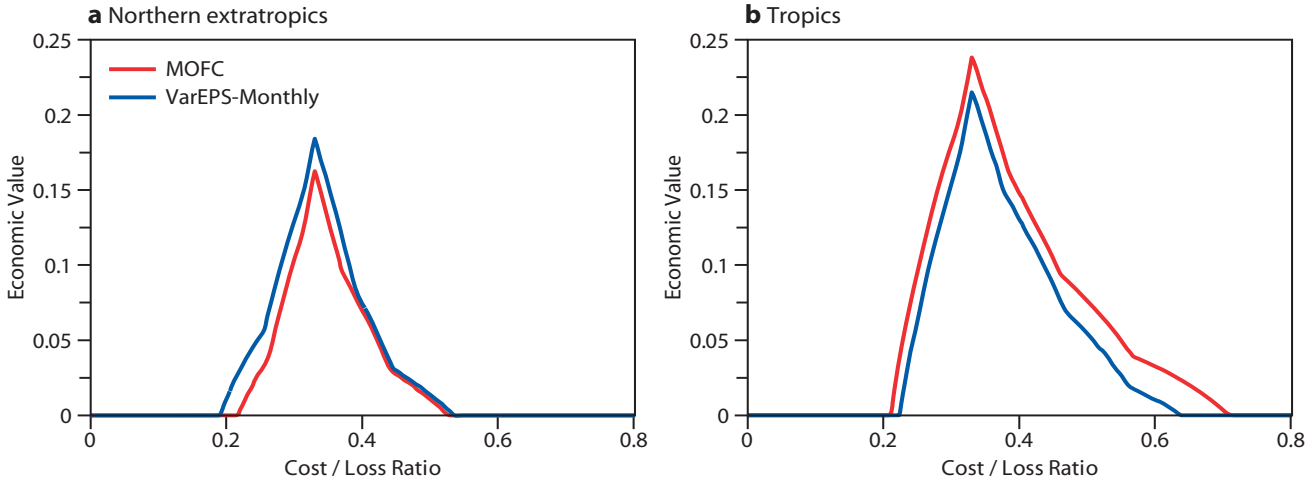

Figure 5 Potential economic value of the probability that 2-metre temperature averaged over days 12–18 is in the upper tercile over (a) northern extratropics and (b) tropics for MOFC and VarEPS-Monthly.

23 July 1991 to 2002. The re-forecasts from 1991 to 2002 are used to calibrate the 2003 forecasts and compute the 2-metre temperature anomalies. Since the model is not the same as in 2003, the same experiment was repeated but with MOFC and IFS Cy31r2.

The 2-metre temperature anomalies of MOFC and VarEPS-Monthly with IFS Cy31r2 are shown in Figures 6(c) and 6(d). Figure 6(d) indicates that the 2-metre temperature anomalies produced by VarEPS-Monthly are significantly larger than those produced by the monthly forecast in 2003 (Figure 6(b)), with anomalies of the ensemble mean exceeding 4°C over a large portion of western Europe. However, VarEPS-Monthly does not seem to predict the heat wave over Portugal, but this was also the case with the pre-operational monthly forecast (Figure 6(b)) and MOFC at Cy31r2

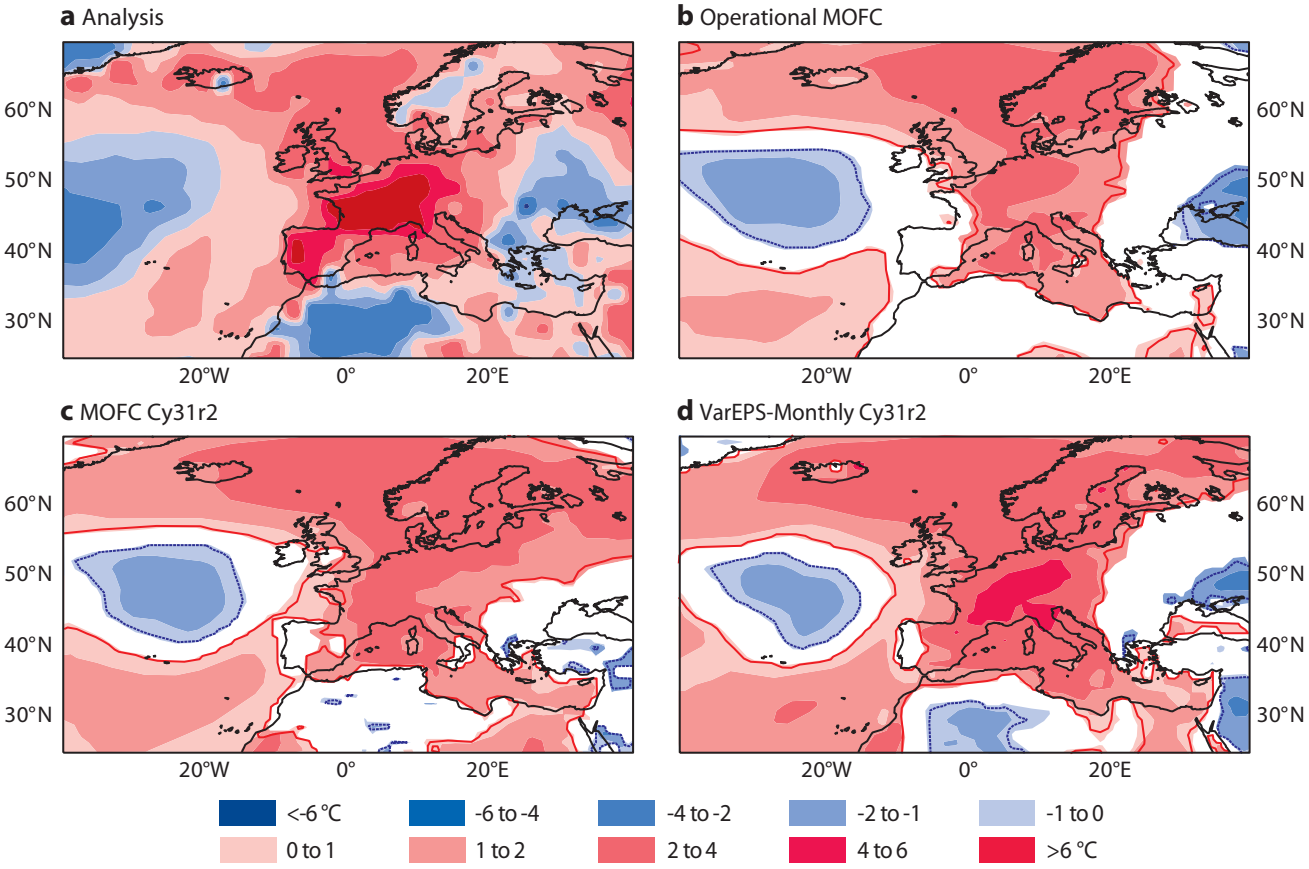

Figure 6 2-metre temperature anomaly relative to the past 12-year climate for 3–9 August 2003. Red colours indicate positive anomalies and blue colours represent negative anomalies. (a) The anomaly from the operational analysis/ERA-40. (b) The pre-operational monthly forecast of days 12 to 18 issued in 2003. (c) Re-forecast using a recent version of the monthly forecasting system with IFS Cy31r2. (d) Re-forecast with VarEPS-Monthly and IFS Cy31r2.

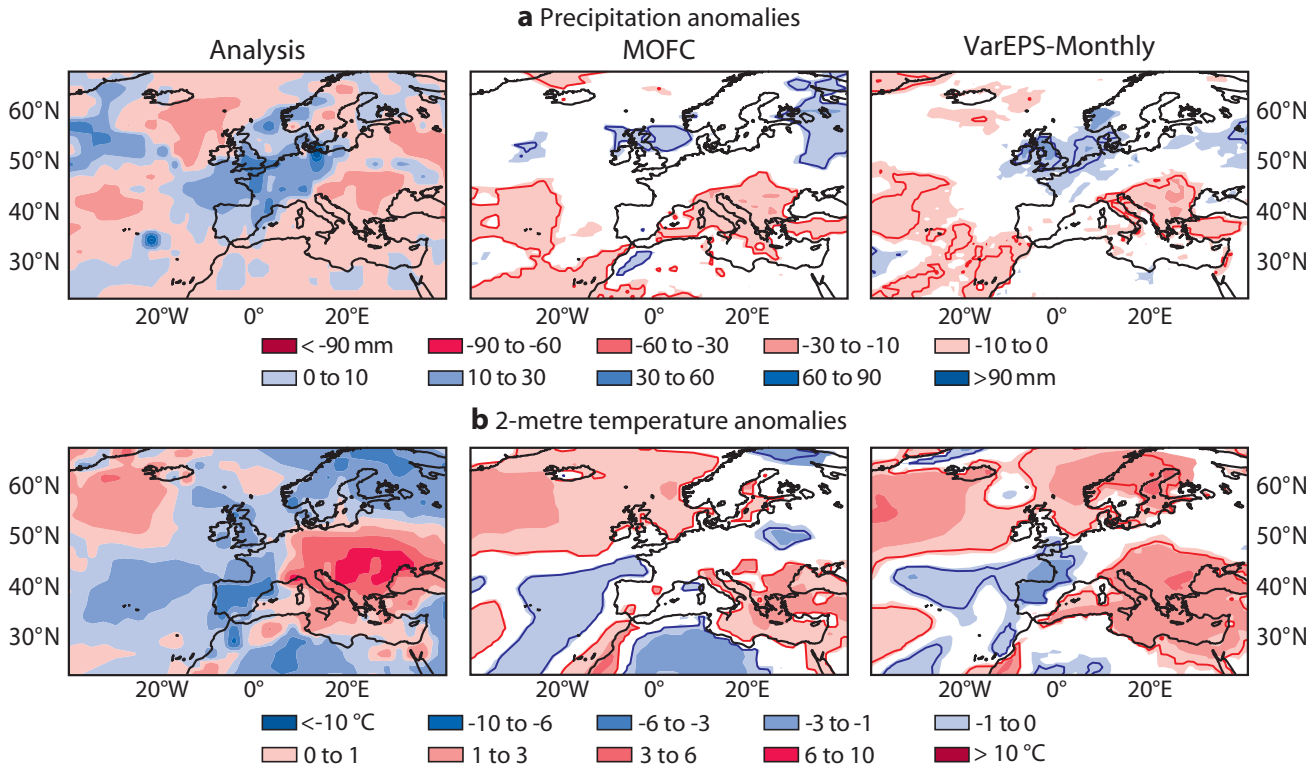

Figure 7 Anomalies averaged over the 16–22 July 2007 for (a) precipitation and (b) 2-metre temperature. The anomalies are computed relative to the past 12-year climate. Left panels: the ensemble mean anomalies computed from ECMWF operational analysis and ERA-40 for the 12-year climate. Middle panels: the operational MOFC forecasts starting on 5 July 2007. Right panels: the VarEPS-Monthly forecasts starting on 5 July 2007. For each model the anomalies are computed relative to the model climate.

(Figure 6(c)). Comparing Figure 6(c) with Figure 6(d) indicates that most of the improvement is not due to the changes in model physics, but rather to the increased horizontal resolution in VarEPS-Monthly. Those results suggest that VarEPS-Monthly could be a useful tool for early warnings of this type of extreme heat wave over Europe.

Wet summer over England in 2007

The summer 2007 over England was exceptionally wet with record precipitation which led to significant flooding over Southwest England, particularly during the week of 16 to 22 July 2007. We will focus on that specific week, where a heat wave also took place in Southeast Europe. Consider the precipitation anomalies (Figure 7(a)) and 2-metre temperature anomalies (Figure 7(b)) that are observed along with those predicted by MOFC and VarEPS/Monthly. The left panels in Figure 7 show the anomalies computed from the ECMWF operational analysis and ERA-40. A VarEPS-Monthly test suite was running routinely last summer with the same ensemble size and model cycle than MOFC. Comparison of the forecasts with the analysis shows that the VarEPS-Monthly test-suite (right panels) appears to better capture the anomalous precipitation over England than MOFC (middle panels) at the time range of 12 to 18 days. Furthermore, the heat wave over Southeast Europe is significantly stronger in VarEPS-Monthly than in MOFC, in agreement with observations.

The heavy precipitation over England was associated with a persistent low pressure system centred over England (Figure 8(a)). This low is also better predicted by VarEPS-Monthly (Figure 8(c)) than by MOFC (Figure 8(b)), along with the wave train across the Atlantic. For longer time ranges, beyond day 18, both VarEPS-Monthly and MOFC forecasts did not predict a particularly high risk of heavy precipitation over England, but the heat wave over Southeast Europe was still stronger in VarEPS-Monthly than in MOFC.

Impact of persisted SST anomalies and of ocean coupling

As described earlier, VarEPS-Monthly consists of 10 days of atmosphere-only integrations followed by 22 days of ocean-coupled integrations. During the first 10 days of integrations, the atmospheric model is forced by persisted SST anomalies instead of persisted SSTs as in the previous VarEPS systems. The reason for using persisted SST anomalies is that for a long-range integration the seasonal cycle starts to have a significant impact on the amplitude of SSTs. In the context of VarEPS-Monthly, persisted SST anomalies provide more realistic initial conditions for the coupled integrations at day 10 than persisted SSTs (Figure 9). This has little impact on the atmospheric scores of medium-range forecasts over land, but the ROC diagram in Figure10 shows that using persisted SST anomalies instead of persisted SSTs has a positive impact on the probabilistic scores beyond day 10.

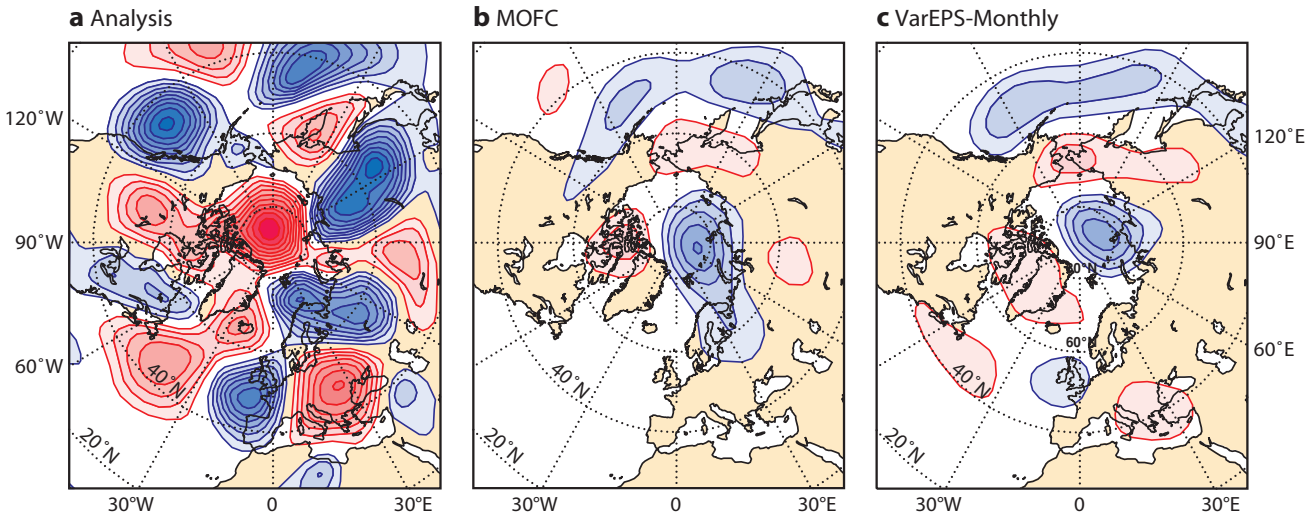

Figure 8 Geopotential at 500 hPa anomalies relative to the past 12-year climate and averaged over the week 16–22 July 2007 for (a) ECMWF analysis and ERA-40, (b) MOFC for the forecast starting on 5 July 2007 (time range days 12–18) and (c) VarEPS-Monthly for the forecast starting on 5 July 2007. The fields are displayed using a contour with intervals of 2 dam between 2 dam and 40 dam (red), and –40 dam –2 dam (blue).

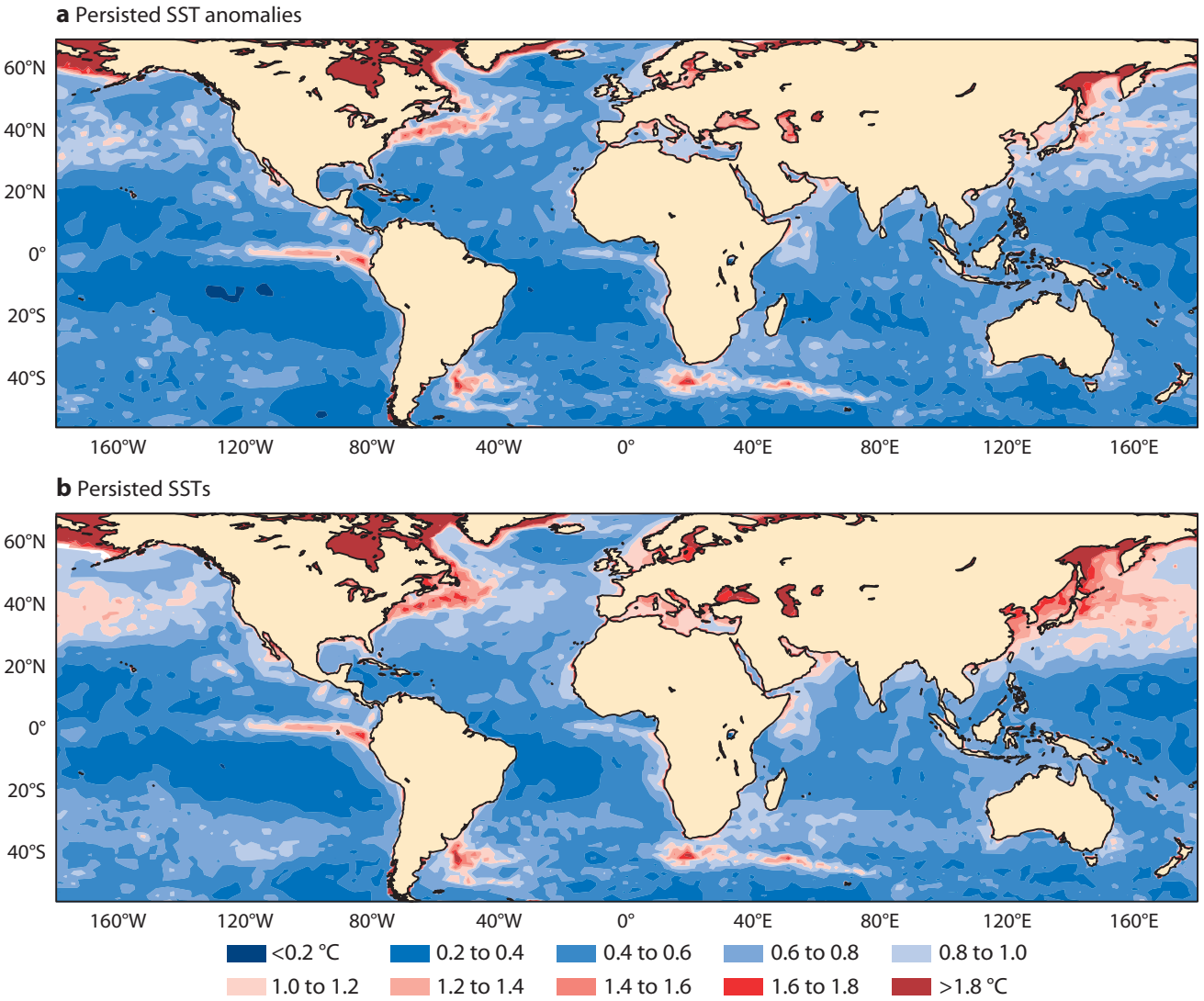

Figure 9 RMS error of sea surface temperatures at day 10 from 52 five-member ensemble cases (four starting dates over 13 years) with (a) persisted SST anomalies and (b) persisted SSTs. The RMS error is significantly lower, particularly in the extratropics, with persisted SST anomalies than with persisted SSTs.

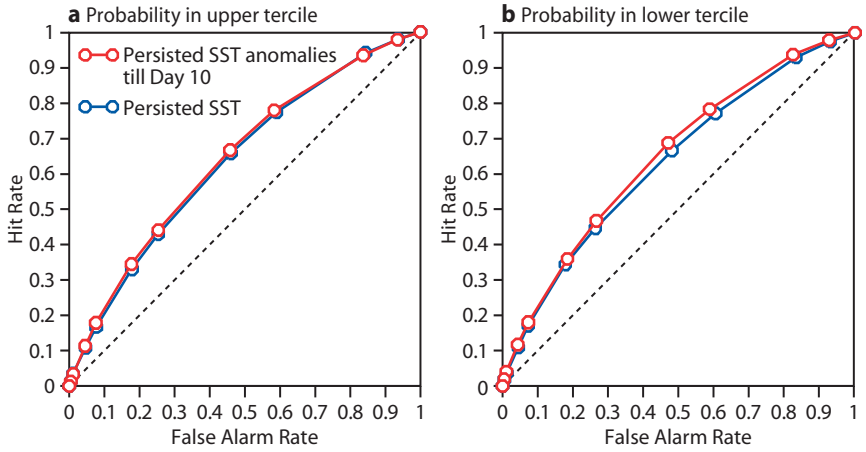

Figure 10 ROC diagrams indicating that the probability of 2-metre temperature averaged over the land points in the northern extratropics for days 12–18 is in (a) the upper tercile and (b) the lower tercile for persisted SST anomalies till day 10 and persisted SSTs. 52 cases were used in the computation of the ROC areas.

One justification for including an interactive ocean below the atmospheric model is the impact of the ocean-atmosphere interactions on the propagation of the Madden-Julian Oscillation (MJO) which is a main source of predictability in the tropics on the sub-seasonal time scale. In order to assess the impact of ocean-atmosphere coupling in the VarEPS-Monthly configuration, a five-member ensemble of 32-day integrations of VarEPS-Monthly was performed each day from 15 December 1992 until 31 January 1993, when a strong MJO event took place. The same experiment was repeated, but with persisted SST anomalies through the 32-day integrations instead of coupling the atmosphere to the ocean model after day 10. The MJO is diagnosed by projecting each ensemble member into the two leading combined Empirical Orthogonal Functions (EOFs) of velocity potential at 200 hPa, zonal wind at 850 hPa and outgoing long-wave radiation (OLR) computed from ERA-40 (see *Woolnough et al.*, 2006 or *Vitart et al.*, 2007 for more details). The skill of the monthly forecasting system is then estimated by computing the anomaly correlations of principal components 1 and 2 (PC1 and PC2) predicted by the model with the PC1 and PC2 computed from the analysis (in this case ECMWF's reanalysis dataset, ERA-40).

Figure 11 shows the time evolution of the mean of the correlations obtained with PC1 and PC2. During the first 10 days, the scores are identical since the experiment setting is identical in both experiments. However when the coupled ocean-atmosphere integrations start, at day 10, the VarEPS-Monthly integrations display higher correlations with analysis than those obtained with 32 days of persisted SST anomalies. This shows that the ocean-atmosphere coupling is important at this time range, and therefore supports the introduction of the ocean in the context of VarEPS-Monthly.

Note that the scores displayed in Figure 11 for the two VarEPS-Monthly experiments are lower than those obtained with MOFC. This is due to MOFC being coupled from day 0 instead of day 10 for VarEPS-Monthly; the ocean-atmosphere coupling seems to have more impact on the MJO propagation than an increase in horizontal resolution (*Vitart et al.*, 2006).

Benefits of the new system

The ECMWF monthly forecasting system was developed and run separately from the EPS system. Now both systems have been merged into a unified forecasting system. The synergy will provide users with an easier access to ensem-

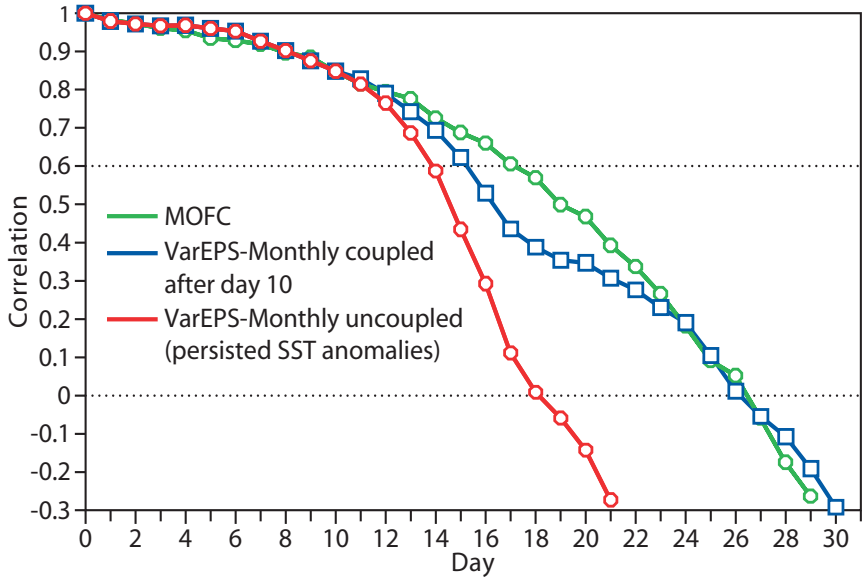

Figure 11 The time evolution of the mean of the correlations obtained with PC1 and PC2 (the individual correlations of PC1 and PC2 look similar) for VarEPS-Monthly uncoupled (persisted SST anomalies), VarEPS-Monthly coupled after day 10 and MOFC. The MJO is diagnosed by projecting each ensemble member into the two leading combined EOFs of velocity potential at 200 hPa, zonal wind at 850 hPa and outgoing long-wave radiation computed using ERA-40. The skill is estimated by computing the anomaly correlations of principal components 1 and 2 (PC1 and PC2) predicted by the model with the PC1 and PC2 computed from the analysis (in this case ERA-40).

ble forecasts from day 0 to day 32, and will give users of monthly forecasts more skilful predictions.

First of all, the change will make the retrieval of data much easier for users. This will also help to build forecasting products across the different time ranges. For instance, EPSgrams could be presented with daily values till day 12 and then weekly mean values afterwards. Some probabilistic products from the EPS (e.g. the Extreme Forecast Index, EFI) can also be applied to the extended forecast range. Another big advantage of this new system is that EPS and monthly forecasting can share the same re-forecast system.

Secondly, as results presented here have shown, monthly forecasts will benefit from the increased horizontal resolution of the atmospheric model. The scores in the extratropics are overall higher at all time ranges, and most particularly the prediction of extreme events seems to benefit from the higher horizontal atmospheric resolution. Furthermore, the case studies discussed in this article have shown that the new merged VarEPS-Monthly system is capable to provide useful warnings of extreme weather events beyond forecast day 15.

The only drawback of the new merged system is the negative impact on the scores of the monthly predictions in the tropical regions caused by running the atmospheric model forced by persisted SST anomalies till day 10 rather than coupling at day 0. Results have indicated that this has a negative impact on MJO predictions. Work is progressing towards the development of a new ocean model that will allow coupling of the merged VarEPS-Monthly system from day 0, and thus this weakness will be addressed.

FURTHER READING

Balmaseda, **M.**, **A. Vidard** & **D. Anderson**, 2007: The ECMWF System-3 ocean analysis system. *ECMWF Tech. Memo. No. 508.*

Buizza, **R.**, **J.-R. Bidlot**, **N. Wedi**, **M. Fuentes**, **M. Hamrud**, **G. Holt** & **F. Vitart**, 2007: The new ECMWF VarEPS. *Q. J. R. Meteorol. Soc.*, **133**, 681–695.

Vitart, **F.**, 2004: Monthly forecasting at ECMWF. *Mon. Wea. Rev.*, **132**, 2761–2779.

Vitart, **F.**, 2005: Monthly Forecast and the summer 2003 heat wave over Europe: a case study. *Atmos. Sci. Lett.*, **6**, 112–117.

Vitart, **F.**, **S. Woolnough**, **M.A. Balmaseda** & **A. Tompkins**, 2006: Monthly forecast of the Madden-Julian Oscillation using a coupled GCM. *Mon. Wea. Rev.*, **135**, 2700–2715.

Woolnough, **S.J.**, **F. Vitart** & **M.A. Balmaseda**, 2007: The role of the ocean in the Madden-Julian Oscillation: Sensitivity of an MJO forecast to ocean coupling. *Q. J. R. Meteorol. Soc.*, **133**, 117–128.

ECMWF's Replacement High Performance Computing Facility 2009–2013

NEIL STORER, ISABELLA WEGER

IN 2007, ECMWF carried out a procurement to replace its High Performance Computing Facility (HPCF) from 2009 onwards. Within the framework of a service contract with IBM United Kingdom Ltd., a POWER6 system will be provided for the period 2009–2011, delivering five times the performance over the current system, which will be replaced with a POWER7 system for the period 2011 to mid-2013.

Summary of the procurement process

The ECMWF Strategy 2006 to 2015 defines the principal goal for the coming years as maintaining the current rapid rate of improvement of its global medium-range weather forecasting products, with particular emphasis on improving early warnings of severe weather. The Strategy includes specific targets for improvements in forecast skill and highlights the fact that the rate of increase in the performance of the HPCF is an essential factor for achieving these targets. It calls for a sustained performance of 20 teraflops from early 2009, with a gradual increase to between 150 and 200 teraflops sustained by 2015.

The Strategy requirements equate to an improvement over the existing HPCF system by a factor of 5 from 2009 (Phase 1 of the new system) and a factor of 10 to 12.5 from 2011 (Phase 2 of the new system).

Since the existing service contract for the current HPCF expires in early 2009, in December 2006 Council approved the proposal to procure a replacement system. Recognizing that the performance of the HPCF is crucial to the successful implementation of the strategy, Council accordingly approved an increased money stream, with the proviso that all ancillary costs (infrastructure enhancements, data archive system upgrades and increased electricity consumption) arising from this increase in HPC funding are to be covered out of this money stream. The Invitation to Tender (ITT) therefore provided vendors with a way of calculating the ancillary costs associated with their particular offer and required them to make a corresponding deduction from the funds available for the new contract.

In March 2007 ECMWF published an ITT (reference: ECMWF/2007/192) for the procurement of a High Performance Computing Facility, with a closing date of 1 June. A number of working groups were established, each charged with performing an in-depth analysis and

comparison of specific aspects of the tenders received. The process was carried out over the summer months and included visits to reference sites and a dialogue with tenderers to refine the solutions bid.

In December 2007, Council authorized ECMWF's Director to sign a contract with the successful tenderer, IBM UK Ltd. The new HPCF will attain a performance improvement factor of 5 for Phase 1 and about 10.5 for Phase 2, based on a benchmark comprising the following set of applications that are representative of the most computationally demanding components of ECMWF's planned operational activities:

- 4D-Var at resolution T799L91 and T95/159/255.
- Deterministic forecast at resolution T1279L126.
- EPS at resolution T639L91.

The new HPCF

The new HPCF will be supplied in two phases; Phase 1 will cover the period 2008 to 2011, while Phase 2 will cover the period 2011 to 2013. Each Phase will be delivered and installed in two stages (Stage 1A and Stage 1B for Phase 1, Stage 2A and Stage 2B for Phase 2). The system delivered for each phase will comprise two identical independent subsystems. Phase 1 for example will comprise two identical POWER6 compute clusters along with two identical I/O storage clusters, so subsystem-1A will comprise one of the compute clusters and one of the I/O storage clusters, while subsystem-1B will comprise the other compute cluster and I/O storage cluster.

Table 1 outlines the main characteristics of one of the two identical subsystems of Phase 1.

Stage 1A will start its formal acceptance tests towards the end of 2008, then, once Stage 1B has been installed, the whole of Phase 1 will start its formal acceptance tests a few months later. Phase 2 will start its formal acceptance tests in 2011.

The staged delivery approach has two main advantages.

- It puts less strain on ECMWF's power and cooling infrastructure, as it will be possible to ensure that during periods of overlap, when systems are being commissioned alongside production systems, only a maximum of three subsystems (two old and one new, or two new and one old), rather than four, need be powered and cooled.
- It will enable one subsystem to reside for a while at IBM's manufacturing and testing plant in Poughkeepsie, USA at the same time as the other subsystem resides at ECMWF. This will enable the two subsystems to be tested concurrently. ECMWF will run a workload that tries to emulate what normally runs on the existing HPCF. At the same time engineers in Poughkeepsie can concentrate more on benchmark and diagnostic testing, as well as having an identical system on which to solve any problems experienced in testing at ECMWF.

Figure 1 is a schematic of the Phase 1 system, showing the two subsystems and the various clusters and components. The only physical difference between 'application' nodes and 'pre/post-processing' nodes is the amount of memory they have. Although the I/O storage clusters are shown as belonging to one subsystem or the other, the multi-cluster GPFS filesystem enables both compute clusters to access data on either I/O cluster as if the data was resident on that compute cluster. Potentially all of the data is accessible to any node in either subsystem and the data will be transferred at a rate that is independent of which of the two I/O clusters serves the data. Also, the I/O storage clusters are independent of the compute clusters, so it will be possible for example to shutdown a compute cluster without affecting either of the I/O clusters or the other compute cluster.

	Subsystem attribute	Description
COMPUTE	Compute nodes	240 32-core 4.7GHz POWER6 'application' nodes
		8 32-core 4.7GHz POWER6 'pre/post-processing' nodes
		2 32-core 4.7GHz POWER6 'spare' nodes
	Memory	2 GB/core on the 'application' and 'spare' nodes
		8 GB/core on the 'pre/post-processing' nodes
	Network nodes	9 32-core 4.7GHz POWER6 (mainly for I/O routing)
	Interconnect	8-plane 4×DDR Infiniband
I/O	I/O nodes	28 (14 pairs of) 4-core 4.2 GHz POWER6
	Disk space	0.9 Petabytes (900,000 GB, or 900 TB)

Table 1 The main characteristics of one of the two identical subsystems of Phase 1.

Figure 2 illustrates the independence of the I/O storage clusters, as well as their constituent parts.

Comparing the current and new HPCFs

The main component of the system is the POWER6 node, which is an evolution of the p5-575 POWER5 node that is used in the existing HPCF. In the compute clusters the POWER6 node has 32 cores, running at 4.7 GHz, while the nodes in the I/O clusters each have 4 cores with a frequency of 4.2 GHz. Figure 3 is a simplified schematic which shows the differences in architecture of the POWER6 and POWER5 chips.

While the POWER6 processor is binary compatible with the POWER5 processor that is used in ECMWF's current HPCF, it has several additional and enhanced architectural features that are outlined in Table 2, which compares the two architectures.

There are other differences between ECMWF's new HPCF and the existing one besides the generation of the

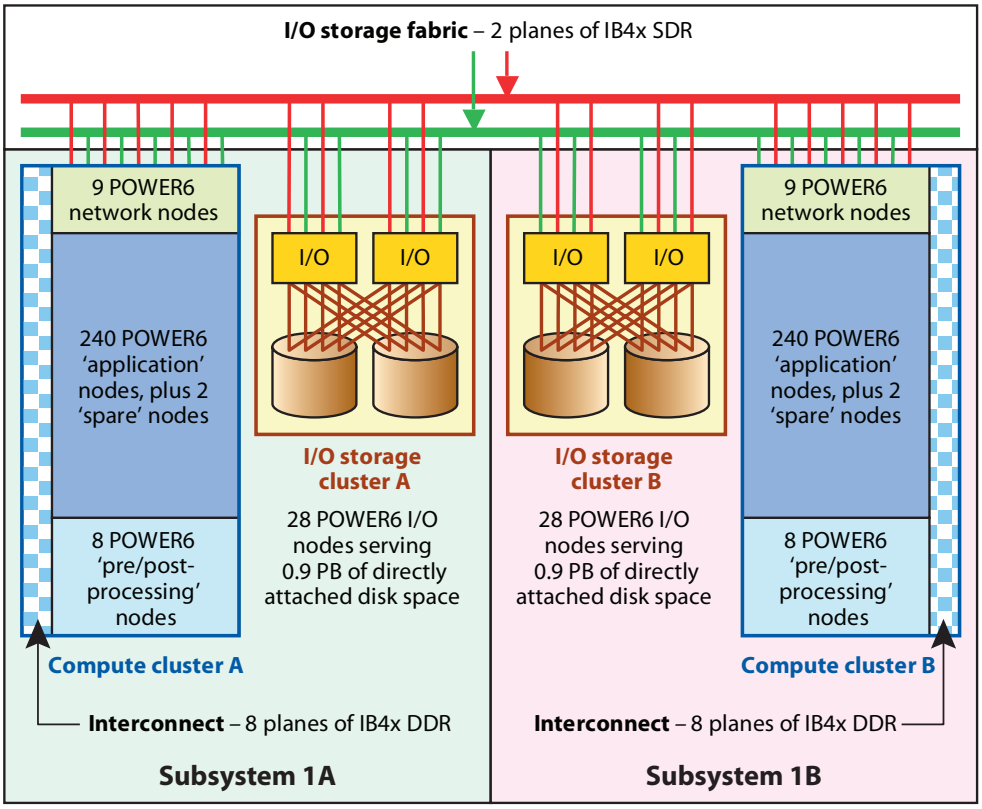

Figure 1 An overview of the Phase 1 system.

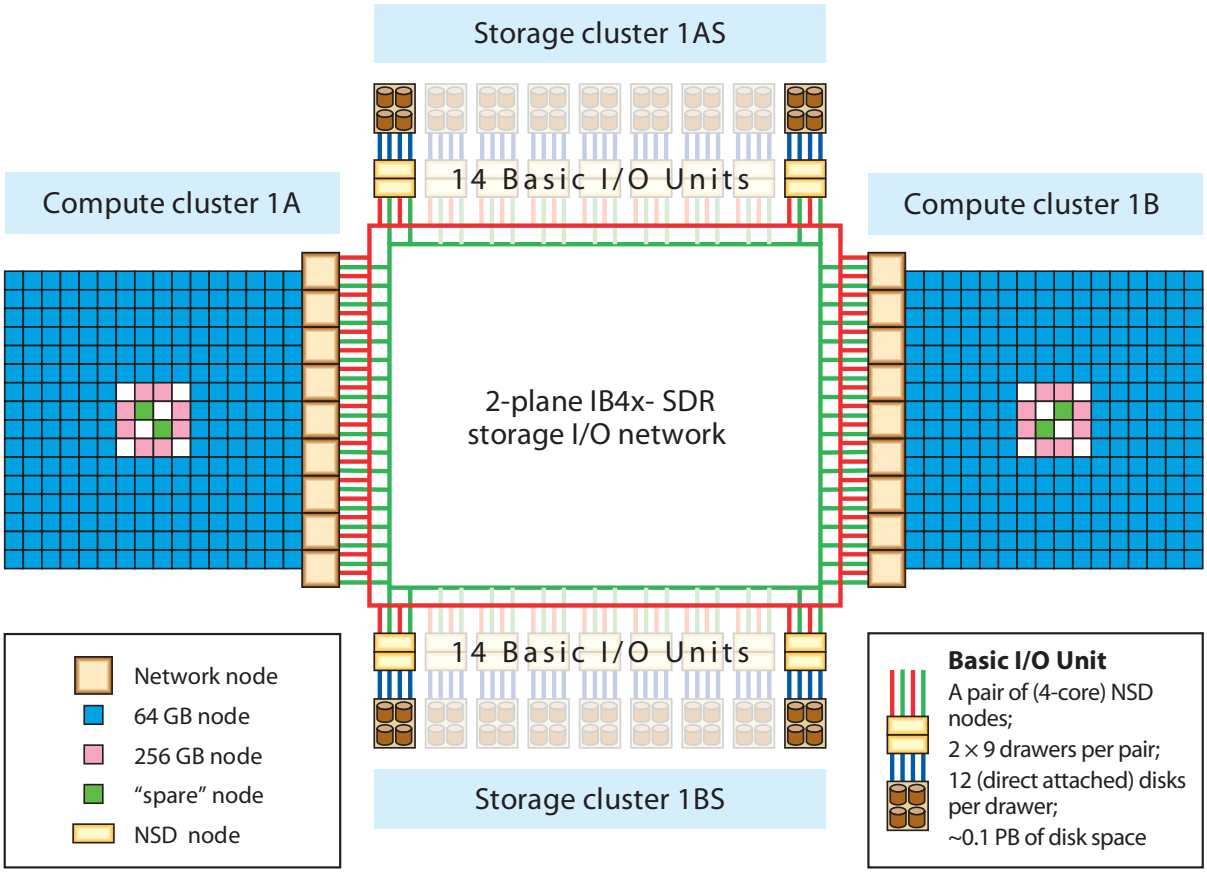

Figure 2 The Phase 1 system in more detail.

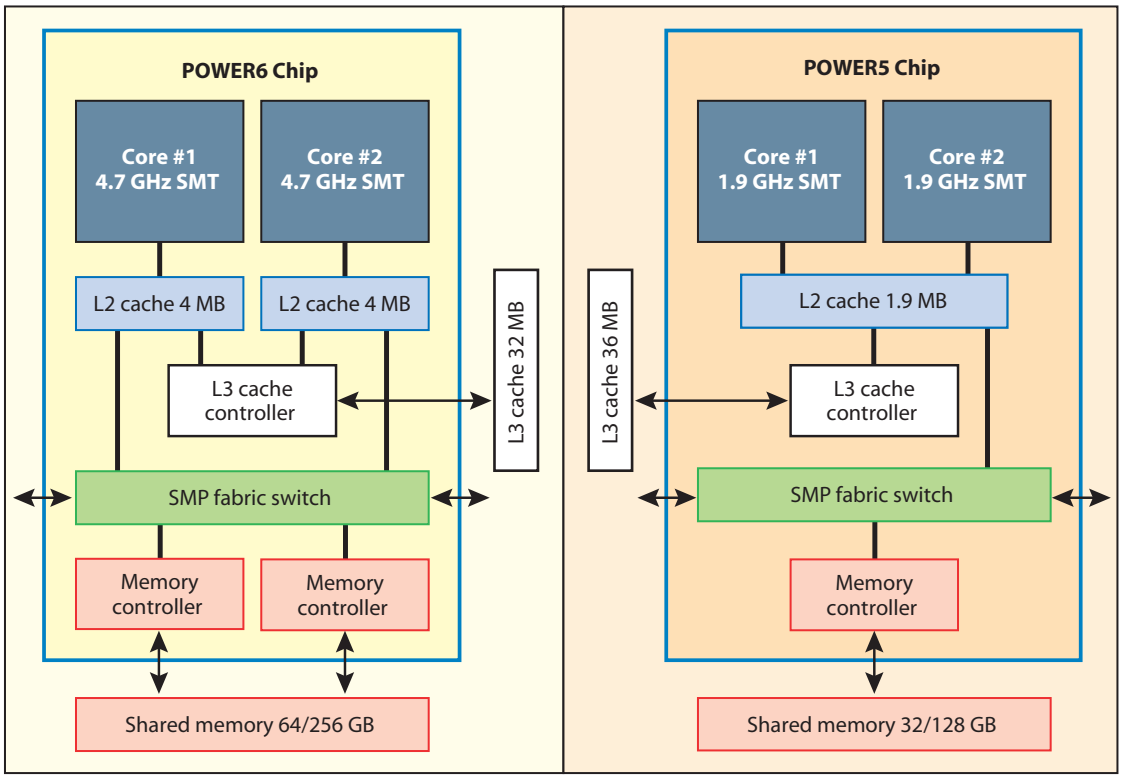

Figure 3 The architecture of the IBM POWER6 and POWER5 at ECMWF.

	POWER6	POWER5
SMP packaging	Dual chip module (DCM)	Dual chip module (DCM)
Transistors per chip	790 million	276 million
Execution style	Mostly in-order, with special case out-of-order execution	General out-of-order execution
Symmetric multi-threading	2 threads/core, priority-based dispatch, simultaneous dispatch from 2 threads (up to 7 instructions)	2 threads/core, priority-based dispatch, alternate dispatch from 2 threads (up to 5 instructions)
Frequency	4.7 GHz (18.8 GFLOPS/core peak)	1.9 GHz (7.6 GFLOPS/core peak)
Functional Units	2 floating-point multiply-add 2 fixed-point (integer) 2 load/store 1 branch 1 decimal-point 1 SIMD (VMX)	2 floating-point multiply-add 2 fixed-point (integer) 2 load/store 1 branch
L1 cache	On-core: 64 KB 4-way instruction 64 KB 8-way data	On-core: 64 KB 2-way instruction 32 KB 4-way data
L2 cache	On-chip, private to a core: 2 × 4 MB 8-way LRU, 150 GB/s	On-chip, shared by the cores: 1.9 MB 10-way LRU, 30 GB/s
L3 cache	Off-chip, but on-DCM, shared by the 2 cores (unused cache can be "borrowed" by other chips): 32 MB 16-way LRU, 32 GB/s	Off-chip, but on-DCM, shared by the 2 cores: 36 MB 12-way LRU, 12 GB/s

Table 2 Comparison of the POWER6 and POWER5 architectures.

processor. The POWER5 nodes in the clusters that comprise ECMWF's current HPCF are interconnected using the pSeries High Performance Switch (also known as the Federation Switch). This is a proprietary switch designed and manufactured by IBM solely for clusters made out of the pSeries POWER range of shared memory processor (SMP) systems. The compute clusters in the new HPCF will use a non-proprietary switch for their interconnect, based on eight planes of 4x Infiniband running at double data rate (i.e. IB4x DDR). "4x" means that four lanes are aggregated into a single link, providing a theoretical peak transfer rate of 2 GB/s bi-directional per IB4x DDR adapter. So an 8-plane IB4x DDR has a theoretical peak transfer rate of 16 GB/s per connection in each direction. This compares to the 2-plane, 4 GB/s Federation switch on the existing HPCF.

The current HPCF has a single GPFS "controlling" cluster, which along with VSD (virtual shared disk) I/O nodes in the compute clusters is connected via a fibrechannel storage area network to RAID storage subsystems having multiple disks and controllers. However, this "controlling" cluster does not serve data to the

	New Phase 1 HPCF	Current HPCF
No. of clusters	2 compute clusters 2 I/O storage clusters 1 small test cluster	2 compute clusters 1 MC-GPFS "controlling" cluster 1 small test cluster
Performance	~20 TFLOPS (sustained)	~4 TFLOPS (sustained)
Energy requirement	~2.5 MW	~1.0 MW
Each compute cluster		
Operating System	AIX 6.1 (probably)	AIX 5.3
Compute nodes	248 × 32-core POWER6 (SMT)	155 × 16-core POWER5 (SMT)
Compute processors	~8000	~2500
Network nodes	9 × 32-core POWER6 (connected to the LAN and the I/O storage fabric)	2 × 16-core POWER5 (connected to the LAN)
I/O nodes	None	8 × 16-core POWER5 (VSD nodes connected to the fibrechannel SAN)
Interconnect	8-plane IB4x-DDR (16 GB/s)	dual-plane pSeries HPS (4 GB/s)
I/O		
Paradigm	Independent I/O storage clusters, each with 28 × 4-core POWER6 NSD nodes transferring data over a dual-plane IB4x SDR network	Fibrechannel SAN
Disk types	Directly attached RAID6 storage	DS4500 RAID5 storage systems
Disk space	1.8 Petabytes (total HPCF) ~6000 disks	100 Terabytes (total HPCF) ~3500 disks
Each compute server (node)		
Memory	64 Gigabytes (8 with 256 GB)	32 Gigabytes (4 with 128 GB)
Dual-core chips	16	8
Processors (cores)	32	16
Each processor (core)		
Lithography	65 nm	90 nm
No. of transistors	790 million	276 million
Clock frequency	4.7 GHz	1.9 GHz
Peak performance	18.8 GFLOPS (~290 TF total HPCF)	7.6 GFLOPS (~37 TF total HPCF)

Table 3 Comparison of the new Phase 1 HPCF and the current facility.

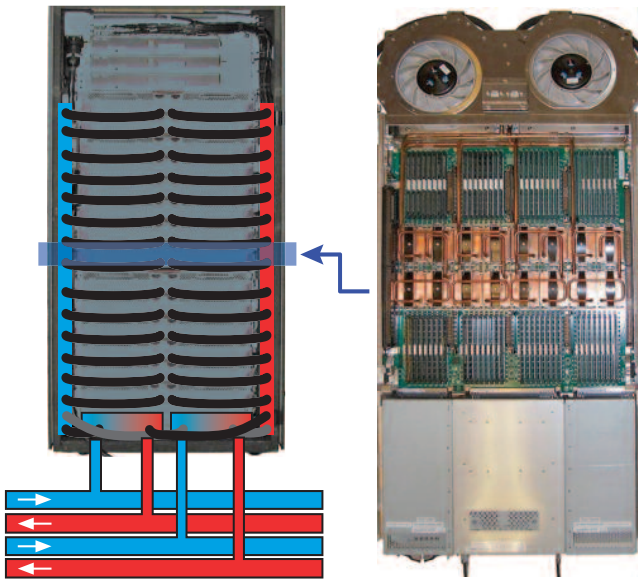

Figure 4 The cooling system based on new technologies.

compute clusters; it solely controls multi-cluster GPFS metadata and tokens. The new HPCF has two separate I/O clusters and only they are directly connected to disks, via RAID adapters. When a compute node in the new HPCF needs to read/write data, the actual disk I/O is performed by the NSD (network shared disk) nodes in the I/O cluster. These nodes route the data over a dedicated dual-plane IB4x SDR network to/from network nodes in the compute cluster, which in turn route the data to/from the compute node requesting the I/O over the cluster's internal Infiniband interconnect.

The use of storage clusters, rather than a fibrechannel storage area network, enables greater flexibility in deployment of the most appropriate technologies; also the simplicity of this scheme should improve reliability. It also means that since neither compute cluster "owns" data it should be relatively simple to perform maintenance on the compute clusters without affecting the I/O capabilities of the other one. Certain datasets will be replicated on the two I/O storage clusters to ensure that the operational suite of jobs can run even if, for whatever reason, one of these clusters becomes unavailable.

Another difference between the new and the existing HPCF is the operating system. The current HPCF runs the AIX 5.3 operating system, but the new one is likely to run AIX 6.1. While in general, users of the system should see very little difference regarding the software, AIX 6.1 has features that improve the security and availability of the system by enabling concurrent kernel updates to be done as well as tracing, debugging and recovery. It also includes improved support for memory management.

The technology of the new p6-575 servers is denser than the current technology. Although the new HPCF has five times the sustained performance compared to the current one, it will still only take up about the same amount of floor space. However, power and cooling requirements will increase significantly. ECMWF will upgrade its infrastructure in 2008 to accommodate an additional uninterruptible power supply machine and two additional chillers. These are needed to power and cool the new system.

New cooling technologies are used within the servers to remove the heat from the denser systems. The processor chips in the new p6-575 servers will be water-cooled, which is a departure for IBM in that up until now their pSeries systems have been air-cooled. The memory DIMMs will continue to be air-cooled, but the heated air will pass through a water jacket attached to the rear door of the servers. These two water cooling features together will enable more than 70% of the heat to be extracted directly by water, with very little remaining to be dissipated into the machine room. The flow of the water is regulated through copper pipes to the heat sink on the chip to match the heat output of the processors. Figure 4 shows how dense the packaging within a frame is, and how the water is fed into and out of each of the individual p6-575 servers, of which there will be twelve per frame.

Table 3 compares the main features of the two systems.

Phase 2

In mid-2011, the POWER6 based Phase 1 system will be replaced by one based on IBM's follow-on processor generation, POWER7. This will be similar to a "petaflop" system being delivered under a contract awarded to IBM by the US National Science Foundation. The Phase 2 system macro-architecture will be identical to that of Phase 1, again comprising of two identical compute clusters. An article on the Phase 2 system will be published in the ECMWF Newsletter closer to the time of its installation.

The Phase 1 system is crucial for ECMWF to meet the strategic target of increasing the resolution of all its forecasting systems in 2010. The Phase 2 system will support further improvement in the operational forecasting system in 2011 and beyond. It will provide the compute resources to support the research and development needed to prepare for the next resolution enhancement in 2015. It will also enable continued efforts to make optimal use of the wealth of information supplied by the observing system, especially for the provision of early warnings of severe weather events.

FURTHER READING

IBM POWER6 Microprocessor Technology.
IBM Journal of Research Development
http://researchweb.watson.ibm.com/journal/rd51-6.html.

ECMWF Calendar 2008

May 6–9	WCRP/WWRP Modelling Summit
May 13–14	Security Representatives' Meeting
May 14–16	Computing Representatives' Meeting
Jun 2–6	Training Course – Use and interpretation of ECMWF products
Jun 9–10	Council (*69th Session*)
Jun 11–13	Forecast Products – Users' Meeting
Jun 12–13	Meeting of the Pensions Administrative Committee of the Co-ordinated Organisations
Jun 16–18	ECMWF-EUMETSAT/GRAS SAF Workshop on "Use of GPS Radio-occultation"
Sep 1–4	Seminar on "Parametrization of Subgrid-scale Physical Processes"
Sep 16–17	Trilateral Meeting of the Co-ordinating Committee on Remuneration
Sep 22–26	Training Course – Use of supercomputing resources
Oct 6–8	Scientific Advisory Committee (*37th Session*)
Oct 8–10	Technical Advisory Committee (*39th Session*)
Oct 13–17	Training Course – Use and interpretation of ECMWF products for WMO Members
Oct 13–14	Finance Committee (*81st Session*)
Oct 14–15	Policy Advisory Committee (*27th Session*)
Oct 20	Advisory Committee of Co-operating States (*14th Session*)
Nov 3–7 (tbc)	13th Workshop on "High Performance Computing in Meteorology"
Nov 10–12	Workshop on "Ocean-atmosphere Interaction"
Dec 2–3	Council (*70th Session*)

ECMWF publications

(see http://www.ecmwf.int/publications/)

Technical Memoranda

559 **Buizza, R.**: Comparison of a 51-member low-resolution (TL399L62) ensemble with a 6-member high-resolution (TL799L91) lagged-forecast ensemble. *March 2008*

557 **Pappenberger, F., J. Bartholmes & J. Thielen**: TIGGE: Medium range multi model weather forecast ensembles in flood forecasting (a case study). *January 2008*

556 **Bechtold, P., M. Köhler, T. Jung, F. Doblas-Reyes, M. Leutbecher, M.J. Rodwell, F. Vitart & G. Balsamo**: Advances in simulating atmospheric variability with the ECMWF model: from synoptic to decadal time-scales. *February 2008*

555 **Wilkinson, J.M., R.J. Hogan, A.J. Illingworth & A. Benedetti**: Use of a lidar forward model for global comparisons of cloud fraction between the ICESat lidar and the ECMWF model. *February 2008*

553 **Taylor, J.W., P.E. McSharry & R. Buizza**: Wind power density forecasting using ensemble predictions and time series models. *February 2008*

552 **Janssen, P.A.E.M., S. Abdalla, L. Aouf, J.-R. Bidlot, P. Challenor, D. Hauser, H. Hersbach, J.-M. Lefevre, D. Vandemark, P. Queffeulou & Y. Quilfen**: 15 years using Altimeter sea state products. *February 2008*

551 **Jung, T. & M. Leutbecher**: Scale-dependent verification of ensemble forecasts. *January 2008*

550 **Casado, M.J., M.A. Pastor & F.J. Doblas-Reyes**. Euro-Atlantic circulation types and modes of variability in winter in ERA-40 and NCEP reanalysis. *January 2008*

549 **Lopez, P.**: A 5-year 40 km resolution global climatology of super-refraction for ground-based radar meteorology. *January 2008*

548 **Park, Y.-Y., R. Buizza & M. Leutbecher**: TIGGE: preliminary results on comparing and combining ensembles. *January 2008*

547 **Richardson, D., J. Bidlot, L. Ferranti, A. Ghelli, G. van der Grijn, M. Leutbecher, F. Vitart & E. Zsoter**: Verification statistics and evaluations of ECMWF forecasts in 2006-2007. *January 2008*

546 **Vidard, A., M. Balmaseda & D. Anderson**: Assimilation of altimeter data in the ECMWF ocean analysis system. *March 2008*

543 **Orr, A. & P. Bechtold**: Improvement in the capturing of short-range warm season orographic precipitation in the ECMWF model. March 2008

527 **Bouniol, D., A. Protat, J. Delanoë, M. Haeffelin, J. Pelon, D.P. Donovan, J.-M. Piriou, F. Bouyssel, A.M. Tompkins, R.J. Hogan, E.J. O'Connor, D.R. Wilson, Y. Morille & A.J. Illingworth**: Evaluating cloud fraction and ice water content in the ECMWF integrated forecast system and three other operational forecasts models using long-term ground-based radar and lidar measurements. *December 2007*

526 **Bouniol, D., A. Protat, J. Delanoë, M. Haeffelin, J. Pelon, D.P. Donovan, J.-M. Piriou, F. Bouyssel, A.M. Tompkins, R.J. Hogan, E.J. O'Connor, D.R. Wilson, Y. Morille & A.J. Illingworth**: Evaluating cloud occurrence in the ECMWF integrated forecast system and three other operational forecasts models using long-term ground-based radar and lidar measurements. *December 2007*

Proceedings

ECMWF Seminar on Recent Developments in the Use of Satellite Observations in Numerical Weather Prediction, 3 to 7 September 2007. *February 2008.*

Index of past newsletter articles

This is a selection of articles published in the ECMWF Newsletter series during the last five years. Articles are arranged in date order within each subject category. Articles can be accessed on the ECMWF public web site – www.ecmwf.int/publications/newsletter/index.html

Useful names and telephone numbers within ECMWF

Telephone
Telephone number of an individual at the Centre is:
International: +44 118 949 9 + three digit extension
UK: (0118) 949 9 + three digit extension
Internal: 2 + three digit extension
e.g. the Director's number is:
+44 118 949 9001 (international),
(0118) 949 9001 (UK) and 2001 (internal).

E-mail
The e-mail address of an individual at the Centre is:
firstinitial.lastname@ecmwf.int
e.g. the Director's address is: D.Marbouty@ecmwf.int
For double-barrelled names use a hyphen
e.g. J-N.Name-Name@ecmwf.int

Internet web site
ECMWF's public web site is: http://www.ecmwf.int

	Ext
Director	
Dominique Marbouty	001
Deputy Director & Head of Research Department	
Philippe Bougeault	005
Head of Operations Department	
Walter Zwieflhofer	003
Head of Administration Department	
Ute Dahremöller	007
Switchboard	
ECMWF switchboard	000
Advisory	
Internet mail addressed to Advisory@ecmwf.int	
Telefax (+44 118 986 9450, marked User Support)	
Computer Division	
Division Head	
Isabella Weger	050
Computer Operations Section Head	
Sylvia Baylis	301
Networking and Computer Security Section Head	
Rémy Giraud	356
Servers and Desktops Section Head	
Richard Fisker	355
Systems Software Section Head	
Neil Storer	353
User Support Section Head	
Umberto Modigliani	382
User Support Staff	
Paul Dando	381
Anne Fouilloux	380
Dominique Lucas	386
Carsten Maaß	389
Pam Prior	384
Computer Operations	
Call Desk	303
Call Desk email: calldesk@ecmwf.int	
Console – Shift Leaders	803
Console fax number +44 118 949 9840	
Console email: newops@ecmwf.int	
Fault reporting – Call Desk	303
Registration – Call Desk	303
Service queries – Call Desk	303
Tape Requests – Tape Librarian	315

	Ext
Meteorological Division	
Division Head	
Horst Böttger	060
Meteorological Applications Section Head	
Alfred Hofstadler	400
Data and Services Section Head	
Baudouin Raoult	404
Graphics Section Head	
Stephan Siemen	375
Meteorological Operations Section Head	
David Richardson	420
Meteorological Analysts	
Antonio Garcia-Mendez	424
Anna Ghelli	425
Claude Gibert (web products)	111
Fernando Prates	421
Meteorological Operations Room	426
Data Division	
Division Head	
Jean-Noël Thépaut	030
Data Assimilation Section Head	
Erik Andersson	627
Satellite Data Section Head	
Peter Bauer	080
Re-Analysis Section Head	
Dick Dee	352
Probabilistic Forecasting & Diagnostics Division	
Division Head	
Tim Palmer	600
Seasonal Forecasting Section Head	
Franco Molteni	108
Model Division	
Division Head	
Martin Miller	070
Numerical Aspects Section Head	
Agathe Untch	704
Physical Aspects Section Head	
Anton Beljaars	035
Ocean Waves Section Head	
Peter Janssen	116
GMES Coordinator	
Adrian Simmons	700
Education & Training	
Renate Hagedorn	257
ECMWF library & documentation distribution	
Els Kooij-Connally	751